Production and use of nuclear tracks: imprinting structure on solids

Bernd Eberhard Fischer and Reimar Spohr

Gesellschaft für Schwerionenforschung GmbH, D-6100 Darmstadt 11, Postfach 110 541, Federal Republic of Germany

Latent nuclear tracks are damaged zones, created along the paths of rapidly moving ions in solids. They are stored indefinitely in many insulators and can be used to initiate a phase separation process by one of several procedures that remove, collect, or transform material along the latent track. The resulting two-step technique is based on separate inscription and development stages, similar to the lithographic techniques using visible light, uv, x rays, or electrons. In contrast to these other techniques, however, it is applicable even to mechanically very stable, chemically inert, radiation-resistant dielectric materials. The most common development procedure is track etching, which acts as a chemical "amplifier" that dissolves the damaged zone of the latent track preferentially, creating etch pits or channels that can be extremely fine. Etched track diameters start around 10 nm and increase linearly with the etching time. The most outstanding feature of the technique is that one single particle is sufficient to create a developable damage. This unique combination of recording and revealing properties makes possible a single-particle structuring tool with a very wide array of applications. With the advent of high-energy, heavy-ion accelerators, with ion ranges between micrometers and centimeters, large-scale application of the technique to the imprinting of structure onto solids has become possible. At present, most frequently random track arrays are employed to induce global property changes of the solid volume or surface. In the future, scanning ion microbeam technology will make possible local generation of oriented track structures with high precision. This "ultimate" microtool should provide the versatility of a computer-controlled mechanical lathe. This review describes the processes involved in track generation. It outlines applications that are on the verge of being commercialized at present and considers future possibilities.

CONTENTS

PREFACE

This review addresses the nonspecialist, the technically curious, and those looking for new trends in rapidly developing fields. More specifically, it addresses those interested in imprinting structure onto unstructured matter, in order to generate (often unexpected) property changes. The reader is assumed to share the long-term goal to adapting techniques developed elsewhere to his own field. Such adaptations are especially important for the transfer of a useful new technique from the research laboratory to industrial application.

The goal of this review is to provide a basic understanding of the physical phenomena in track production and etching. It intends to convey the necessary information for a newcomer in the form of a "starter kit." For this purpose, recent survey articles are recommended in the cited literature, through which the earlier, original reports can be found. To facilitate the setting up of priorities for further reading, complete reference titles are given.

Up to now, the strongest interest in this field has come from the observation of heavy particles produced in nature, generally ions much heavier than protons. Natural tracks have been recorded in various minerals and glasses since the early days of our solar system. From the etched track shapes, the charge and energy of the unknown projectile ions can be determined. In contrast to the observation of already existing natural tracks, this review is concerned with the active generation of tracks for practical purposes, using a recently developed new generation of ion accelerators. In this context, the nuclear track technique is seen as a practical tool for shaping solids and changing their properties, not as a method for particle detection.

In this review, we do not ask "what particle caused the observed effect." Instead of natural particle sources with an often unknown spectrum of properties, we use accelerated heavy ions of known nuclear mass, charge, specific energy, and direction, and we ask "what is the observed effect of these ions." We therefore prefer the technology-oriented term "track recorder" to the science-oriented term "track detector," which is reserved for the observation of nuclear events. The most convenient way to tell the story is to follow the course of time, beginning with the track production, then describing the observed effects, and finally arriving at practical applications.

The new technology is based on the preferential etchability of latent nuclear tracks, due to ion-induced defects which have a very large size in comparison to the size of atoms. The observed property modifications are not due to the spatial distribution of the ions themselves, as in implantation technology (Dearnaley, 1975; Gibbons, 1972). Therefore not the ions but the inscribed defects are the real "actors on the scene." The latent tracks are conceptually discrete entities, which are distributed at random with a negligible amount of overlap. The discreteness condition is restricted to areal track densities below approximately 10^{12} ions per cm^2. Above this limit, the distinction between the defect zones and the unaltered bulk material gradually vanishes.

The effect of nuclear track defects on solid-state properties can be enhanced by several orders of magnitude using various development processes. Therefore, nuclear track technology uses much lower ion doses in general, ranging between 10^0 and 10^{12} ions per cm^2, than implantation, which usually requires areal doses above 10^{15} ions per cm^2 and rarely goes down below 10^{11} ions per cm^2.

Because of the freshness of the field, nuclear track research is far from being a closed subject. Much remains to be done in theory as well as in applications. In order to stimulate further research and development, we have included some speculative thoughts in our discussion of nuclear track uses. Any foreseeable future application will depend heavily on a better understanding of the processes involved in track formation and etching.

Up until now, most practical applications were restricted to using fission sources or nuclear reactors. With the advent of powerful high-energy, heavy-ion accelerators during the seventies, much better conditions for practical applications have been created. As it appears to the authors of this review, this new opportunity has not yet been fully perceived and seems to invite innovations in the near future.

I. INTRODUCTION

> "The first views of tracks were brief because of the frustrating tendency of the tracks in natural micas to fade in the electron beam of the microscope while they were being observed" (Fleischer *et al.*, 1975).

As recalled in the standard reference book on nuclear tracks (Fleischer *et al.*, 1975), the etching of latent tracks was motivated by the need to improve their stability. This book reviews nuclear track work published until about 1975 and has been the entrance into the field for many workers since then. The earliest observation of chemically etched tracks cited therein dates back to 1958 (Young, 1958). A broad view of this rapidly moving field since 1976 can be obtained from the recent conferences on solid-state nuclear track detectors (Granzer *et al.*, 1978; Khan and Kristiansson, 1980; Francois *et al.*, 1980; Fowler and Clapham, 1982).

At the time when the etchability of nuclear tracks were discovered, photography and lithography had already been used for more than a century, the principles of cloud (Wilson, 1897) and bubble (Glaser, 1954) chambers were well understood (York, 1958; Glaser, 1958), and the preferential etchability of crystal dislocations had been known for several years.

As it turned out recently, nature had anticipated human creativity even in the field of track etching: in

TABLE I. Basic properties of the nuclear track etch technique.

Single-particle drilling tool. Each hole corresponds to exactly one particle track.
Adjustable hole diameter. Lower limit about 10 nm. Present upper limit about 1 mm (given by ion energy, foil thickness, homogeneity, and etch rates).
Uniform hole sizes. Size distribution depends on homogeneity of recording material. Areal dispersion usually between 2% and 20%.
Uniform hole length. Maximum attainable length depends on the ion range and the sensitivity of the recording material. For example, a 10-MeV/nucleon heavy ion has a range of about 100 μm. Range straggling is normally of the order of 1%.
Uniform hole orientation. Holes are usually parallel to within a few degrees. Their straightness is limited by the angular straggling of the ions, mainly due to atomic collisions. Angular straggling in crystals may be minimized in the future by ion channeling.
Adjustable hole density. Areal density can range between one single hole per sample and more than 10^{10} holes per cm^2.
Random hole distribution. Holes are statistically distributed over the irradiated area of the sample. In the future, it should be possible to generate defined hole patterns using the scanning ion beam technique.
Applies to a large variety of materials. The technique is applicable to most dielectric materials (crystals, glasses, and polymers), yielding a variety of different etched track shapes.

minerals containing uranium, the alpha decay of ^{238}U leads to a recoiling daughter nucleus ^{234}Th capable of creating an etchable nuclear track. The preferential loss of the daughter nucleus into solution gives direct evidence for this process of natural track etching (Huang and Walker, 1967; Fleischer, 1980). Recoil track etching has most important implications in the field of nuclear power generation. At present, α-recoil aging of radioactive waste storage materials (Dran *et al.*, 1980) is a problem where track etchability gives rise to some sobering frustration.

Looking back on more than two decades of productive activity in the field of nuclear tracks, we may ask what has been achieved and what are the future prospects.

The technique provides, as far as basic research is concerned, a very simple and inexpensive means for observing fast atomic particles. It is capable of recording all ions from protons to transuranium elements. The threshold of detection can be tuned to a specific minimum atomic mass by varying the composition and treatment of the track-recording material. The track recorder can store these "events" for an almost infinite time.

These are the reasons why solid-state nuclear track recorders are, nowadays, applied in many diverse branches of science, such as nuclear physics, geochronology, archeology, and space physics. They are used for fission track dating, determination of the thermal history of minerals, diagnosis of pellet burning in fusion experiments, uranium prospecting, low-level dosimetry, and heavy-ion radiography, to name but a few applications. This "detector" aspect of nuclear tracks, however, will be neglected in this review almost completely, since it is treated in detail by several recent review articles (Ahlen *et al.*, 1981; Fleischer, 1981; Hepburn and Windle, 1980).

Rather, we shall be concerned in this review mostly with the practical goal of imprinting structure on solids, since the track-etching technique can be used to manufacture tiny, regularly shaped holes in many dielectric materials. This technique has already been successfully commercialized.[1] It is a spinoff from ideas created at General Electric in the early sixties (Fleischer *et al.*, 1975), and the resulting homoporous nuclear track filters (Price and Walker, 1967) find applications in as diverse fields as cytology and ultrapure water generation.

The nuclear track technique is a unique tool for manufacturing statistically distributed holes of predictable cross section and areal density. Etched track diameters start around 10 nm and increase linearly with the time of etching. The nuclear track technique has decreased the smallest attainable diameter of conventional drilling tools down to the submicron range, not very far from dimensions where molecular forces become predominant.

The main properties of this new tool, which a potential user should be aware of, are summarized in Table I.

In Table II the nuclear track technique is compared with other techniques for "drilling" fine precise holes. Unlike many other techniques yielding regular hole arrays, the nuclear track technique is at present used mostly to generate random hole arrays, and it requires a dielectric "recording" material. The achieved random distributions of nuclear tracks provide a surprisingly wide range of property changes on a global scale. In the future, however, the scanning ion microbeam technique will also permit

[1]Nuclepore Corporation, 7035 Commerce Circle, Pleasanton, California 94566, USA.

TABLE II. Alternative techniques for generating fine precise channels.

Method	Smallest hole size (μm)	Corresp. rate of production (s^{-1})	Aspect ratio (length/diameter)	Restrictions	Reference
Direct writing electron beam	10^1	10^4	10^1	Phase changes around channel, due to hot plasma	von Dobeneck, 1975
Direct writing laser beam	10^0	10^2	10^0	Phase changes around channel, due to hot plasma	Nakada and Giles, 1971
Glass composite etching	10^1		∞	Requires pair of chemically different glasses	Washington *et al.*, 1971
Unidirectional solidification	10^{-1}		∞	Phase separation process; dependent on cooling rate	DeSorbo and Cline, 1970
Preferential crystal etching	depends on mask	10^5	10^2	Depends on crystal orientation	Kendall, 1979
Electron lithography	10^{-1}	10^5	10^0	Electron scattering limited; requires resist	Wallmark, 1975
X-ray lithography	10^{-1}	10^5	10^1	Requires physical mask; requires resist	Spiller and Feder, 1977
Nuclear track technology	10^{-2}	10^{10}	10^4	Yields random arrays; requires dielectric material	Fleischer *et al.*, 1975

the manufacture of regular hole arrays for inducing local changes on a submicroscopic scale.

II. PRODUCTION OF NUCLEAR TRACKS

A. Irradiation with heavy ions

One serious barrier to a broader application of nuclear tracks in research and industry is the difficulty encountered by the newcomer in obtaining access to suitable radiation sources, especially if feasibility studies are required beforehand. There exist three practical ways to expose track recorders to heavy ions: fission sources, nuclear reactors, and heavy-ion accelerators.

1. Spontaneous fission sources

Spontaneous fission from artificial nuclides is a very convenient way to obtain energetic heavy particles of about 1-MeV/nucleon specific energy, corresponding to penetration ranges in solids of the order of 10 μm. The fastest way to get started with track studies is to buy a californium fission-fragment source from a supplier of radioactive calibration sources.[2] Such sources have the approximate size of a coin. Weak sources (0.1 μCi or less) pose a small radiation hazard and can be handled even at schools. Because of their convenience, such sources should be part of any newcomer's starter kit (Enge, 1980). Fission sources (Fig. 1) yield a broad distribution of different fission fragments with different energies (Hyde, 1964; Schmitt and Pleasonton, 1966; Henschel *et al.*, 1981). They enable one to study track-etching phenomena quite satisfactorily in a dose range up to about 10^6 fission fragments per cm^2.

2. Nuclear reactors

Improved beam intensity and collimation is provided by nuclear reactors, from which much higher doses can be obtained rapidly. Reactors make possible large-scale ap-

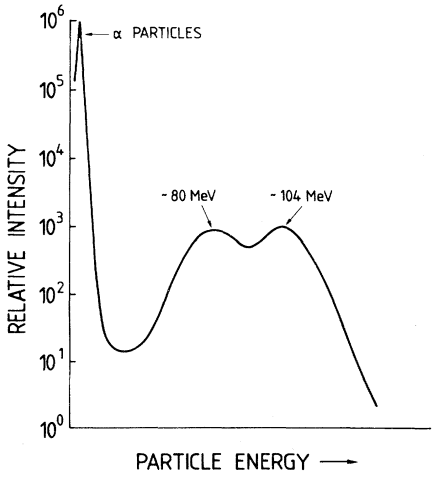

FIG. 1. Energy spectrum of a commercial spontaneous fission source. (See footnote 2.) Because of its compactness and convenience, such a source should be part of any newcomer's starter kit: isotope, ^{252}Cf; half-life, 2.65 years; alpha particles, 96.9%; fission fragments, 3.1%; alpha energies, 5.975—6.119 MeV; fission-fragment energies, two broad maxima, fission rate, about 10^9 fissions/(s Ci); neutron emission, about 4×10^9 neutrons/(s Ci).

[2]Amersham, The Radiochemical Centre Ltd., White Lion Road, Amersham, Buckinghamshire, HP7 9LL, UK.

TABLE III. Stopping power of ^{238}U ions in five elemental solids (Geissel *et al.*, 1982a). From this experimentally obtained table, the stopping power of ^{238}U ions in other elemental solids, characterized by their corresponding nuclear charges, can be obtained by interpolation. The stopping power of ^{238}U ions in any arbitrary nonelemental solid compound can be obtained, according to the Bragg rule (e.g., Northcliffe and Schilling, 1970), by summing the stopping powers of the constituent elements, while using their relative mass abundance within that compound as a weight factor.

Energy	Stopping power [MeV/(mg/cm^2)]				
MeV/nucleon	$_{6}C$	$_{13}Al$	$_{28}Ni$	$_{50}Sn$	$_{79}Au$
0.5	90.5	51.0	34.4	31.1	18.7
1.0	116.3	80.6	57.7	46.3	29.9
1.5	130.3	95.1	69.0	53.1	35.4
2.0	139.4	103.8	75.8	56.8	38.7
2.5	145.9	109.5	80.2	59.1	41.0
3.0	150.5	113.3	83.3	60.6	42.7
3.5	153.9	115.9	85.5	61.6	44.0
4.0	156.3	117.6	87.2	62.3	45.0
4.5	158.0	118.7	88.3	62.8	45.9
5.0	158.9	119.2	89.2	63.2	46.6
5.5	159.3	119.3	89.9	63.5	47.3
6.0	159.2	119.1	90.3	63.9	47.9
6.5	158.6	118.7	90.7	64.2	48.5
7.0	157.5	118.0	90.9	64.6	49.0
7.5	156.1	117.1	91.1	65.1	49.6
8.0	154.3	116.0	91.3	65.6	50.2
8.5	152.2	114.7	91.4		50.8
9.0	149.7	113.4	91.4		51.4
9.5	147.0	111.9	91.5		52.0
10.0	143.9	110.3	91.6		52.7

plications like the commerical production of nuclear track filters[1] with areal densities up to 10^{10} fission fragments per cm^2. The irradiations require access to one of the neutron outlet ports of a reactor. They also require a neutron converter foil that transforms the neutron flux into fission fragments. For this purpose, usually a ^{235}U foil is inserted between the reactor and the track recorder. Nuclear reactors yield principally the same broad distribution of energies and masses as the physically much smaller fission-fragment sources. However, because of the much higher intensity of reactor-generated fission fragments, reactors make possible a much better beam collimation.

3. Heavy-ion accelerators

The third, rather exclusive way to irradiate track-recording materials with excellent control is to use a heavy-ion accelerator. Such an accelerator can provide monoenergetic, monoisotopic, highly parallel ion beams leading to damage trails in the form of latent tracks. Their intensities range between 10^{10} and 10^{13} ions per second. The achieved damage increases with the atomic number of the ion and is highest for uranium ions (see Table III). For uranium ions, energy loss is about two times larger than for fission fragments and many times larger than for protons. Uranium ions provide the highest available specific energy loss within the periodic system. The damage depends on the specific energy of the ion and has a broad maximum between about 1 and 10 MeV/nucleon, depending on the ion and composition of the recording material. The corresponding ranges in normal solids are between about 10 and 100 μm (see Table IV). Up to now, only very little track work has been performed using relativistic uranium ions with ranges of the order of centimeters (Ahlen *et al.*, 1982). Several high-energy ("large") accelerators exist arond the world with attainable ion ranges between 100 μm and more than 10 cm, depending on the type and size of the accelerator.[3–9] An example of a high-energy linear accelerator with its experimental switchyard is shown in Fig. 2.

---

[3]Lawerence Berkeley Laboratory, 1 Cyclotron Blvd., Berkeley, California 94720, USA.

[4]Joint Institute of Nuclear Research, Laboratory of Nuclear Reactions, 141980 Dubna, Post Box 79, Moscow, USSR.

[5]Gesellschaft für Schwerionenforschung, Postfach 110 541, D-6100 Darmstadt, FRG.

[6]Oak Ridge National Laboratory, Nuclear Division, P.O. Box X, Oak Ridge, Tennessee 37830, USA.

[7]VICKSI Accelerator, Hahn Meitner Institut, Glienicker Str. 100, D-1000 Berlin 39, FRG.

[8]GANIL Accelerator, P.O. Box 5027, F-14021 Caen Cedex, France.

[9]Daresbury Research Laboratory, Warrington, WA4 4AD, UK.

TABLE IV. Range of ^{238}U ions in five elemental solids (Geissel *et al.*, 1982a). The range corresponds to the integral of the inverse of the experimentally obtained stopping power (i.e., the integral of the "penetration" power) of ^{238}U ions in the corresponding solid (Table III), integrated from zero up to the initial energy of the impinging ion. As usual, range is not given in units of μm, but in units of the areal mass density mg/cm^2 of the recording material, yielding identical numbers for a density of 10 g/cm^3.

Energy	Range (mg/cm^2)				
MeV/nucleon	$_{6}C$	$_{13}Al$	$_{28}Ni$	$_{50}Sn$	$_{79}Au$
0.5	2.7	3.7	6.2	7.3	10.5
1.0	3.8	5.5	9.0	10.3	15.3
1.5	4.8	6.9	10.8	12.7	18.9
2.0	5.7	8.1	12.5	14.9	22.1
2.5	6.5	9.2	14.0	16.9	25.1
3.0	7.3	10.2	15.5	18.9	28.0
3.5	8.1	11.3	16.9	20.8	30.7
4.0	8.8	12.3	18.2	22.8	33.4
4.5	9.6	13.3	19.6	24.7	36.0
5.0	10.4	14.3	29.9	26.6	38.6
5.5	11.1	15.3	22.3	28.4	41.1
6.0	11.8	16.3	23.6	30.3	43.6
6.5	12.6	17.3	24.9	32.2	46.1
7.0	13.4	18.3	26.2	34.0	48.5
7.5	14.1	19.3	27.5	35.9	50.9
8.0	14.9	20.3	28.8	37.7	53.3
8.5	15.7	21.4	30.1		55.7
9.0	16.4	22.4	31.4		58.0
9.5	17.2	23.5	32.7		60.3
10.0	18.1	24.5	34.0		62.6

Even low-energy ("small") accelerators with ion ranges between 1 and 10 μm offer rather interesting applications. For example, they may be used for surface texturing, where the recording material must not necessarily be penetrated by the impinging ions. Small accelerators are as capable as large ones of producing irradiations with a given isotope, ion range, areal density, and angle of incidence, using virtually any arbitrary insulator as the recording material. Thus they provide a valuable testing ground for applications requiring higher energy, especially in view of their high reliability. In heavy-ion lithography, they can even provide advantages if fine, but not very deep, structures have to be manufactured using low-energy beams.

The ion energy of high-frequency accelerators is often given in units of MeV/nucleon, the so-called "specific" energy of the accelerated ion. The specific energy unit corresponds to the ion's total energy divided by the number of its nucleons and is a measure of the ion velocity. For example, a 1-MeV/nucleon ^{238}U ion has 238-MeV total energy, corresponding to roughly 5% of the speed of light (see Fig. 8 below). Heavy-ion ranges are roughly proportional to the specific ion energy for the range between 0.1 and 10 MeV/nucleon, independent of the ion mass and recorder composition. The corresponding ion ranges are roughly between 1 and 100 μm.

Typical irradiation requirements for track formation by using heavy-ion accelerators are the following (Spohr, 1980).

Well-defined ion mass and energy. The ion beam should be free of spurious contributions from ions of different masses and energies. The existence of such ions is overlooked by many other accelerator users working in the fields of nuclear and atomic physics, since their experiments are usually tuned electronically to the desired class of events. However, in nuclear track technology, even a very few wrong ions can have a disastrous effect. For example, overshooting ranges can decrease depth resolution in heavy-ion lithography dramatically.

Highly parallel beam. This is an inherent advantage of charged-particle beams from accelerators over those from fission sources and nuclear reactors. Beam divergencies between 1 and 10 mrad can easily be achieved, depending on the specific irradiation geometry.

Homogeneous dose distribution. For high doses, a rapid scanning of the beam and/or a rapid lateral movement of the track recorder is necessary to smooth out beam inhomogeneities (Fig. 3). For low doses, a homogeneous beam profile can be obtained by defocusing the ion beam. The homogeneity of the ion beam over the recording area should normally be better than about 10%. Many other accelerator users require simply the absence of "hot" spots which can destroy their targets. But most nuclear track irradiations aiming at bulk property changes require a flat intensity profile of the beam over the target area.

Preset dose control. In contrast to most other electronically observed experiments at heavy-ion accelerators, experiments in track formation require the ion beam to be

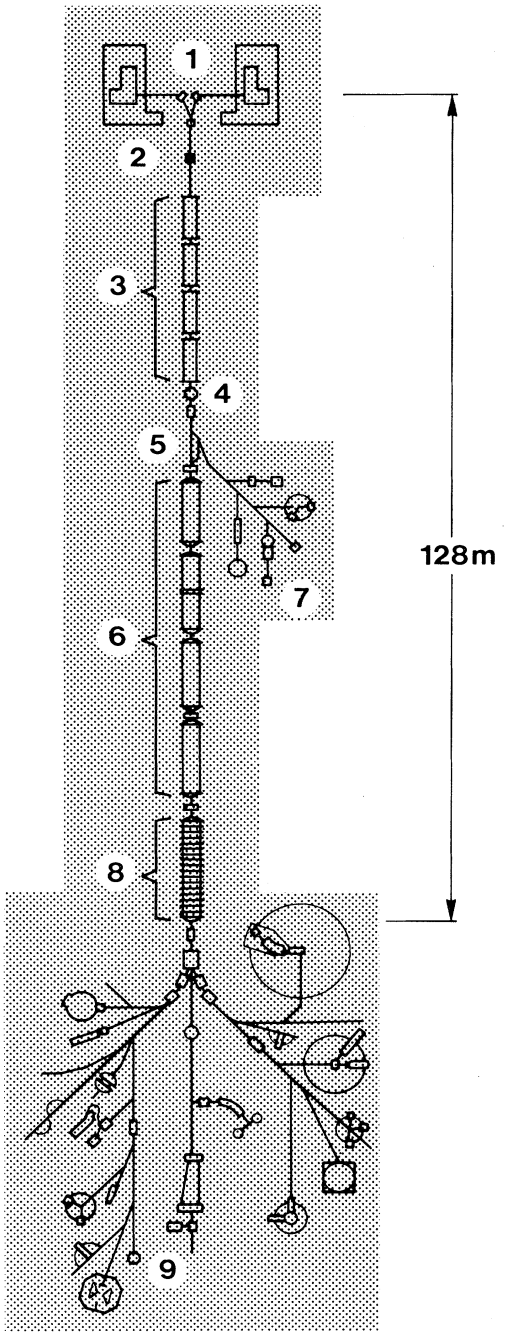

FIG. 2. Example of a linear high-energy heavy-ion accelerator. (See footnote 5.) This high-frequency accelerator yields an ion beam, pulsed at 50 Hz, with ions as heavy as uranium at particle currents between 10^{11} and 10^{13} ions/s at a maximum specific energy of about 20 MeV/nucleon. The accelerator is 128 m long and has two beam distribution switchyards with four simultaneously ion-beam-furnished experimental sites. It consists of (1) twin ion sources and injector, (2) electrostatic beam shutter (≤ 1 ms), (3) 27-MHz Wideroe-type preaccelerator, (4) gas or foil stripper, (5) charge separator, (6) 108-MHz Alvarez-type postaccelerator, (7) low-energy experimental area (≤ 1.4 MeV/nucleon), (8) single-resonator cavities, and (9) high-energy experimental area (1.4 to about 20 MeV/nucleon).

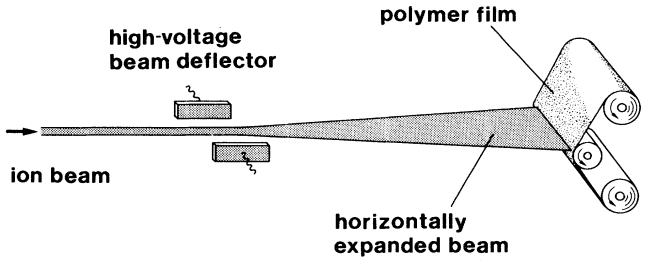

FIG. 3. Plan of an irradiation facility using a scanning ion beam (Flerov, private communication). The accelerated ion beam is passed horizontally over the sample area by a pair of electrostatic deflection plates. Simultaneously, a foil band is pulled continuously through the scanning ion beam at a speed of several meters per second at 90° to the scanning direction. Primarily conceived for the production of large quantities of nuclear track filters, this facility uses a bending roll to increase the angular spread of the recorded tracks in one plane and thus to optimize the selectivity of the filters at a given filter transmission.

switched off not electronically but physically and in real time, as soon as a preset dose is reached. The areal dose should be adjustable between 10^0 and 10^{12} ions per cm^2. It should be reproducible within about 10%. This broad dynamic range of areal doses requires an elaborate transition in measuring the beam intensity when irradiations with both low and high areal dose have to be performed: low doses require small beam intensities that can only be monitored by individual ion counting. High doses require high beam intensities that can only be monitored by measuring the electrical current.

Rapid replacement of recorders. The irradiation apparatus (see, e.g., Fig. 4) should accommodate track recorders (crystals, glasses, and polymers) of different sizes, shapes, and mechanical properties. For an economic use of the allotted beam time, it must permit a rapid replacement of irradiated recorders by fresh ones. In most cases the irradiation requires vacuum conditions. However, at low doses and high energies, thin foil windows may be used for obtaining an external beam, that is, one outside the vacuum system of the accelerator.

The primary motive for building heavy-ion accelerators during the last decade has been basic nuclear and atomic research. Therefore, at present, not many heavy-ion accelerators provide facilities for low-dose irradiations of track recorders. However, as basic research moves gradually to heavier ions and higher energies, applied research will find a broader support at such accelerators in the future. Furthermore, it is possible to build highly reliable accelerators devoted exclusively to technological applications with fixed ion species and energy that cost only a fraction of the presently used universal research accelerators. Therefore, we may soon see in the use of large accelerators for creating nuclear tracks an analog to the increasing use of small accelerators in the field of ion implantation during the last decade.

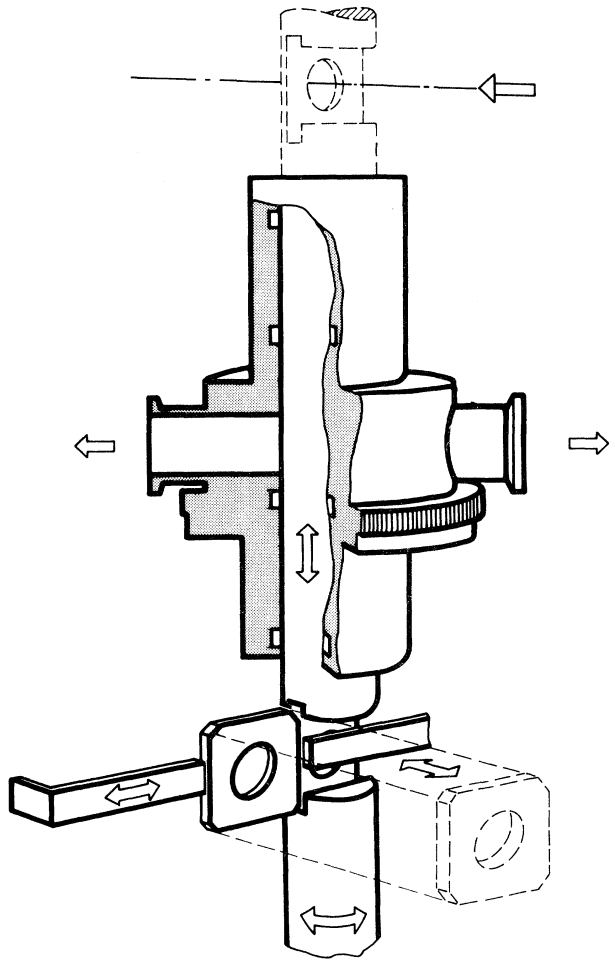

FIG. 4. Diagram of a sample exchanger for nuclear track irradiations. (See footnote 5.) The track-recording material (maximum size $50\times50\times1$ mm^3) is mounted on a sample holder (outer size $64\times64\times10$ mm^3). A vertically sliding, rotatable, slotted cylindrical piston transports one sample holder at a time from air (bottom) over a pumping station (middle) into the irradiation position within the vacuum system (top). After irradiation at a selected angle and areal dose (ions/cm^2), the piston is retracted and the sample holder is replaced by a fresh one from up to twenty sample holders stored in a magazine. During the irradiation and throughout the 1-min replacement cycle, four lubricated sealing rings, arranged at distances slightly larger than the size of the sample uptake slot, assure vacuum tightness.

B. Formation of the latent track

A very successful approach to understanding phenomena that occur in nature has been the concept of concatenated hierarchies, as, for example, the breakdown of solids into molecules, atoms, and elementary particles. In addition, several time-scale hierarchies must also be accounted for in the formation of nuclear tracks (Benton, 1970; Fleischer, 1981), namely:

Defect creation: The passing ion has a very short primary interaction time in the vicinity of the atoms of the solid (of the order of 10^{-17} s for a 5-MeV/nucleon ion which has a velocity of about 10% of the speed of light). The primary interaction is followed by an electronic collision cascade spreading out rapidly from the particle trajectory, which lasts more than a thousand times longer than the primary interaction ($\geq 10^{-14}$ s) and leaves behind a highly positively charged cylindrical plasma zone. In the case of organic polymers, in addition, many chemically activated molecules are produced outside this zone. In dielectric solids, the remaining charged-plasma cloud "explodes" via the electrostatic repulsion of the formed positive ions. This process is often referred to as the "Coulomb explosion" (Fig. 5). This triggers an atomic collision cascade, which in turn comes to a halt on a time scale that again can be stretched by a factor of about a hundred ($\simeq 10^{-12}$ s), leaving behind a cloud of interstitial atoms and vacancies. The radial range of the electronic collision cascade ($\simeq 100-1000$ nm) is 1 or 2 orders of magnitude greater than that of the atomic collision cascade ($\simeq 10$ nm).

Relaxation of atomic defects: Immediately after the passage of the heavy ion, the latent track core consists of a highly agitated zone with a density that deviates significantly from the matrix itself. The interstitial atoms and vacancies find themselves in intensely agitated surroundings corresponding to a locally confined "thermal spike" (Ollerhead *et al.*, 1980; Seiberling *et al.*, 1980); i.e., a very hot cylindrical zone of atoms in quasi-thermal-equilibrium (corresponding hypothetically to several thousand degrees centigrade). During cool down (10^{-10} s is an upper time limit), the atomic defects aggregate to an almost contingent string of "extended defects," the so-called track core (diameter $\simeq 10$ nm), surrounded by a

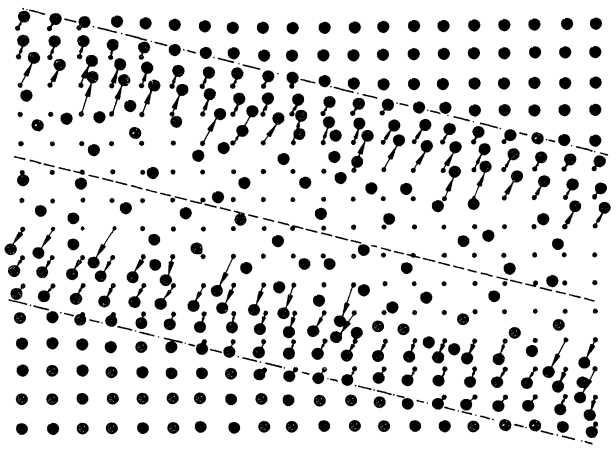

FIG. 5. Axial cut through a latent nuclear track in a crystal (schematic representation) (Hansen *et al.*, 1983). The penetrating ion creates a positive ion cloud around its path, which "explodes" by electrostatic repulsion. This leads to atomic displacements (arrows), the magnitude of which decreases with the original distance of the atoms from the ion path. A disordered zone results, with a core of decreased density surrounded by a sheath of increased density.

remaining cloud of point defects (Dartyge *et al.*, 1981). In organic polymers, the track core consists of a zone of drastically reduced molecular weight, corresponding to broken molecular bonds.

Relaxation of molecular defects: Finally, in organic polymers, farther away from the track core (in the track "halo"), chemically activated species (radicals) undergo secondary reactions on a time scale of seconds. Also, reactions with the surrounding atmosphere take place (especially with oxygen). They have typical time constants of weeks or months. Therefore, inorganic solids and organic polymers record different defects, confined to "tubes" of quite different sizes; in organic polymers the track core is additionally surrounded by a track halo (diameters $\simeq 10-100$ nm) with modified chemical properties, consisting of depolymerized and polymerized zones (Fig. 6).

Ab initio calculations (Paretzke, 1982) of the electronic collision processes yield the starting spatial distribution of the generated point defects and chemically altered molecules. Calculations to describe the successive long-term processes (the collision cascade and the relaxation of atomic and molecular defects) seem to tax the presently available simulation capabilities. A promising step towards overcoming this problem is the recently proposed homogeneous nucleation model (Dartyge *et al.*, 1981). Based on calculated original defect densities and on experimental defect mobilities, such a model may ultimately arrive at the final defect distribution and thus circumvent additional assumptions about intermediate stages and transient processes that cannot be observed directly. This approach is similar to the treatment of the photographic process as a phase-transition process (Granzer and Moisar, 1981).

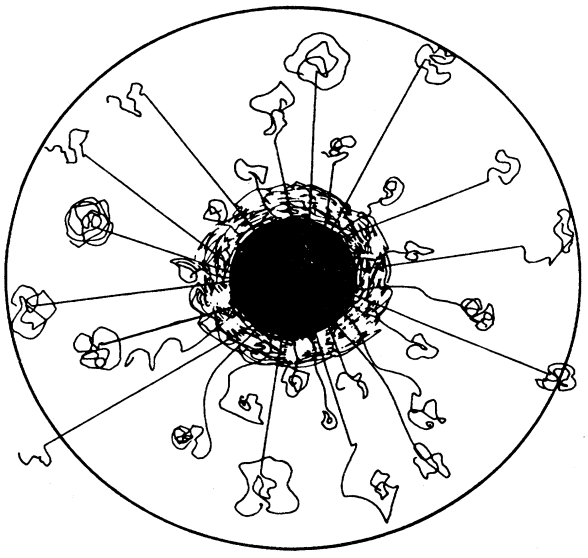

FIG. 6. Radial cut through a latent nuclear track in a polymer (schematic representation) (Chatterjee and Magee, 1980). The track core (innermost black circle) corresponds to the range of the atomic collision cascade and has a diameter of roughly 10 nm. It is surrounded by a much larger halo (outer encircled zone) with a diameter of roughly 100—1000 nm, corresponding to the electronic collision cascade. In polymers, a preferentially etching sheath of chemically activated molecules (diameter somewhere between 10 and 100 nm) exists between the track core and the track halo.

A series of different phenomena occurs between the irradiation of the sample and the preferential etching of the established latent tracks. The following methods can be used to observe them: x-ray, electron, and ion spectroscopies (Remillieux *et al.*, 1982), energy-loss and range measurements (Geissel *et al.*, 1980), optical absorption measurements from small defects (Perez *et al.*, 1976), magnetization and related properties (Heitmann *et al.*, 1978; Hansen and Heitmann, 1979, 1981), thermoluminescence (Edmonds and Durrani, 1979; Bangert *et al.*, 1979), electron spin resonance (Edmonds and Durrani, 1979; Teicher and Beserman, 1982), small-angle scattering of x rays (Dartyge *et al.*, 1981) and neutrons (Albrecht *et al.*, 1982) from latent tracks, track-sensitization and annealing measurements, observation of the track-etch threshold, of the track-etch ratio, and of the etched track itself (Fleischer *et al.*, 1975).

1. Energy-loss phenomena

> "The best known physical quantity relating to an etched particle track is the stopping power of the ion" (Chatterjee and Magee, 1980).

Each individual ion is a "power package" of unique energy density. On its way through the solid, the ion deposits per atomic layer more than a thousand times the energy required to ionize individual atoms. At the same time, the available kinetic energy of the ion is almost inexhaustible compared to the relatively small energy loss per atomic layer. The ion follows a very long (compared to atomic dimensions), almost linear trajectory through the solid until it finally comes to a halt. The penetration range depends on the mass and energy of the ion and on the atomic composition and density of the track-recording solid.

a. Stopping power

The stopping power of an ion, penetrating into a solid, is defined as the energy loss per unit length of path. Since stopping power is related to the damage remaining in the form of the latent track, any description of track structure usually has stopping-power theory as its starting point. At low ion energies, the energy loss is dominated by "nuclear stopping," corresponding to close encounters between the nucleus of the primary ion and the target nuclei. These "atomic collisions" lead to abrupt changes of the projectile energy and direction. At high ion energies, the energy loss is dominated by "electronic stopping," corresponding to interactions between the primary ion and the electrons of the target material. These electronic collisions lead to a smooth, quasicontinuous braking pro-

cess, leaving the projectile direction virtually unchanged. Electronic stopping increases at low energies approximately as $\sqrt{E}$, up to a maximum between about 1 and 10 MeV/nucleon (depending mainly on the penetrating ion), and decreases beyond this maximum approximately as $1/E$.

Different stopping-power theories have been developed for distinct projectile energy ranges (Lindhard *et al.*, 1963). If we follow a relativistic heavy ion on its path through the solid as it gradually slows down, we will encounter the following phenomena (Hepburn and Windle, 1980) (Fig. 7):

(1) The very fast ion is stripped of all its electrons almost instantaneously when entering the solid. In many cases (Fig. 8) its energy loss is too small to be registered in the form of a latent track. In organic substances, the emitted high-energy electrons may have ranges too long to lead to a sufficiently high defect density around the ion path to be registered. The energy loss per unit path length is roughly proportional to the square of the interaction time, i.e., inversely proportional to the projectile energy.

(2) As the ion slows down, its stopping power increases gradually and may exceed the threshold for track registration. Simultaneously, as it slows down, the ion gradually recovers its neutrality via electron capture, corresponding to a decreasing effective charge. Therefore, the stopping power reaches a flat maximum, somewhere between 1 and 10 MeV/nucleon specific ion energy, depending on the ion nuclear charge. As the ion slows down further, its stopping power decreases rapidly with the projectile velocity. The ion may ultimately fall short of the registration threshold for a second time.

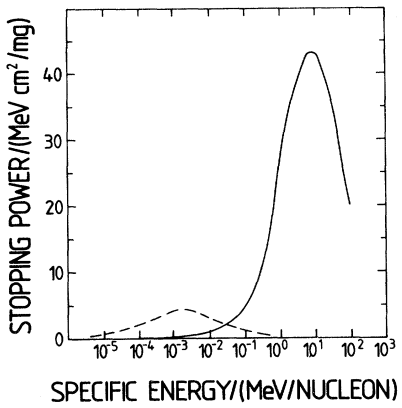

FIG. 7. Nuclear and electronic stopping of a heavy ion in a solid (here, stopping power of ^{208}Pb ions penetrating through gold), (Geissel, 1982). *Nuclear stopping* (dashed curve) is dominant at small specific energies, below about 0.01 MeV/nucleon. It corresponds to discrete encounters between the penetrating ion and the atoms of the solid, exchanging substantial fractions of the ion energy, and is responsible for most of the angular and range straggling of the penetrating ion. *Electronic stopping* (solid curve) prevails at high specific energies, beyond about 0.1 MeV/nucleon. It corresponds to a quasicontinuous transfer of energy between the penetrating ion and the electrons of the solid, yielding a straight ion path.

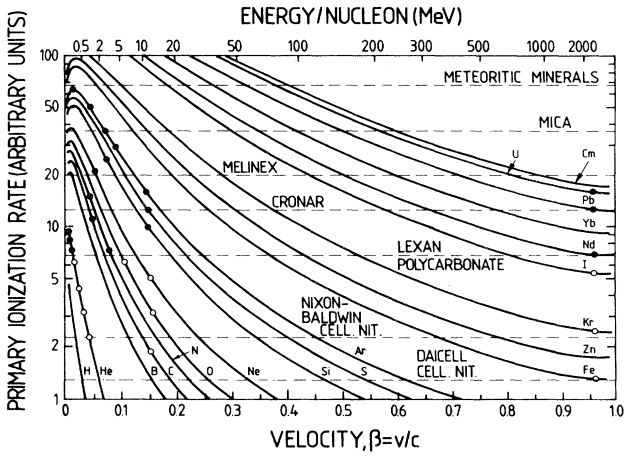

FIG. 8. Primary ionization rate of several different ions in solids (Fleischer, 1981). The primary ionization rate corresponds to the number of secondary ions created per unit path length along the path of the penetrating (primary) ion. It has roughly the shape of the electronic stopping function (Fig. 7) and is a measure of the density of the developable damage along the latent track. Track-recording materials can be ranked in order of minimum primary ionization density required for obtaining developable tracks (dashed horizontal lines), so that the sensitivity increases from the top to the bottom of the figure. For example, Lexan® polycarbonate yields etchable tracks (black circles) above and nonetchable tracks (open circles) below about seven arbitrary units of the primary ionization rate, independent of the penetrating ion.

(3) For a certain distance close to the end point of the ion trajectory, corresponding to the so-called "range deficit" of etched tracks, the energy loss may be too small for track registration if the threshold for registration is high enough.

(4) So far the ion has decelerated quasicontinuously due to the smooth braking power of the comparatively light electrons. Close encounters with nuclei of the solid were rare events. Therefore most of the ion path has been a straight line up to here. However, at very low ion energies, of the order of 1 μm before the ion reaches its final stopping point, nuclear stopping becomes important. This process deflects the ion from its straight path in an erratic way, corresponding to a "bumpy" braking process, leading to the exchange of substantial fractions of the total ion momentum and energy during each atomic collision. Nuclear stopping yields very dense secondary atomic collision cascades, which do register even in semiconductors and metals. In metals, nuclear stopping is the only important mechanism for radiation damage.

As a rule of thumb, nuclear stopping becomes dominant whenever the specific energy of the ion, in keV/nucleon, falls below a few keV/nucleon, regardless of the material in which it moves (Dienes and Vineyard, 1957). In silicon surface-barrier particle detectors, nuclear stopping, in addition to ion-electron recombination,

yields a considerable fraction of the observed "pulse-height defect" (Martin and Stelzer, 1978) corresponding to an incomplete conversion of the kinetic energy of the ion into secondary electrons.

In crystals, it is possible to suppress nuclear stopping over a substantial fraction of the range by "ion channeling" (Gemmel, 1974; Datz and Moak, 1982). Therefore ion channeling may be used in the future to generate extremely parallel etched track channels. An instance of this effect was reported for fission fragments in mica minerals in the form of etch-range variations (Belyaev *et al.*, 1979). Depending on the crystal orientation, etched track length variations of 17% were observed.

Few experiments using ions with atomic number Z greater than 20 and specific energies greater than 1 MeV/nucleon have been performed up until now (Geissel *et al.*, 1980, 1981, 1982b) and only very few experiments using relativistic heavy ions (Tarle and Solarz, 1978; Salamon *et al.*, 1981; Ahlen *et al.*, 1982; Ahlen and Tarle, 1983). The latter experiments showed higher-order effects in the conventional specific-energy-loss formula, increasing in magnitude with the nuclear charge Z. The effect was very large for uranium at specific energies of the order of GeV/nucleon. In response to a lack of data on experimental stopping powers for heavier ions at higher energies, scaling laws and the concept of the "effective charge" were developed to generate stopping-power tables (Northcliffe and Schilling, 1970; Ziegler, 1977; Hubert *et al.*, 1980), which have been steadily improved during the last decade and now reproduce data to within 20%.

To obtain an approximate value for the stopping power S in units of MeV/nucleon for a target of an "areal mass density" of 1 mg/cm^2, one can use (Schmidt-Boecking, 1978)

$$S \simeq 0.14(Z_p^{*2})(Z_t/A_t)\ln(250E/Z_t) , \quad (1)$$

where the effective charge Z_p^* is

$$Z_p^* = Z_p[1-\exp(-6E^{1/2}/A_p^{2/3})] , \quad (2)$$

and S is the stopping power of the projectile in MeV/nucleon per mg/cm^2, E is the projectile energy in MeV/nucleon, Z is the atomic charge number, A is the atomic mass number, p denotes the projectile, and t denotes the target. This equation gives values which are correct to 10% for light ions and target atoms and can deviate by a factor of 3 for arbitrary ion-target combinations.

b. Range

The integral of the inverse stopping power (i.e., the integral of the "penetration" power) is a measure of the range R of the particle in the solid:

$$R = -\int_0^E (dE/dx)^{-1} dE , \quad (3)$$

which corresponds approximately to the length of the generated nuclear track; nuclear stopping is responsible for most range straggling.

As a rule of thumb, a heavy ion of 0.1-MeV/nucleon specific energy has a range in solids of about 1 μm, a heavy ion of 1 MeV/nucleon about 10 μm, and a heavy ion of 10 MeV/nucleon about 100 μm. The ion range can be roughly approximated by the empirical formula (Dienes and Vineyard, 1957)

$$R = CE^{\gamma} , \quad (4)$$

where C and γ have to be empirically determined. Better approximations (Benton and Henke, 1969; Güttner *et al.*, 1977) require physics-related model functions or simply a greater number of fitting parameters.

2. Atomic defect creation

a. Coulomb explosion

Electrostatic repulsion between the positive ions created along the ion path is the driving force of the so-called "Coulomb explosion." Evidence for the occurrence of such an ion explosion mechanism in dieletrics can be derived from molecular systems (Groeneveld *et al.*, 1980; Frischkorn *et al.*, 1982). The average energy loss per atomic layer may range between 10^3 and 10^4 eV per atomic layer, well above the required threshold energy of about 50 eV per created pair of defects.

Previously, sputtering was thought to be due exclusively to atomic collision cascades, close to the end of the ion range, where nuclear stopping prevails. This description is valid only for metals, where the phenomenon of ion explosion is completely absent. In dielectrics, the ion explosion leads to enhanced sputtering (Seiberling *et al.*, 1980), which is not described by previous sputtering theories (Siegmund, 1981).

A necessary condition for the occurrence of an ion explosion in insulating solids is their low electron mobility. This is a characteristic property of dielectrics. In metals, mobile electrons provide "virtually an instantaneous repair kit" (Hepburn and Windle, 1980), which neutralizes the charged plasma cloud around the ion path. More recently, the existence of an ion explosion in dielectrics and its absence in metals was directly proved (Knippelberg *et al.*, 1982); the sputtered ion yields from metallic and dielectric surfaces correlated directly with nuclear and electronic stopping, respectively.

Displacement cascades can be observed in metals only at the end of the ion range, where nuclear stopping prevails. The resulting disorder anneals out at a relatively low temperature, due to the high mobility of defects in metals. Metals are therefore very litttle susceptible to radiation damage.

b. Resulting primary defects

During the 1950s, nuclear reactor technology was the strongest motivation for radiation damage studies in metals (Dienes and Vineyard, 1957). In recent times, the

problem of nuclear waste disposal in the form of glassy compounds has replaced this incentive with the study of defects in insulators (Dran *et al.*, 1980). Up until now, point defects and low-order aggregates have been investigated almost exclusively, in part because of the low ionization density of the available radiation, and in part because optical absorption spectra of low-order defects are easy to interpret (Perez *et al.*, 1976).

As a result of a heavy-ion-induced ion explosion, a collision cascade spreads radially from the projectile trajectory and leaves behind a densely populated cloud of defects. The cloud consists at first of an identical number of complementary defects in the form of interstitial atoms and vacancies. This dense defect distribution is far from thermal equilibrium, and the dielectric can be considered heavily supersaturated with these point defects.

3. Defect rearrangement

a. Relaxation of atomic defects

Point defects have a very high mobility compared to larger defect aggregates. Thereby interstitial atoms and vacancies can annihilate by mutual recombination. Another possibility is the formation of aggregates, whereby the interstitial atoms have the tendency to aggregate on "outer" surfaces and the vacancies on "inner" surfaces of the solid. This corresponds to repulsive forces between interstitial atoms and attractive forces between vacancies. The latter forces can be understood in terms of the surface energy of two tiny cavities, which is reduced by the merging process. During the "thermal spike," which corresponds to a rapid heating followed by a rapid thermal quenching, the diffusion process is drastically enhanced within a small "tube." This leaves a cloud of unreacted point defects around a frozen (immobilized) distribution of larger defect aggregates. Formation and growth of a new phase require that the system be supersaturated with the components of the new phase.

According to nucleation theory (Zettlemoyer, 1969) a condensation process consists of different successive stages. Transmission electron microscope studies reveal that clusters are the evolutionary end product of the damage induced along the track. Their formation has been tentatively associated with a condensation process (Ruault *et al.*, 1982). In addition, periodic constrictions of latent tracks have been observed in polyethylene terephtalate (Albrecht *et al.*, 1981). They have been tentatively attributed to the action of surface tension, similar to the gradual formation of discrete droplets from a contingent filament of water. Therefore, for an originally homogeneous defect distribution confined within a cylinder, the following agglomeration stages can be assumed.

(1) Subcritical stage. Formation of unstable small aggregate "embryos" of various sizes, which may decay again into point defects.

(2) Nucleation. The largest aggregates reach a critical size and form a condensation nucleus.

(3) Growth. Growth of the condensation nuclei at the expense of the subcritically sized embryos, creating a depleted zone around the growing aggregates in the form of a "capture" zone. This process leads to a linear array of extended defects.

(4) Coalescence. For a sufficiently high defect concentration, close neighbors touch each other, coalesce, and form a contingent string of defects.

(5) Periodic constriction. A contingent string of defects is subject to surface tension and tends to reduce its surface energy. This may lead to periodic constrictions of the latent track (Albrecht *et al.*, 1981), or ultimately to the formation of discrete defect droplets.

b. Stored energy

Stopping power is a rough measure of the damage created along the ion trajectory. Only a small fraction of this energy input, generally assumed to be of the order of a few to several tens percent, is actually stored in the close vicinity of the ion trajectory and can ultimately lead to a latent track. Still, the locally deposited energy density is higher by several orders of magnitude than in the photographic process. This stored energy can be released during annealing and measured, e.g., by differential scanning calorimetry (Turi, 1981).

Maximum track damage occurs at a lower energy than would be inferred from the energy-loss curve. This is due to the fact that fast ions yield a higher fraction of fast electrons leaving the core zone of the track without interactions. Therefore the track-forming capability of fast ions is smaller than that of slow ions of the same specific energy loss.

Several approaches exist, based on the energy-loss theory, for describing the amount of energy stored along the latent track. The observable effect (i.e., the track-etch rate) has been related to the energy deposited by electrons within a narrow cylinder of arbitrary diameter (Katz and Kobetich, 1968); the energy deposited by electrons below a certain maximum energy ("restricted energy loss"; Benton, 1970); and the total number of created electrons ("primary ionization"; Fleischer, 1981).

In polycarbonate, only the last approach (primary ionization) is a compatible process for describing the track-etch threshold (Fleischer, 1981; see Fig. 8). The primary ionization density J is given by (Fleischer, 1981)

$$J=\frac{C_1C_2Z_{\text{eff}}^2}{I_0\beta^2}[\ln(W_{\max}/I_0)-\beta^2-\delta+K]$$

$$\rightarrow J\propto Z^2/\beta^2 \text{ for } \beta\rightarrow 1\ , \tag{5}$$

where I_0 is the ionization potential of the most loosely bound electrons of the recording material, $W_{\max}=2mc^2/(1-\beta^2)$, m is the electron mass, c is the velocity of light, $\beta=v/c$ is the projectile velocity in units of the velocity of light, δ is a polarization correction for

relativistic velocities, K is a recorder-specific constant, $C_1=2\pi ne^4/mc^2$, n is the number of electrons per cm^3, e is the electronic charge, C_2 is the fraction of electrons in the most loosely bound state, and Z_{eff} is the effective charge,

$$Z_{\text{eff}}=Z[1-\exp(-130\beta/Z^{2/3})] , \tag{6}$$

where Z is the atomic number of the particle.

The primary ionization density J has roughly the shape of the electronic stopping-power curve of the penetrating ion (cf. Fig. 7) and is a measure of the density of the developable damage along the latent track.

c. Track-etch threshold

The most significant property of a track recorder is its track-etch "threshold," which is the minimum primary ionization required for the formation of an etchable track. Although the track-etch threshold cannot be defined in a more rigorous sense than, for example, the threshold of a rectifying diode, it is governed by a well-defined power-law function (Somogyi *et al.*, 1976) leading to an abrupt change of etched track visibility within a small margin of primary ionization variation.

Track-recording materials can be ranked in order of increasing sensitivity. The spectrum of existing materials ranges from very radiation-resistant crystals that do not even register uranium ions at any energy (at least, with respect to their track etchability) to very track-sensitive polymers, recording even fast protons at high energies beyond their energy-loss maximum, up to about 20 MeV/nucleon. Below the threshold, the defects are more or less discrete on an atomic scale, while they form a string of contiguous defects above that threshold. In dielectric crystals, the threshold is directly related to thermal conductivity (Siegrist and Balzer, 1977). Heat conductivity, in turn, is related to the atomic binding energies within the crystal, as long as the electric conductivity is low. No tracks have been observed, up until now, in crystals with very high thermal conductivity, such as MgO, Al_2O_3 (sapphire), and diamond. One reason for this resistance could be the immobilization of defects in these hard crystals, before they can migrate to and merge with larger aggregates, due to the much shorter duration and lower "temperature" of the thermal spike. The density of such frozen defects in crystals with high heat conductivity (i.e., high atomic binding energy) can be very high. A catastrophic stored-energy release has been observed for neutron-irradiated diamond at very high doses (Dienes and Vineyard, 1957).

d. Track annealing

Latent tracks can be stored for a quasi-infinite time at room temperature. There exist terrestrial and extraterrestrial minerals and glasses that have stored nuclear tracks for millions of years (Fleischer *et al.*, 1975). However, if the temperature is sufficiently high, the radiation-produced atomic defects are capable of moving around. Latent tracks, in inorganic crystals and glasses, correspond to a frozen disequilibrium which can be restored at elevated temperatures. In this way the damage can be altered and the latent track can ultimately be erased in most inorganic materials.

First the interstitials, then the vacancies become mobile with increasing temperature. The corresponding activation energies are of the order of eV, typical for point defects in solids. It is also possible for both kinds of point defects to be trapped by impurity atoms or by crystal dislocations. Moreover, complementary point defects can annihilate mutually by recombination. Point defects diffuse through the crystal lattice until they encounter traps, where they are immobilized. At much higher temperatures, the extended defects disappear by absorbing or emitting point defects.

The most successful approach to describing track annealing is based on the diffusion of elementary point defects. According to this assumption, the defects have a certain activation energy for recombination. In close analogy with chemical reaction rates, such a process is governed by an Arrhenius equation:

$$t=\text{const}\exp(E_0/kT) , \tag{7}$$

where t is the annealing time for the point defect, E_0 is the activation energy for recombination, k is the Boltzmann constant, T is the temperature in K.

A more realistic model assumes that defects of different sizes have different stabilities. This more elaborate approach, directed at the age-temperature relationship of natural tracks in minerals, assumes different activation energies E_i for defects of different sizes (Naeser and Faul, 1969; Gold *et al.*, 1981; Märk and Märk, 1982).

Although track etching can be suppressed even after annealing at relatively low temperatures, the latent tracks themselves are much more stable and can still be observed at much higher temperatures. For example, track etching in mica is completely suppressed after annealing for 1 h around 550 °C. But the latent tracks can still be observed at much higher temperatures by transmission electron microscopy (Price and Walker, 1962). During annealing, the latent tracks gradually become intermittent and finally vanish between 800 °C and 900 °C. These observations are consistent with the recently developed "gap" model (Dartyge *et al.*, 1981). According to this model, the etchable track corresponds to a statistical array of extended defects surrounded by a cloud of point defects, whereby track etching requires a string of contiguous defects. For partially annealed tracks, therefore, etchability is dominated by the much more stable extended defects. The statistical distribution of the distances amongst the extended defects as well as range straggling, causes different etched track lengths even for monoenergetic, monoisotopic ion beams. This contribution to track length variations is dominant close to the track-etch threshold. During annealing, the extended defects are much more stable than the point defects, leading to an interruption of the preferential etch attack whenever the etching medium reaches a "gap."

This offers the possibility of fine-tuning the track registration threshold by partial track annealing.

Track annealing is quite closely related to track formation, at least with respect to the temperature-activated aggregation of small point defects into larger extended defects. Both processes are governed by diffusion processes. However, they occur on quite different time scales. Further light should be shed on the annealing process by observing the release of stored energy during annealing.

e. *Relaxation of molecular defects*

Organic polymers are much more susceptible to radiation damage than most inorganic solids. This property is due more to the track halo than to the track core. The electronic collision cascade produced in organic polymers leaves behind chemically active species (radicals), which are located mostly in the track halo. These species are ready to react with each other and with small molecules, especially oxygen molecules (Gruhn and Benton, 1982) that are capable of diffusing rapidly through the polymer network. The primary effect of the electronic collision cascade on the polymer molecules can be either strand breaking of the backbone of individual molecules or cross linking between neighboring molecules via the activation of the side groups. In lithography, the prevalence of strand breaking or cross linking is used to characterize the recording resist as "positve" or "negative," respectively (Fig. 9). The response of the resist to the developing solution is defined as "positive" if the irradiation increases its dissolution rate. For a sufficiently high local dose, strand breaking leads to fragments with sizes that do not depend on the original molecular weight (Wittels, 1980). Cross linking, on the other hand, leads to larger molecules, the size of which is initially proportional to their original molecular weight, and for high doses yields a continuous giant molecule. Both processes are counteractive and depend on the specific chemical properties of the polymer.

Figure 10 shows the distinct existence of a track "core" and track "halo" in polycarbonate material (Schnoor *et al.*, 1982). In spite of the radially decreasing energy density, the mutually opposing effects of strand breaking and cross linking in the track "halo" lead to a flat step in the radial etch ratio. This corresponds to a sheath of practically constant radial etch rate.

4. Track sensitization

Track-etch response depends on the environmental conditions before, during, and after irradiation with heavy ions, especially on the influence of other types of ionizing radiations, temperature, and environmental oxygen. The radiation used for track sensitization should have simultaneously a high penetration range and a low ionization density. For example, uv light, γ radiation, or high-energy proton beams can be used for creating a quasihomogeneous damage density throughout the volume of the solid. This type of irradiation is characterized as a "volume irradiation" of the solid. Quite different approaches should be followed for inorganic solids and for organic polymers.

For crystals and glasses, immobilized "frozen" point defects can be created within the total volume by irradiation with high-energy protons or gamma rays. The build-up of defects in very "hard" materials, such as diamond, can involve displacements of about half of the atoms of

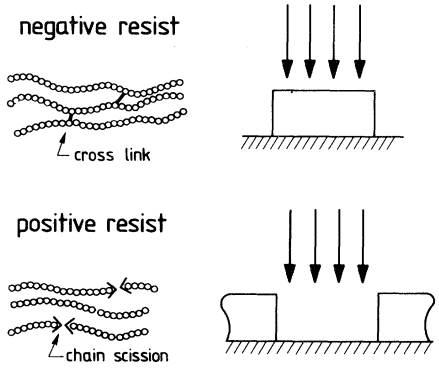

FIG. 9. Basic mechanisms for the radiation response of polymer films (Hall *et al.*, 1980). *Left side*: irradiation-induced molecular changes. The prevalence of strand breaking or cross linking characterizes the recording resist film as "positive" or "negative," respectively. *Right side*: Macroscopic response of the resist film after irradiation and development. Good etchable track recorders should be of the "positive" resist type, in which chain breaking prevails. Such track recorders have an increased dissolution rate in the vicinity of the ion path.

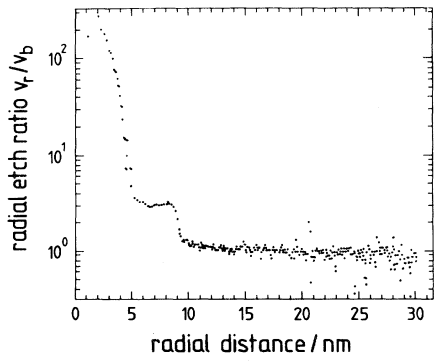

FIG. 10. Radial etch ratio of a single track in a polycarbonate foil (Schnoor *et al.*, 1982)—the ratio of the radial etch rate v_r to the bulk etch rate v_b, as a function of the radial distance from the track axis. The observed values correspond to the time dependence of the electrical conductivity through a single pore during the etching process. (1) The track "core" (up to 5-nm radius) has a drastically enhanced etch ratio, varying rapidly as a function of the radial distance from the track axis. (2) The track "halo" (between 5- and 10-nm radius) has a much smaller, but still significantly enhanced etch ratio, corresponding to a sheath with almost constant radial etch rate.

the solid (Dienes and Vineyard, 1957). It should be possible to mobilize these "frozen" defects by a postirradiation with heavy ions during the "thermal spike" time regime. In this way, the already existing defects may aggregate to form a stable nuclear track, even in cases where no stable tracks have been observed up until now without pre-irradiation.

A similar "volume irradiation" with uv light can be used to sensitize the track recorder in the case of organic polymers.

Every polymer is characterized by a specific dose-response curve, defining its behavior under the influence of ionizing radiation (Wittels, 1980). This leads to a change in molecular weight that is inversely proportional to its dissolution rate in a solvent. Sizable effects occur normally at doses of the order of Mrad. Polymethylmethacrylate (PMMA), one of the most commonly used microlithographic resist materials, has a scission rate of about 1 scission per 100 eV absorbed energy (Willson *et al.*, 1982). Such a dose-response curve exists, in principle, for any polymer (Fig. 11). In analogy to photolithography, "response" is defined as that fraction of a polymer film which remains (negative resist) or is removed (positive resist) after a volume irradiation at a given "dose" (i.e., deposited energy density), followed by a given development (dissolution) procedure.

A "negative" resist will polymerize increasingly with increasing energy density, becoming less soluble in the developing solution, causing a protrusion. However, at a sufficiently high dose, a "positive" resist behavior appears, in such a way that the resist will progressively decompose with increasing energy density. Since chain breaking always prevails in the track core, one can assume

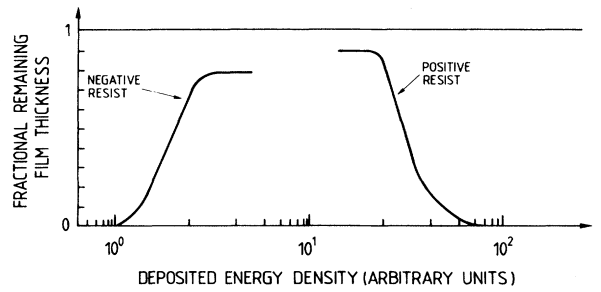

FIG. 11. Schematic dose-response curve for organic polymers (Wittels, 1980). *Response* is defined as the fraction of the polymer film remaining after a "volume irradiation" at a given deposited energy density ("dose") followed by a given (dissolving) development procedure. A "volume irradiation" is defined as a homogeneous energy deposition throughout the film thickness. It induces primarily either cross links (left curve) or chain scissions (right curve). *Radiation sensitivity* is defined as the negative slope of the dose-response curve and depends on the pre-irradiation history of the polymer. The track etchability of a polymer can be "sensitized" by a pre-irradiation which sets the "working point" immediatly below the slope corresponding to the prevalence of chain scission (right curve). In this case, any further radiation damage will lead to an increased dissolution rate along the latent track.

that in cross-linking materials a highly polymerized sheath exists around the track core, that can withstand the attack of the etching medium and thus impedes track etching. In this case, it should be possible to improve track-etching ratios dramatically by subjecting the total volume of the track recorder to a homogeneously ionizing radiation (e.g., uv light or γ radiation) before (or after) the irradiation-induced track formation. Such an irradiation shifts the "working point" of the dose-response curve to a higher dose value. In this case, the "working point" corresponds to the level of the volume dose without the heavy-ion irradiation. Therefore the threshold of track etchability can be exceeded even in cases where no etchable track can be observed without a "volume irradiation." The shifting of the "working point" can be compared to the shifting of the working point of a rectifying diode by applying a bias voltage, leading to a change in the current/voltage characteristics.

For example, the track-etching properties of polycarbonate, which even when untreated is one of the best track recorders, can be futher improved by using a uv postirradiation simultaneously with an oxygen treatment (DeSorbo, 1979). Untreated polycarbonate has an etch-rate ratio v_t/v_b of about 10^3, using an aqueous sodium hydroxide solution as etching bath. It is inherently a "positive" resist material, in which chain-breaking processes prevail (see Fig. 11). The track-to-bulk etch ratio of polycarbonate can be increased by about a factor of 10, using a uv irradiation in a wavelength range between 300 and 400 nm (Guillot and Rondelez, 1981). This kind of irradiation has produced calibrated pores as small as 10 nm in diameter.

5. Track response function

Latent tracks consist of a heavily damaged core zone, which in organic polymers is surrounded by a halo with increased chemical reactivity, due to secondary- and higher-generation electrons ejected from the ion path (Chatterjee and Magee, 1980). Track etching in crystals and inorganic glasses is dominated by changes in the core zone. In organic polymers it will depend additionally on chemical changes in the track halo.

One approach to describing track structure in organic polymers is based on the radial distribution of local dose, deposited by secondary electrons in concentric cylinders around the ion trajectory (Fig. 12) (Katz and Kobetich, 1968; Fain *et al.*, 1974). This model has been successfully used to describe track structure in radiobiology and radiation detection (Katz, 1978). Its local dose calculations are based on semiempirical formulas for secondary electron emission, energy deposition by electrons, and range of electrons in solids. In this model the local etch response is set equal to the observed global etch response for homogeneously ionizing gamma radiation. The global etch response can be described, independently, on the basis of target theory. It is assumed that the track recorder is composed of sensitive subunits (grains) which require the passage of a certain minimum number of elec-

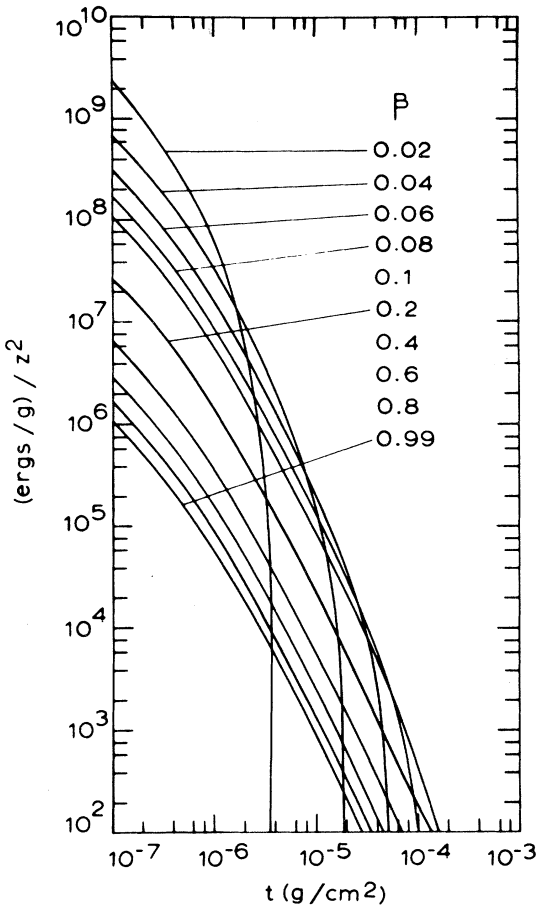

FIG. 12. Radial energy deposition around an ion path, due to electrons (Katz and Kobetich, 1968). With increasing ion velocity, the deposited energy due to secondary electrons decreases simultaneously with the electronic stopping power. At the same time, the energy deposition becomes locally more diffuse (i.e., less concentrated around the ion path); therefore in organic materials the available fraction of the deposited energy density due to electrons, which may induce developable radiation damage in the vicinity of the ion path, decreases with increasing ion velocity. The curves are calculated for an arbitrary ion of nuclear charge Z of, relative velocity $\beta=v/c$ (given in units of the velocity of light), in silicon dioxide (quartz). The radius t is given in units of the areal mass density (g/cm^2).

trons to become developable. The minimum number of required passages ("multihittedness") characterizes the response function of the track recorder.

C. Track etching

Latent tracks consist of metastable or permanently changed zones with increased chemical reactivity (Fig. 13). The etching transforms the latent track into an unerasable structure by supplying the required amount of energy for the enlargement process. This chemical "amplifier" is extremely sensitive. It compares favorably even

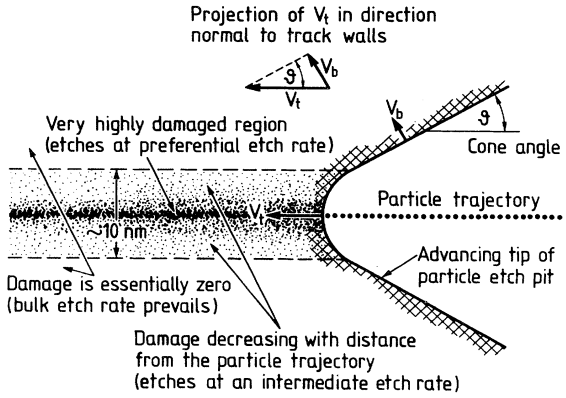

FIG. 13. Schematic model for track etching on a submicroscopic scale (Henke and Benton, 1971).

with very sensitive electronic amplifiers. Etched tracks of 100 μm diameter, for example, have a volume that is 10^8 times larger than the volume of the original latent track. In contrast to other two-stage techniques, such as the photographic process, even one single particle is sufficient to create a developable damage in the recording material. In principle, any phase transformation destabilizing the system can serve as an amplifier for the existing inhomogeneities. Therefore track etching, that is, removing material, is only one of many possible ways to reveal latent tracks. There exist several other ways to "decorate" latent tracks, of which only very few have been considered up to now, for example, additive processes such as track grafting (Somogyi *et al.*, 1979), or transformation processes such as the silver chloride recorder (Haase *et al.*, 1977). Other possible schemes are sputter etching (Krumme *et al.*, 1977) and reactive ion etching. In other cases a development process may even be completely unnecessary to produce a global property change. This is the case for ferrimagnetic iron garnets (Krumme *et al.*, 1977; Heitmann *et al.*, 1978). Up to now, however, chemical etching has been the method most frequently used.

1. Track-etch requirements

Because of the very high deposited energy density of heavy ions, practically all dielectrics (i.e., almost any insulating solid) can record heavy-ion tracks. A very broad spectrum of suitable materials and development schemes exists, with different recording and development characteristics. This is quite a different situation from that of photography, which still depends almost exclusively on silver halides. In view of this wealth of materials, how do we choose a suitable track-recording process? Several criteria must be met for obtaining an etchable track (Fleischer *et al.*, 1975). Any systematic development of a new track-recording process must follow certain guidelines (Cartwright *et al.*, 1978; Fleischer, 1981; O'Sullivan *et al.*, 1982). A good recording material should fulfill the following conditions:

Homogeneity. Etching is an extremely sensitive chemi-

cal "amplifier" for any variation in density or composition. It will reveal any previously existing inhomogeneities as well as the latent tracks. Such "background noise" may conceal the etched tracks. Therefore the track recording material should be as homogeneous as possible.

Absence of polycrystallinity. Chemical attack is extremely sensitive to crystallographic orientation. Crystal grains of different orientation, encountered along the etching track, will etch differently. A good track recorder should therefore be free of regimes with different orientations corresponding to different etch rates. This requirement is fulfilled by ideal single crystals and by amorphous solids, i.e., glasses. In glasses, the formation of microcrystals can be inhibited by (a) rapid quenching from the melt, (b) glass-forming substances (only for inorganic glasses), (c) plasticizers that keep the molecular chains at a safe distance from each other, preventing crystallization (only for organic glasses; Tarle *et al.*, 1981).

Radiation sensitivity. The energy density required to induce a stable, irreversible phase change along the ion path should be as small as possible. The new phase should have distinctly different chemical properties from the bulk material.

(a) In the case of crystals and inorganic glasses, the interatomic binding energy should be as small as possible. A global measure of the interatomic binding energy of dielectric solids is their mechanical strength. In dielectric crystals, the track-etch threshold is proportional to thermal conductivity (Siegrist and Balzer, 1977).

(b) In the case of organic polymers, chain breaking should prevail over cross linking. The required amount of energy per chain rupture should be as small as possible. Gaseous products of radiolysis released around the latent track and collected bubbles along the track seem to influence particle track etching (Lück, 1982), in such a way that etch attack occurs predominantly at the surfaces of these "free reaction volumes." This is attributed to the fact that hydrated ions, for electrostatic reasons, prefer to remain in the high-dielectric-constant medium, water, rather than pass into the tight, low-dielectric-constant medium, i.e., the polymer.

Phase instability. A characteristic property of good track-recording materials is their inherent phase instability. This leads to a stable new phase along the ion path, with distinctly different properties. An example of this type is the silver chloride recorder. Technologically promising are inherently unstable glasses that are supersaturated with metals (e.g., lead, copper, silver, gold; Haase *et al.*, 1978). Another example of an inherently phase-unstable system is the recently proposed "unzipping molecule" (Wilson *et al.*, 1982). This molecule decomposes into purely gaseous compounds upon one single chain rupture, circumventing the etching process completely. The size of the "unzipping molecule" terminates the development process at a predetermined dimension. Therefore this system may become the basis of a future self-developing, self-terminating process.

Existence of a suitable etchant. Track etching is a chemical process governed by several mutually interdependent parameters, like temperature, concentration, and chemical reactivity of the various components. This is the reason why finding a suitable track etchant has remained, up until now, mostly an empirical science in which the fundamental processes involved are largely unknown. Accordingly one aims roughly at optimizing the etch selectivity, surface activity, and viscosity of the etchant.

(a) Selectivity. The etchant should be capable of "distinguishing" between regions of different chemical properties. It must provide just the right amount of chemical attack: ideally, its chemical potential should be just sufficient to dissolve the irradiated zone and stop at the virgin material. A dislocation-selective etchant must be found in the case of inorganic crystals and glasses, which preferentially removes atoms from sites of reduced binding energy. On the other hand, an etchant must be found, in the case of organic polymers, that can degrade the molecules at the liquid-solid interface slowly and carefully. The degradation should occur solely by bond breaking and without swelling or dissolving the matrix. Consequently, the etchant must not be a good solvent for the polymer. A nonswelling selective etchant will preferentially remove fragments of reduced molecular weight in the vicinity of the track core.

(b) Surface activity. The etchant should remove or disintegrate passivated surface layers formed by chemical-reaction products. Surface-active chemicals improve the etching conditions by removing such passivated surface layers. To this end one sometimes adds minor amounts of a polar organic solvent (methanol, ethanol, etc.) to the etchant, or includes a not-degrading surfactant or detergent that is not degrading in the etching bath. Surface activity has to be maintained even in a strongly acidic or caustic environment. Another possibility would be to use, in addition to the track-sensitive etchant, a second etchant for degrading and dissolving built-up surface layers.

(c) Viscosity. The etchant should have low viscosity in order to permit efficient convective transport from the surface of the track recorder to the bulk of the etch solution. To some extent, viscosity can be decreased by diluting the etchant with a "passive" low-viscosity medium, for example, water, requiring prolonged etching times. Another approach is to increase the temperature, reducing the selectivity of the chemical attack.

2. Track-etch sensitive materials

A necessary condition for a track recorder is high ($>10^3$ Ω cm) electrical resistivity (Fleischer, 1981). This is the reason why most dielectrics record tracks and most semiconductors do not. Thin metallic films on dielectric substrates, however, behave differently: their resistivity can be several orders of magnitude smaller (Fleischer, 1981). The production of tracks in such films may be due to Coulomb-enhanced sputtering in the case of dielectric-substrate-supported metal films. Another possible explanation is the enhanced diffusion of the metal into the

defect zone of the latent track in the substrate. Etchable track recorders exist in the following three classes of dielectric materials.

a. Crystals

Most of the crystals investigated up to now are minerals found in nature. Of these, the ubiquitous mineral muscovite mica is commercially available[10] and could in principle be used even in future large-scale technical applications. Mica is used in electronics as a high-voltage insulating material up to 600 °C, mainly because of its good thermal and electrical properties. Since its etch rate normal to the cleavage plane of the crystal is virtually zero, mica has a very high relative track-etch ratio in hydrofluoric acid ($v_t/v_b \gg 10^4$). Very tiny holes (≤ 10 nm diameter), as well as very large holes (≥ 0.3 mm diameter), can be generated in mica, limited only by amplification of background crystal defects. Mineral inclusions, fission tracks, and crystal dislocations yield a natural background which cannot be completely annealed before the track irradiation. The etched-track hole has, because of the crystal structure, an approximately rhombic cross section with a minor angle of about 60°. A disadvantage of this material is that large variations of the lateral etch rate exist from batch to batch (of the order of 300% or more). Another drawback is its relatively low mechanical stability, which is characteristic of a soft and easily cleavable mineral. However, mica has been the most used model material for feasibility studies of various nuclear track applications up until now. Other natural crystals have been investigated mainly for their natural track records of cosmic rays and fission products (Thiel and Külzer, 1978).

As far as single-crystal recorders are concerned, solid-state technology provides several highly perfect single crystals which can be produced on a routine basis. Gadolinium gallium garnets, which are a spinoff from magnetic bubble technology, with an atomic composition of $Gd_3Ga_5O_{12}$, are an example. Garnets provide a very high mechanical and thermal stability up to 900 °C. They also provide a wide range of possible compositions with different etch properties (Thiel *et al.*, 1978), allowing an ion of one element to be replaced by another ion of similar size. For example, gadolinium may be replaced by another rare-earth element, and gallium may be replaced by iron. The material has an extremely low dislocation density. A disadvantage of the material is its relatively high cost in comparison to mica.

b. Inorganic glasses

One of the most abundant isotropic materials of modern civilization is regular soda-lime glass. This very cheap material offers a low but highly reproducible etch ratio for highly ionizing particles (e.g., full energy fission fragments) of the order of $v_t/v_b \simeq 2$. On this basis it appears to be a promising candidate for a breakthrough in practical applications, for example, in surface texturing that could increase the adhesion or lower the optical reflection coefficient of technical glass.

Another promising candidate for a technological application is the very homogeneous and isotropic phosphate glass (Aschenbach *et al.*, 1974). For highly ionizing heavy ions, phosphate glass has an etch ratio v_t/v_b of the order of $\simeq 10$. For prolonged etching and sufficiently low areal dose, the tracks can be easily etched to spherical sections of relatively large diameter (≥ 200 μm). Metalized multispherical surfaces may offer interesting optical reflectance properties for future applications.

c. Organic polymers

The development of track-etch recipes for polymers has involved, up until now, only commercially available polymers (Roff *et al.*, 1971), originally designed for different purposes, as the track-recording medium. Any attempt to standardize track-etch processes has been hampered in the past by the wide variety of track-etch responses for identical formulations with different trade names and even for foils of different thicknesses purchased from the same company. Additionally, various additives used as uv stabilizers and plasticizers have a strong influence on their etch characteristics, while environmental effects, for example, oxygen from the surrounding atmosphere, can have a strong influence on the track-etch rate as a function of depth. Standardization of materials and developing procedures, therefore, is necessary for progress in this field, to enable different laboratories to compare results.

One very promising step in this direction is the material known as "CR39" (allyl diglycol carbonate) (Cartwright *et al.*, 1978), the now widely studied "Wunderwaffe" of nuclear track detection, which is commercially available as a "standardized" material.[11] It is a thermosetting, three-dimensionally cross-linked polymer with plasticizer additives, consisting of virtually one large molecule, which by definition can be attacked only by a degrading etchant and not by a solvent.

A very unconventional approach to creating a track-recording material with a built-in developer is the "unzipping" molecule (Willson *et al.*, 1982), a polymer molecule which, when subjected to a single radiation-induced bond scission or rearrangement, undergoes spontaneous, exoenergetic depolymerization, resulting in a complete reversion to monomer molecules. Its radiation sensitivity is proportional to the length of the polymer strand, thus enhancing the response to the original initiating event by a multiplicative factor that can be tailored to specific

[10]R. Jahre GmbH & Co KG, Lützowstr. 90, P.O. Box 3644, D-1000 Berlin 30, FRG.

[11]Pershore Mouldings Ltd., Pershore, Worcestershire WR102DH, UK.

needs. This is very similar to the sensitivity of silver halides in photoemulsions, which is proportional to their grain size. The unstable polymer polyphthalaldehyde (molecular weight about 10^5) was stabilized by capping the end groups at low temperature by an alkylating agent (Willson *et al.*, 1982). The resulting product was soluble in common organic solvents. Spin-coated, it provided a clear, isotropic, noncrystalline film that was stable up to 200 °C. When subjected to electron beams, x rays, and uv exposure, it gave high-resolution relief images without any development step. The relief images corresponded to approximately 10% loss in film thickness. An improved copolymer designed for greater efficiency in the initial radiochemical event yielded up to 60% loss in film thickness. Since heavy ions yield local radiation densities in nuclear tracks that are several orders of magnitude higher than those obtainable for electrons, uv, and x radiation, these "unzipping" polymers are very promising track recorders for the future.

Any future development of track-recording processes should benefit from the vast amount of information available in the field of radiation chemistry (Dole, 1973) and photoresist technology (DeForest, 1975), one of the cornerstones of microcircuit fabrication. Photoresists are readily available commercial products (Marshall, 1982) of high quality. They are organic molecules with specifically tailored chain-breaking and cross-linking properties, achieved by the proper selection of backbone and side branches of the molecule.

3. Etch recipes

The etching of a latent track in a given solid depends on the chemical nature of the etching medium, its concentration, the temperature, and the etch time. Efficient stirring or ultrasound agitation of the etch bath is necessary, in most cases, for a successful etching procedure. The main effect of this precaution is to prevent the buildup of etch products on the liquid-solid interface by convective transport. Since the dissolved track material may itself drastically influence the etching rates, stationary concentration conditions must exist throughout the duration of the etch process. Typical etch conditions for some track recorders are given in Table V.

Dislocation-sensitive etchants are widely applied in the field of semiconductor materials, to make crystal defects observable. On the other hand, nonselective smoothing etchants have been developed for chemically polishing crystal surfaces. The chemical polishing removes strains from the surface that were introduced by a mechanical prepolishing. The information accumulated in this field (Bogenschütz, 1967) will be a valuable source of future etching recipes for developing nuclear tracks in crystals and for smoothing their entrance aperture edges. Such

TABLE V. Typical etching conditions for some useful track recorders yielding microscopically observable etched tracks.

Material	Etchant	Temp.	Time	Reference
Crystals:				
gadolinium gallium garnet	25% HNO_3/25% CH_3COOH/50% H_2O	70 °C	30 min	Krumme *et al.*, 1977
muscovite mica	48% HF	20 °C	20 min	Blok *et al.*, 1974
quartz	(a) KOH (aq)	150 °C	3 h	Fleischer *et al.*, 1975
	(b) 48% HF	23 °C	24 h	Fleischer *et al.*, 1975
Glasses:				
lead phosphate glass	1 ml 70% HNO_3/3 ml H_2O		2–20 min	Fleischer *et al.*, 1975
phosphate glass	48% HF		5–20 min	Fleischer *et al.*, 1975
quartz glass	48% HF		1 min	Fleischer *et al.*, 1975
soda lime glass	(a) 48% HF		5 s	Fleischer *et al.*, 1975
	(b) 24% HBF_4/5% HNO_3/0.5% acetic acid		1 h	Fleischer *et al.*, 1975
Polymers:				
allyl diglycol carbonate	NaOH,KOH $\leq$ 40%	$\leq$ 70 °C		Amin and Henshaw, 1981
cellulose acetate	1 ml 15% NaClO/2 ml 6.25*N* NaOH	40 °C	1 h	Fleischer *et al.*, 1975
cellulose acetate butyrate	6.25*N* NaOH	70 °C	12 min	Fleischer *et al.*, 1975
cellulose nitrate	$\leq$ 16*N* LiOH,NaOH,KOH	$\leq$ 50 °C	$\leq$ 6 h	Hilderbrand and Benton, 1980
polyamide	(a)$KMnO_4$ (25% aq)	100 °C	1.5 h	Fleischer *et al.*, 1975
	(b)6*N* NaOH			Fleischer *et al.*, 1975
polycarbonate	6.25*N* NaOH	50 °C	20 min	Fleischer *et al.*, 1975
polyethylene terephtalate	6.25*N* NaOH	70 °C	10 min	Fleischer *et al.*, 1975
polyimide	$KMnO_4$ in H_2O			Fleischer *et al.*, 1975
polystyrene	(a) sat. $KMnO_4$	85 °C	2.5 h	Fleischer *et al.*, 1975
	(b) 10 g $K_2Cr_2O_7$/35 ml 30% H_2SO_4	85 °C	3 h	Fleischer *et al.*, 1975
polyvinylidene fluoride	5–12*N* NaOH	65–85 °C	$\leq$ 100 h	Komaki, 1979

selective etchants are even commercially available as ready-mixed solutions for insulators as well as for metals.[12]

4. Shape of the etched track

Chemical etching results in a preferential attack on the latent track, leading to an etch "pit." In general, the track-etch rate is a smooth monotone function of the stored energy density along the track. Above the track-etch threshold, the etch rate increases rapidly with increasing specific ion energy. It reaches a maximum at a specific ion energy between 1 and 10 MeV/nucleon, and, after the maximum, decreases relatively slowly at still higher energies. However, close to the track-etch threshold, fluctuations occur in the stored energy density from track to track. This can lead to a broad distribution of track lengths. Above the track-etch threshold the etch rate gradually becomes a smooth function. If track and bulk etch rates are known, the shape of the resulting etched track can be constructed (Fleischer *et al.*, 1969). It corresponds to the superposition of elementary time-delayed waves (Fig. 14), emitted from the moving end point of the etched track as it proceeds into the depth of the track recorder. This process corresponds to the shock wave of a supersonic bullet, or, in a two-dimensional situation, to the bow wave of a ship. For accelerating, constant, or decelerating track-etch rates in an isotropic medium, the etched track shape is concave, conical, or convex, respectively. For a crystal, in general more than one etch rate exists, complicating the construction of the etched track shape. This leads to faceted etched tracks, whose shapes can be quite complex.

a. Constant track-etch rate in an isotropic medium

In many practical applications, the etch pit can be approximated by a cone. This holds for briefly etched tracks in an isotropic medium. A track cone corresponds to a constant or slowly varying track-etch rate. This approximation is justified at least locally, due to the smoothness of the track-etch function sufficiently above the track etch threshold. The idealized case (Henke and Benton, 1971) is determined by the following parameters: α is the angle of irradiation (measured with respect to the surface plane), R is the range of the incident ion, v_t is the track etch rate, v_b is the bulk etch rate, and t is the etch time.

Three distinct phases, subdivided here into stages, can be recognized as the etching proceeds along the track into the (thick) recording medium (Fig. 15): the "cone phase" (Fig. 16), the "transition phase," and the "sphere phase" (Fig. 17) (Ali and Durrani, 1977).

[12]Transene Company, Inc., Route 1, Rouwley, Mass. 01969, USA.

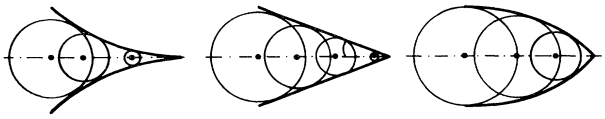

FIG. 14. Construction of etched track shapes from elementary waves (Paretzke *et al.*, 1973). For known track and bulk etch rates, the shape of the resulting etched track can be constructed (Fleischer *et al.*, 1969). Elementary waves, originating along the latent track as the etch front proceeds, merge to an envelope that corresponds to the actual shape of the etched track. The superposition resembles the shock wave of a supersonic bullet, or, in two dimensions, the bow wave of a ship. From left to right: Increasing, constant, and decreasing track-etch rate along the latent track, assuming that the etch attack always occurs from left to right. Reversal of the etch attack, for example, by etching from the back side of the track recorder, reverses the resulting track shapes from concave to convex and vice versa, with practical consequences.

(1) Cone phase ($0 \le t \le t_2$). The most prominent observables are:

(a) The half-angle ϑ of the etch cone (defined for $0 \le t \le t_4$),

$$\sin\vartheta = v_b/v_t \rightarrow \vartheta = v_b/v_t \quad \text{for } v_t \gg v_b \ . \tag{8}$$

(b) The actual length L of the conical track, measured from the etched surface along the latent track axis (defined for $0 \le t \le t_2$),

$$L = v_t t - v_b t/\sin\alpha \ , \tag{9}$$

$$L \rightarrow v_t t \quad \text{for } v_t \gg v_b \ , \tag{10}$$

$$L \rightarrow 0 \quad \text{for } \sin\alpha = v_b/v_t \text{ or for } \alpha = \vartheta \ . \tag{11}$$

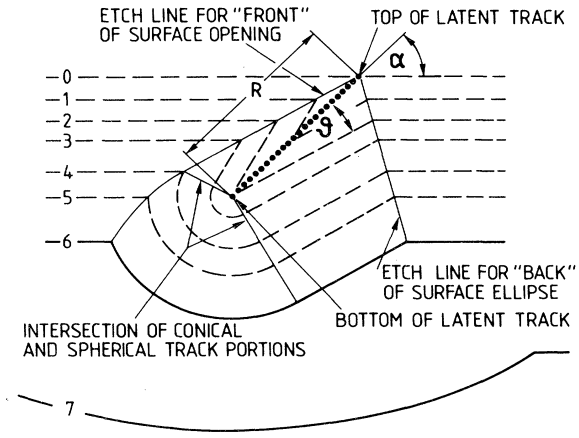

FIG. 15. Sequential steps for track etching in an isotropic medium, assuming constant track-etch rate (Henke and Benton, 1971). *Cone phase*: t_0, pre-etch surface of the track recorder; t_1, partially etched, conical track; t_2, completely etched latent track (down to the stopping point). *Transition phase*: t_3, partially developed spherical tip; t_4, spherical tip intersects etched surface; t_5, termination of track undercut ($0 \le t \le t_5$); t_6, vertical projection (surface contour) is a half circle, joined to a half ellipse. *Sphere phase*: t_7, etched track becomes a spherical section (shown shifted upward with respect to the rest of the figure).

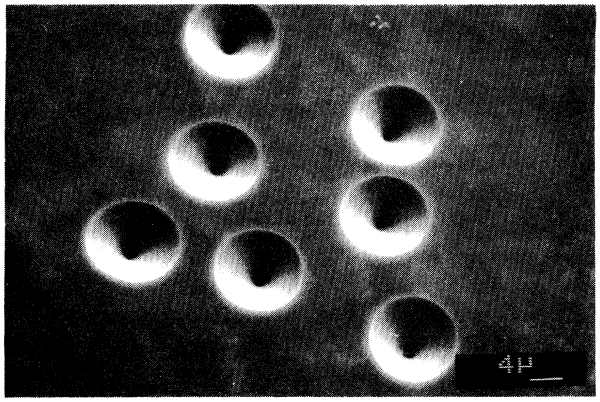

FIG. 16. Etch cones obtained in regular glass after a short etching.

The last relation defines a critical threshold angle $\alpha_0=\vartheta$ for creating an observable track.

(c) The intersection of the track cone with the etched surface. This forms an ellipse with the major half-axis a and the minor half-axis b (defined for $0\le t\le t_4$),

$$a=v_b t[\cos\vartheta/(\sin\alpha+\sin\vartheta)]\ ,$$
$$b=v_b t[(\sin\alpha-\sin\vartheta)/(\sin\alpha+\sin\vartheta)]^{1/2}\ . \tag{12}$$

The first etch phase terminates at time $t_2=R/v_t$, when the preferential etching reaches the stopping point of the heavy ion. Henceforth no preferential etching takes place, and the etching proceeds in all directions with the same velocity v_b.

(2) Transition phase ($t_2\le t\le t_7$). During this phase, the bottom of the track becomes progressively more rounded, while the surface opening at first remains elliptical and then becomes partly circular and partly elliptical.

Rounding of track cone ($t\ge t_2$). Starting at $t=t_2$, the etching proceeds everywhere at the same rate v_b, normal to all surfaces, resulting in a spherical rounding of the track vertex. The most prominent observables are:

(a) The radius of the rounded tip (defined for all times $t\ge t_2$),

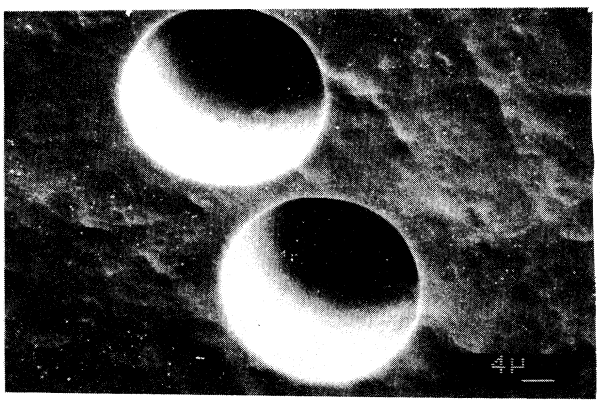

FIG. 17. Spherical etch pits in regular glass after prolonged etching.

$$r=v_b(t-R/v_t)\ \text{ for } t\ge t_2\ . \tag{13}$$

(b) The depth $L_\perp$ of the etch pit with respect to the etched surface, which stays constant for all times $t\ge t_2$,

$$L_\perp=R(\sin\alpha-\sin\vartheta)=\text{const}\ \text{ for } t\ge t_2\ . \tag{14}$$

At time

$$t_4=R\{\sin\vartheta+\sin[(\alpha-\vartheta)/2]/\cos[(\alpha+\vartheta)/2]\}/v_b\ ,$$

the spherical part of the track touches the etched surface.

Elimination of an eventual track undercut ($0\le t\le t_5$). This elimination occurs when the etched surface reaches the stopping level of the heavy ion. Undercutting cannot occur if the irradiation angle $\alpha\ge(\pi/2-\vartheta)$. This etch stage is terminated at $t_5=R\sin\alpha/v_b$.

Approaching half-circle/half-ellipse state ($t_4\le t\le t_6$). At time $t_6=R(\sin\alpha+\sin\vartheta)/v_b$, the vertical projection (surface contour) of the etched track consists of a half-circle joined to a half-ellipse.

Approaching sphere phase ($t_6\le t\le t_7$). This phase is reached for $t_7=R\cos\vartheta\{v_b\tan[(\alpha-\vartheta)/2]\}$.

(3). Sphere phase ($t\ge t_7$). Finally, the whole track profile becomes a spherical section and the surface opening becomes a complete circle. In an ideal, infinitely thick track recorder, this phase would persist forever. However, the actual precision of the spherical section is limited by "noise" caused by inhomogeneities of the used recorder material, leading to surface ripples. The surface contour is a circle with a radius that increases infinitely as the square root of time. The spherical section has the constant depth $L_\perp$. Therefore its visibility decreases with time. Besides the depth $L_\perp$, the most prominent observable is the radius of the circular surface contour,

$$r_{\text{sphere}}=\{(2r-L_\perp)L_\perp\}^{1/2}\ \text{ for } t\ge t_7$$
$$=\{[2v_b t-R(\sin\alpha+\sin\vartheta)]$$
$$\times R[\sin\alpha-\sin\vartheta]\}^{1/2}\ . \tag{15}$$

b. Varying track-etch rate in an isotropic medium

The previous description of track etching applies to an isotropic medium with constant track-etch rate. A simplified case can be solved, assuming a fixed irradiation angle $\alpha=\pi/2$ (i.e., beam axis normal to the surface of the track recorder), if the track-etch rate is not constant but a monotonic function along the track. This leads to a convex or a concave track shape (Paretzke *et al.*, 1973), depending on whether the etch rate decreases or increases as the etching proceeds, respectively. A more complicated problem arises for an arbitrary irradiation angle. Quite complex intersections of the convex or concave track shapes with the etched surface occur in this case (Somogyi, 1980).

c. Track etching in crystals

An additional complication arises in crystals. Track shapes depend on the mutual orientation of the track and

the crystal. Therefore, the morphology of etched tracks in crystals is an interesting but intricate subject. Faceted etch pits with a great variety of different geometries can be created, offering a wide array of possibilities for surface texturing. The main features of track evolution in crystals have been demonstrated in a two-dimensional case (Somogyi and Szalay, 1973), for which three different etch rates were assumed: one track-etch rate and two different bulk etch rates parallel and perpendicular to the surface plane. In this model faceted etch pits are formed. Beyond this, no general track-formation model exists, at present, for arbitrary orientation of track and crystal.

The faceted etch pits represent a kind of inverse crystal growth, evolving from a quasi-one-dimensional condensation nucleus represented by the latent track. Therefore a suitable model for describing track etching in crystals may be found in the field of crystal growth. More immediate help, however, may come from numerical methods developed in photolithography to simulate the development of resist patterns in three dimensions (Jones and Paraszszak, 1981).

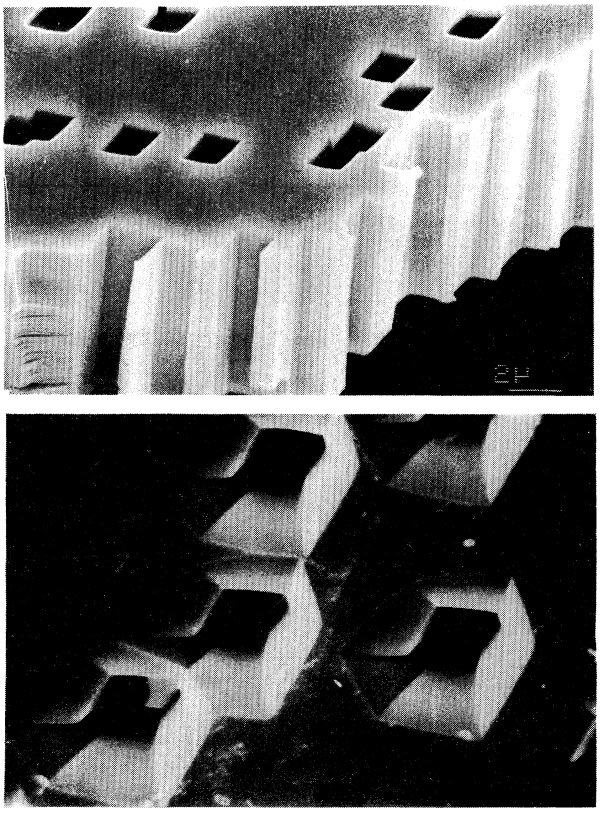

FIG. 18. Influence of the etchant on the track morphology in mica (Khan *et al.*, 1981). In addition to the composition of the recording material and the irradiating ion and energy, track morphology depends on the chemical nature, reactivity, viscosity, and temperature of the etchant. *Top*: Etching of the latent tracks by hydrofluoric acid leads to rhombic holes with sharp edges. *Bottom*: Etching in boiling sodium hydroxide solution leads to smooth hexagonal funnels.

The morphology of etched tracks in crystals depends heavily on the chemical nature and reactivity of the etching medium. This dependence may lead to new ways of shaping tracks in the future. For example, hydrofluoric acid etching of latent tracks in mica leads to almost rhombic holes (Fig. 18, top), whereas etching in boiling sodium hydroxide solution leads to approximately hexagonal funnels (Fig. 18, bottom). Thus a two-stage etching process, using first hydrofluoric acid and then boiling sodium hydroxide solution, can be used to trim the sharp edges of the rhombic holes to obtain smooth hexagonal funnels (Khan *et al.*, 1981). As an alternative "deburring" technique for sharp nuclear track edges, ion beam sputtering can be used.

5. Multiple-track pattern

Unlike many other processes used to create holes, the nuclear track technique yields only random arrays of holes at present. Therefore, with increasing density and size of the holes, close neighbors will merge to multiple holes of irregular shape with larger areas than a single hole (Riedel and Spohr, 1979, 1980a). A basic question in this context is the effective porosity of a two-dimensional statistical array of identical holes,

$$P_{\text{eff}} = 1 - \exp(-P) , \tag{16}$$

where the nominal porosity $P = NS_1$ is the product of the areal density N (ions per cm^2) and the single-hole area S_1. The effective porosity governs the mechanical stability of the track structure. A measure of the discreteness of track holes is the probability of the occurrence of single holes,

$$P_1 = \exp(-4P) . \tag{17}$$

A measure of the probability of overlapping hole neighbors at low nominal porosity is

$$P_2 \simeq 4P \exp(-4P) , \tag{18}$$

or just the probability of the occurrence of double holes. With increasing nominal porosity, holes of higher multiplicity rapidly become more likely at the expense of lower-multiplicity holes. Closed multiple-hole rings are formed at a nominal porosity of about 70% (Riedel and Spohr, 1979). For thick track recorders, discrete islands occur, separated from the rest of the material by deep grooves. For thin recorders, a complete perforation around the discrete islands leads to mechanical breakdown of the etched-track structure, whereby the irradiated area decays into small fragments.

D. Special etching techniques

1. Electrochemical etching

Electrical breakdown in insulators is characterized by a "treeing" phenomenon: the discharge does not occur on a straight path along the strongest field gradient, but rather

propagates on branched paths in the form of a tree. This phenomenon occurs whenever the electric field strength exceeds a certain threshold value. The electric field strength can be locally enhanced by a protruding conductor, for example in the form of a pointed etch pit, filled with the surrounding etchant or another electrolyte. The branches of the discharge tree are susceptible to an accelerated chemical attack, similar to that along latent tracks. The treeing phenomenon can be employed to enlarge etched tracks rapidly into visible dimensions, e.g., for track counting (Tommasino, 1980) by chemical means. The resulting large, high-contrast blobs, can be easily observed.

The technique has two rather unexpected features which eventually might be used for practical purposes:

The inherent tendency of the discharge process prevents a merger between neighboring trees. Therefore, even very large trees from closely spaced latent tracks are distinct and can be counted separately.

The strong directionality of response leads to a preferential amplification of tracks pointing in the field direction. The electrical field thus introduces an axial anisotropy into the system, corresponding to an additional degree of freedom to modify track shapes. For example, tracks that are oblique to the field direction (i.e., oblique to the surface normal of the track recorder) could yield kinked etch pits. The etching would first follow the direction of the latent track and later the direction of the electric field.

2. Double-layer track recorders

Conventional photolithography makes use of two-layer resists to generate very fine, deep structures. The idea behind this is that a single layer alone cannot perform the task satisfactorily, so different functions are delegated to different layers. The following two-layer technique is used in the production of submicrometer lines: the silicon wafer is spin-coated first with a thick layer of a light-insensitive polymer that evens the surface roughness of the substrate and can be selectively etched. A thin second polymer layer of different composition is deposited on top of the first. The second layer carries out the function of the photosensitive resist and can be selectively removed by the developer.

Such a technique can be used in nuclear track technology to generate bottle-shaped microcavities embedded in the recording material. A garnet substrate with a thin, epitaxially grown iron garnet film on top is such a two-layer system, for example. Differences in composition between substrate and epitaxial film lead to differences in their etching rates. For certain combinations of substrate and epitaxial film, the etch-rate differences can be quite drastic. Thus very fine microcavities can be manufactured, connected to the external world only by much thinner bottle-necks (Fig. 19). The immobilization of enzymes in biological reactors constitutes one of the possible applications of such microcavities. Up to now, porous glasses have been used for the attachment of the enzymes.

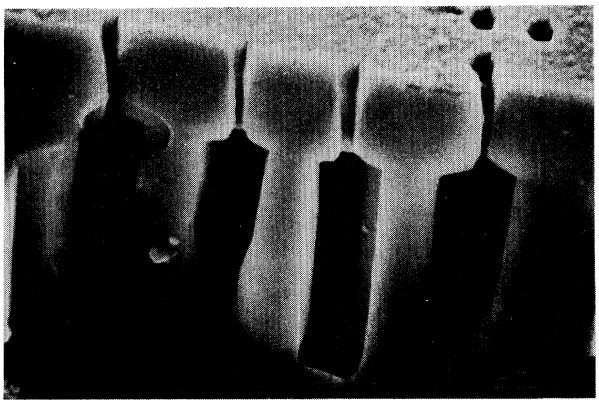

FIG. 19. Microcavities generated in a double-layer track recorder (Hansen *et al.*, 1983). Epitaxially grown iron garnet film on top of a single-crystal garnet substrate with etched nuclear tracks. The different lateral etch rates in the top film and in the substrate lead to hexagonal microcavities, connected to the outside world only by fine bottlenecks.

These maintain valuable enzymes at a stationary phase so that they can later be recovered from the reacted solution. Porous glasses are generated by a phase-separation process followed by selective dissolution of one of the phases. They have pore sizes that vary by a factor of about 2. Nuclear track cavities may provide attachment sites in cases which depend critically on pore size.

3. Sandwiches

Nuclear track applications can benefit greatly from technologies developed in the semiconductor field. A good example of a successful transfer from thin-film technology is the three-layer system used in the production of photo masks (Price *et al.*, 1982). Here, for the first time in track technology, a metallic film and a three-layer system is used. The structure consists of a thin alkali-resistant metal film (normally chromium), evaporated onto a glass substrate. A very thin track-recording polymer (e.g., a photoresist) is spin coated on top of the chromium. Even very slow ions can penetrate the thin polymer film. The assembly is subject to a two-stage etching process after the ion exposure. First, the latent tracks are etched selectively, opening tiny channels down to the top of the metal film. Second, a chromium-specific etchant is used to dissolve the chromium film laterally through these channels. In this way, large, high-contrast circular holes are etched into the chromium film beneath the photoresist. The track-etched holes in the upper layer are concentric with these large holes. The whole system, including the selective etchants, is commercially available with or without the photoresist layer on top of the metal/glass substrate.

4. Multilayer systems

Up to now, most track recorders have consisted of one material, providing a more or less constant etch rate, in-

dependent of depth. Multilayer techniques might be used in the future to generate a variety of unusual track shapes. Almost any arbitrary volume of rotation could be achieved, comparable to the shapes obtainable on the classical lathe. These miniature-sized "turned" bodies might open up new territory at the boundaries of classical physics.

Molecular monolayer films, another spinoff from semiconductor technology, are a new class of ultrathin resist materials (Barraud, 1980), which might be applied in this context.

E. Etch alternatives

1. Track grafting

Etchable tracks are obtained only above a well-defined material-specific track-etch threshold (Fig. 8). For a very fast ion, this condition is sometimes not met at the surface, but only in the interior of the track recorder, after the ion has slowed down somewhat. This raises the question of how such "internal" tracks can be revealed.

Organic polymers consist of a network of entangled molecules providing internal spaces for small molecules. For example, most polymers can absorb at least a few percent of water. This opens up the possibility of revealing internal tracks, hidden deep inside the polymer, by decorating the tracks with polymerizing small molecules (Somogyi *et al.*, 1979), an example of an additive track revelation process, as opposed to one that removes material. To this end, unsaturated organic molecules, i.e., monomers, are diffused through the irradiated material. The required time is proportional to the square of the penetration depth. For polymerization, the temperature is raised after completion of the diffusion process so that the monomers meet the catalytically active species (radicals) in the close vicinity of the latent track, and are polymerized into long strands. For microscopic observation purposes, a second monomer in the form of a dye can be added to the system. The resulting grafted copolymer provides improved contrast in such observations.

2. Metal precipitation

Noble metals, dissolved at high temperatures in a dielectric matrix, have a strong tendency to aggregate in the form of metallic clusters. The aggregation process can be triggered by the passage of a highly ionizing ion. It results in an array of metallic aggregates along the ion track. In the future it might be possible to create contingent metallic needles, for example, oriented microscopic dipole antennas of identical lengths, in this way. Along the preferred axis of anisotropy, such a composite material would have an unusually high dielectric constant at low frequencies. At 90° to the dipole axis, however, the dielectric constant would stay quite low. At high frequencies, the resonant absorption or emission of electromagnetic radiation by such a well-oriented system of dipole antennas could provide interesting information in the future.

a. The silver chloride recorder

The single-crystal silver chloride detector is a spinoff from basic research in photography. It is based on a fundamental process which also rules the photographic action of light in silver halide systems. The system uses visible light rather than wet chemical processing for stabilization of the latent tracks and development into visible dimensions. It represents a study case at the boundary between classical photography and nuclear track technology (Haase *et al.*, 1977; Schmidt *et al.*, 1977; Wendnagel *et al.*, 1980). Derived from "nuclear emulsions" (Shapiro, 1958) which have been already used for decades to record nuclear events, the silver chloride recorder is one of the forerunners of nuclear track technology, combining the properties of "nuclear emulsions" with the high spatial resolution of etchable nuclear track recorders. In contrast to any other nuclear track recorder, it can be switched on and off, in a way analogous to the "gating" of electronic counters.

In a simplified scheme, the recorder is characterized by a two-step process. The first "electronic" step consists of the formation of free electrons and holes along the path of the penetrating ion, followed by the trapping of electrons at lattice defects. It is followed by a second "ionic" step based on a unique property of the silver halides, namely the high mobility of interstitial silver ions in the crystal lattice at room temperature. Their migration leads to a charge neutralization at the negatively charged traps and to the formation of neutral silver. Ultimately, by a self-enforcing process, submicroscopic stable silver agglomerates are formed along the ion path. This latent track, normally not visible in optical microscopy, can be amplified into visible dimensions ("grains") by irradiation with shorter-wavelength light, close to the threshold for photoelectron production ($\lambda \simeq 405$ nm).

The properties of real crystals complicate the idealized scheme above; in order to fulfill the necessary conditions for the formation and development of nuclear tracks, one must prepare the crystal by special means, such as thermal treatment, or plastic deformation (between 1% and 20%) and doping, for example with cadmium.

Because of the divalent state of the cadmium ion, for any cadmium atom introduced into the crystal, one extra silver vacancy is created. Thus the tendency of interstitial silver to aggregate is reduced, i.e., the recorder is desensitized. In this way, doping by the divalent ion "paralyzes" the aggregating power of the existing crystal grain boundaries (Haase *et al.*, 1973). In an undoped recorder even the crystal grain boundaries provide sufficiently deep traps for the silver decoration process, and the simultaneously decorated heavy-ion tracks are obscured by the silver-decorated grain boundaries.

As a result of long-term research efforts, silver chloride sheets can be produced, unsupported or supported, in sizes up to several hundered cm^2, with typical thicknesses

of 200 μm (Wendnagel *et al.*, 1980).

The silver chloride detector has several features which make it unique among track recorders:

An obvious disadvantage associated with desensitization by doping is that the undeveloped latent tracks are unstable in time and will fade under normal circumstances. The fading constant depends on the preparation of the recorder, the temperature during and after exposure, and the specific energy loss of the ion, and varies from about 0.1 s to several days. The latent tracks, however, can be stabilized by a factor of 10^3 in time by irradiating the recorder volume by longer-wavelength (yellow) light ($500 \leq \lambda \leq 650$ nm), during or shortly after ion irradiation. Hence track recording can be restricted to a desired period of time: the recorder can be switched on and off at will. For this stabilization an irradiation of the order of 5×10^{14} photons per cm^2 is administered over a time span of the order of a tenth of a second or more. In this process, the longer-wavelength photons liberate electrons from shallow traps at the site of impurity or doping atoms (such as cadmium), thus reducing the silver ions existing in the vicinity of the ion path to neutral silver atoms that are capable of aggregating. In this way the latent track is stabilized.

The stabilized tracks consisting of small submicroscopic silver aggregates along the ion path can be amplified ("decorated") to larger, microscopically visible silver "grains," using light of shorter wavelength ($\lambda \simeq 405$ nm). This process is comparable to instant-picture photography and is completely free of the problems associated with wet chemical processing. In addition, the dry process avoids shrinkage and other deformations of the recorder. It requires about 5×10^{18} photons per cm^2. This process can be performed simultaneously with or much later than the heavy-ion irradiation. Wet chemical development is completely circumvented.

Developed tracks can be bleached by a dose of green or yellow light of the order of 5×10^{22} photons per cm^2, which dissolves the silver grains. This "bleaching" process, however, under special conditions does not dissolve the latent tracks, which at a later time can be revealed again by the development procedure described above.

The recorder is sensitive to ultraviolet light ($\lambda \leq 405$ nm). One is therefore able to inscribe high-resolution optical information into a thin surface layer of the recorder by conventional microscopic projection through the eyepiece side, and during the evaluation of the tracks.

In future applications, the silver chloride recorder may make possible the creation of a three-dimensionally addressed high-resolution storage device, in which silver grains would be exclusively created at the intersection between individual heavy-ion tracks and a laser beam (Schopper, private communication).

b. Photo-etchable glasses

A recent counterpart to the photolithographic etching of metals is the photo-etching of glasses. This process is already used for mass producing precise insulating parts with complicated shapes. Here, the precipitating metal is silver or copper. The latent track in such glasses (Dürolf *et al.*, 1978) consists of a discrete array of small metallic grains. During a later, two-step thermal annealing process, a lithium metasilicate phase is aggregated around the grains. First, the new phase is nucleated at relatively low temperature. Then the crystallites are grown ("ripened") at a somewhat higher temperature for which the growing rate is sufficiently high. The process is continued until a continuous string of the new phase is formed along the latent track. This new phase has a much higher etching rate in hydrofluoric acid than the matrix material itself. Preferential etching of the latent track exists only if the metasilicate crystallites form a continuous string. Therefore, in this case, the track-etch threshold can be fine tuned by the duration of the second thermal annealing stage.

F. Track observation

1. Electronic track counting

a. Spark counter

Track counting with an optical microscope is a time-consuming process with a natural tendency toward subjective errors. To avoid these errors, one can make a track counter out of any track-perforated foil by a simple method. According to this method (Tommasino, 1980), the perforated foil serves as the dielectric of a self-healing capacitor. A metallic base plate represents one of the capacitor electrodes. The other electrode is the aluminum evaporated surface of a separate plastic foil pressed flat on top of the etched recorder foil. The whole assembly is held tightly together by a clamping device. Still better would be thin metal electrodes evaporated on both sides of the etched recorder surface itself. As the voltage over the capacitor is gradually increased, a succession of sparks occurs. The sparks are counted electronically, and each one vaporizes a well-defined circular area of the thin metal electrode on top of the actually counted track hole. In this way, a second spark cannot come through the same etched track hole.

b. Breakdown counter

A slightly advanced scheme makes use of thin-film technology. The avalanche-type breakdown counter (Tommasino, 1980) is a hybrid, combining the principles of the ionization chamber and the track recorder. In contrast to the storing property of other nuclear track recorders, it provides real-time counting of nuclear track events at the time they occur. This feature could be useful for areal-dose determinations during track irradiations. The thin-film breakdown counter is a nonetching device, consisting of a self-healing metal/oxide/metal capacitor (Klein, 1969). Any heavy particle penetrating the structure initiates a breakdown that vaporizes some of

the metal film around its impinging site.

It may be possible to develop this system further towards a storing detector of the following type: it would be irradiated without applying a voltage between the electrodes and evaluated at a later time by counting successive sparks occurring through the latent tracks. In this way, a valuable combination of a storing recorder and an event counter might be achieved.

2. Diffraction techniques

Elastic scattering experiments yielding diffraction patterns are a classical domain for observations in physics, in which the wavelength of the scattered particle and the angular range of observation must be adapted to the size of the object. From the scattering distribution of oriented nuclear tracks, their average size, density, and shape can be obtained. Up to now, mostly latent nuclear tracks have been observed in this way, using small-angle x-ray (Dartyge *et al.*, 1981) and neutron (Albrecht *et al.*, 1982) scattering. Etched tracks can, however, be observed using visible light from a laser. In future large-scale processes, this could facilitate continuous on-line control during the etching procedure. A necessary condition for such laser diffraction observations would be a proper wavelength selection in order to obtain a different refractive index of etchant and track recorder.

3. Microscopic methods

Any manufacture of nuclear tracks of specified size and shape requires a microscopic control. In choosing such an instrument, the available amout of money is an important factor.

The simplest instrument for enlarging etched tracks to visible sizes is a *slide projector* for diapositives.

At present, most observations in the field of nuclear track detection are performed using an *optical microscope.* Optical microscopy provides adequate resolution in many applications, determined by the wavelength of visible light (about 500 nm). Several techniques are available for enhancing microscopic contrast (Hepburn and Windle, 1980): application of a dyed track-recording material, metal evaporation of a thin metallic film on top of the track recorder, and deposition of a thin metallic film on the total recorder surface or even inside the etched tracks, using a supersaturated metal solution. The main disadvantage of the optical microscope for observing long tracks is its small depth of focus. Additionally, there are many applications in which a higher resolution is desirable.

The *scanning electron microscope* provides excellent shape contrast, resolution, and depth of focus. Its resolution is about 1 order of magnitude higher than that of the optical microscope. It is limited mainly by the diffusion radius of backscattered electrons from the depth of the sample (about 10 nm). The disadvantage of scanning electron microscopy is that it requires replica techniques to observe structures deep inside track channels.

For the observation of individual latent nuclear tracks, the *transmission electron microscope* is an indispensable tool. It has several advantages over the scanning electron microscope for observing fine details of etched tracks, but it requires replica techniques for producing thin, electron-transparent samples (≤ 1 μm). For this purpose elaborate thinning and replica techniques have been developed. The transmission electron microscope provides a resolution that is again an order of magnitude higher (about 1 nm) than that of the scanning electron microscope.

Microscopic methods always require a skillful observer. They are time-consuming, and quantitative observations depend on the subjective judgment of the observer. Therefore, at present, considerable efforts are being made to automate the evaluation of microscopic pictures using *computer image analysis.* Commercial pattern-recognition systems yield global properties such as the areal dose and the average track size very accurately and rapidly (Riedel and Spohr, 1980a). Additionally, image analysis is very useful for screening large numbers of tracks for unusual shapes.

4. Macroscopic methods

Macroscopic observations are imperative in processes that have to be continuously controlled and rapidly optimized, especially for industrial-scale applications. At the same time, the subjectivity of the observer can be minimized in dealing with important parameters like the areal density of tracks, their length, and diameter. Macroscopic control is required for *interruption of the etch process* at a time precisely defined by the track size; *screening of track recorders,* i.e., determination of etch rates in a large sample of different track materials, especially if track-recording properties have to be optimized; *screening of selective etchants* for optimizing track selectivity.

a. Thickness gauge

In isotropic materials, the diameter of the etch pit is proportional to the material removed along the surface normal. For perforated thin foils with high track-etch ratios, the hole diameter corresponds directly to the thickness lost by the foil during etching. This yields a simple method for controlling track size by continuously or intermittently measuring the thickness of the etched foil, using a suitable thickness gauge.

b. Conductivity cell

One of the most precise methods for simultaneously determining bulk and track-etch rates in a thin recorder foil throughout the duration of the etching process is the use of a conductivity cell (DeBlois *et al.*, 1977). This device is sensitive enough to observe single pores (DeSorbo, 1979) and determine radial etch rates close to the ion tra-

jectory (Schnoor *et al.*, 1982). It consists of an electrochemical cell, in which the track-irradiated foil forms an electrical barrier between two inert metal electrodes. The conductivity cell provides two modes of operation, namely, *continuous observation* during the etch process, involving a cell filled with the track etchant as the electrolyte solution, and *intermittent sampling* measurements, involving a cell filled with a passive electrolyte that does not etch the tracks further.

The equivalent circuit of a conductivity cell is a complex resistor, consisting of a capacitor and a real resistor connected in parallel. By means of the lock-in technique used in electronics, real and imaginary parts of this complex resistor can be separately measured. The *imaginary part* yields the foil thickness and, as function of the etch time, the bulk etch rate. The *real part* yields the etched-track diameter and, as function of the etch time, the radial etch rate in the close vicinity of the track. For this, a precise knowledge of the areal dose is required. The average track-etch rate along the track can be obtained from the time of pore breakthrough, characterized by a rapid increase in the cell current. The electronic control can also be used to interrupt the etching process precisely at a desired pore size by flooding the cell with a nonetching medium (cf. Fig. 28).

c. Double-exposure technique

The double-exposure technique is an example of a technological development in the field of photolithography that may be fruitfully adapted to the field of track technology (Lin, 1978). In this technique a test zone on the sample is irradiated with a significantly higher dose than the rest of the sample. As the removal of the resist film approaches a critical value during development, the optical reflectance from the test zone changes abruptly. This macroscopically observable change can be used to interrupt the development process at a precisely defined time. A similar technique may be used for terminating track etching at a precisely defined hole size without the need for repeated microscopic checks.

A slightly modified version is the graded-exposure technique (Brault and Miller, 1980), which uses a graded exposure of the resist-covered silicon wafer along one axis, followed by a graded development along the other axis. In this way, optimum dose and development conditions for a given resist/developer combination can be rapidly determined. For this purpose only one single wafer is required.

The nuclear track analog of this technique is based on the statistical properties of etched nuclear tracks. During track etching, multiple-hole rings lead to discrete islands of separated matter (Riedel and Spohr, 1979). When this occurs, around a nominal porosity of about 70%, an abrupt change of mechanical and optical properties can be observed, very similar to a phase transition. Perforated samples will suddenly break apart. Surface resistivity increases dramatically (Fischer *et al.*, 1982). Macroscopic observation of such changes can be used to interrupt the etching process at a precisely defined nominal porosity. The double-exposure technique requires precise dose control. It may become a valuable means for rapidly screening track recorders and etchants. It may also become useful for interrupting the etching process at a precisely defined pore size, even for bulk etch rates varying from sample to sample.

III. APPLICATION OF NUCLEAR TRACKS

A. Influencing bulk properties

1. Nuclear track filters

Almost immediately after the first observation of etched nuclear tracks in mica, the potential of nuclear track filters for the mechanical separation of small particles was recognized (Fleischer *et al.*, 1975). Nuclear track filters offer distinct advantages over conventional filters, which consist normally either of porous foams or of bonded fibers and depend on serveral mutually interconnected processing parameters. In constrast, nuclear track filters are defined by very few, almost independent parameters: track length, track diameter, and areal density of the tracks. These parameters can be varied in an easily controllable manner over several orders of magnitude.

Since 1972, fission fragments from nuclear reactors have been used for the commercial manufacture of nuclear track filters up to about 10-μm track lengths.[1] This is the first example of a large-scale commerical use of individual atomic particles. Heavy-ion accelerators are a promising alternative for generating nuclear track filters (Kuznetsov *et al.*, 1982). The etching may be performed either on-line or off-line, i.e., simultaneously with the irradiation or after irradiation in a separate chemical processing facility, respectively. The concept of an on-line filter production facility (Flerov, private communication) is shown in Fig. 20. It is possible to irradiate several square meters of foil material per second. Off-line treatment is feasible at low track densities, where uv treatment and chemical etching are the throughput-limiting steps. In this case even waste beams from nuclear physics research experiments might be used for commerical purposes. The main advantage of track filters over conventional filters is their well-defined pore size. Also, the retained particles can be observed directly on the filter surface. Well-defined pore size is a necessary condition for selecting biological cells at almost uniform size. Unfortunately, in aerosol filtration, selectivity is reduced by the electrostatic adhesion of impacting particles in the vicinity of pore entrances (Spurny *et al.*, 1969). This is even truer of conventional aerosol filters because of the higher tortuosity of their holes. The retained particles can be much smaller than the pore size. One way to circumvent this problem is to improve aerodynamic flow through the pores. In track technology, originally rhombic holes (Vater *et al.*, 1980) can be modified by rounding the pore entrances to the approximate shape of a funnel (Khan

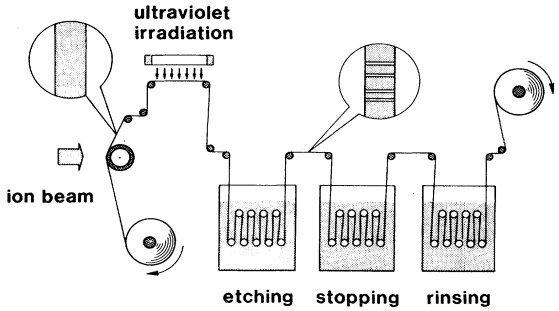

FIG. 20. Diagram of a heavy-ion nuclear track filter production line (Flerov, private communication). A heavy-ion accelerator provides an expanded ion beam through which a polymer foil band is pulled transversely at a speed of several meters per second. The irradiated foil passes through an ultraviolet irradiation station in order to increase the track-etch ratio of the recorded nuclear tracks by adjusting the "working point" of the dose-response function. Then the foil band passes through the etching bath, where the latent tracks are etched to the desired size, through the stopping bath, where the etching process is interrupted, and finally through a rinsing water bath. After passing through a drying station, the finished nuclear track filter band is stored on a roll for later processing steps.

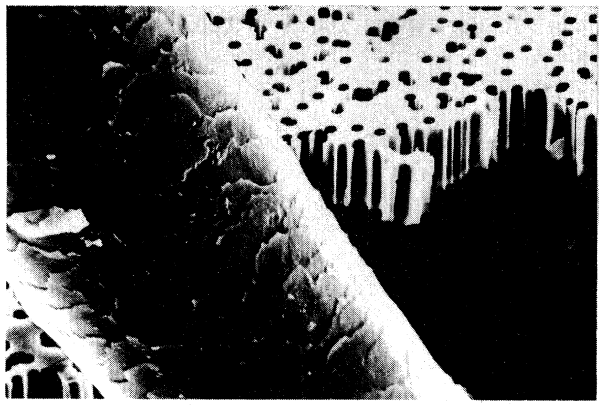

FIG. 21. Nuclear track filter dimensions, compared to a human hair. The etched track holes (background right) are about ten times smaller in diameter than a human hair (foreground left; diameter about 100 μm). The track-etch technique enables one to make holes with a minimum diameter of about 0.01 μm (10 nm), that is, about a thousand times smaller than the etched track holes shown here.

et al., 1981). Funneled nuclear track filters can be used in aerosol filtration (Tress *et al.*, 1982) and whenever the sharp rim of a hole might create turbulent flow or disrupt sensitive biological cells.

One apparent disadvantage of nuclear track filters is that they may contain multiple pores of larger sizes (Riedel and Spohr, 1980b). This, however, can be quite efficiently prevented, by using irradiations with a wide angular spread of the ion trajectories, and thus producing many independent track arrays that do not mutually interfere; such an approach is especially useful for thick nuclear track filters. Figure 21 shows the fineness of etched track holes by comparing them with a human hair.

2. Membranes for separation processes

A membrane is a structure acting as a barrier to the flow of matter, electrical charge, or heat betweeen two compartments. Membranes exist in a wide range of complexity, from very simple, homogeneous phases to highly asymmetric composites. "Passive" membranes can selectively transmit various components of a solution by applying an external force in the form of a gradient in pressure, voltage, temperature, or concentration.

"Active" membranes are still the exclusive domain of biology. They are capable of serving as pumps, working against concentration gradients without external forces. In this process biochemical energy is consumed. Active membranes are the essential components of all living organisms on the cellular and subcellular level. They consist of a monolayer sandwich of lipid molecules, interspersed through which are highly differentiated proteins serving as biochemically controlled "gate" channels for specific ions or molecules.

Artificial membranes (Pusch and Walch, 1982) are finding large-scale application in a variety of industrial fields where liquid or gas mixtures have to be separated. The main advantage of conventional membrane separation processes is their low energy consumption in comparison to alternative methods. Examples are the following.

The diffusion seperation of ^{238}U and ^{235}U, for which, however, the ultracentrifuge seems to be a competitive alternative. This process is based on the permeation of controlled-pore glasses or ceramics with gaseous uranium compounds.

The separation and purification of helium.

Desalination of sea water by reverse osmosis.

The filtration of waste water in galvanotechnic and photographic processes using ion-selective membranes. This bears the additional advantage of an almost complete recovery of valuable substances.

Separation of liquid/liquid and liquid/gas phases in batteries and fuel cells. In hydrogen fuel cells, even a three-phase separation between gas/liquid/solid is established within porous electrodes. In fuel cells, the gas loss through larger pores is a problem.

Artificial as well as biological membranes have, therefore, become the subject of intensive laboratory investigations. The task of membrane science is to find the relationship between membrane structure and observable properties.

The structure of a membrane is, however, often very complex. Conventional polymer membranes are characterized by pore size and by the tortuosity of their network. Solvent and solute molecules diffuse through this network, jumping in succession from adsorption site to adsorption site. In order to describe the phenomenon of semipermeability, one must adapt model parameters to fit the experiment.

The nuclear track technique produces membranes of precisely defined pore structure and can help to provide theoretical direction for what has until now been largely an empirical field (Quinn *et al.*, 1972; Klump and Woermann, 1977). The technique is capable of forming extremely fine, uniform pores of almost molecular dimensions thus making possible well-defined observation of restricted transport phenomena through track membranes (Beck and Schultz, 1972; Anderson and Quinn, 1974; Malone and Anderson, 1978). In nuclear track membranes the flux decreases sharply as the particle radius approaches the pore diameter. An interesting "switching" phenomenon involving an abrupt flux enhancement has been observed for long polymer chains, above a certain critical polymer concentration (Cannel and Rondelez, 1980). This switching phenomenon occurs even in situations where the transmission should be completely blocked according to the size of the molecule. The effect is analogous to the rapidly increasing current/voltage characteristics of a semiconductor diode beyond a certain voltage threshold. Just as the nonlinear behavior of semiconductors has been a key to microelectronics, this finding might become a starting point for externally controlled membrane separation processes, in which the transmissive flux is controlled by a third chemical agent. Up to now, only living organisms have achieved this. However, controlled membrane transmission is urgently needed for the controlled dosage of drugs.

Nuclear track membranes are inert supporting structures. They can be coated by monolayers of molecules to decrease the inner pore diameter in discrete steps (Quinn *et al.*, 1972). The pore walls can be further modified by the attachment of charged groups. The space-charge region in the vicinity of the walls causes co-ion exclusion and counterion enhancement (Koh and Anderson, 1975). The result is an ion-selective membrane.

All investigations of track membranes up until now were based on natural mica, irradiated by fission-fragment sources. The membranes were limited to a very fragile thickness of about 10 μm and took much time and care to fabricate. Accelerated heavy ions can be reliably and easily used for the production of such membranes in sufficient quantities. They may give new impetus to further development in this field. Track technology, therefore, seems destined to play a prominent role in future investigations in membrane science. The advantages of track structures in membrane science are the following:

Pores have almost identical, accurately adjustable diameters, which can be readily adapted to specific requirements.

Pore length is directly defined by the membrane thickness.

Pores can be oriented parallel to each other.

Pore length-to-diameter ratios can be very large, yielding very large active wall areas.

Pores can be modified by attaching monolayers, or by affixing charged groups, enzymes, or catalysts to the pore walls.

Track structures can be used as passive support structures for overlayed, much finer active membranes.

The nuclear track technique also offers interesting possibilities for generating *controlled-pore substrates* for use in liquid and gas chromatography as well as in enzyme reactors. There exist at present two kinds of conventional controlled-pore substrates: the "molecular sieves" (e.g., the zeolites) and the preferentially etched two-phase glasses (Messing, 1974). Two-phase glasses have a relatively broad pore-size distribution and, therefore, are not very size selective. In the future, the nuclear track technique could be used to generate solids with very large surface-to-volume ratios. Their precisely defined pores could be used for the selective attachment of catalysts, enzymes, or even larger biological entities.

3. Fining of magneto-optic materials

> "When the dimensions of artificial structures approach or become smaller than certain characteristic distances (e.g., grain size, domain size, wavelength, mean free path, coherence length, molecular size) it becomes possible to access phenomena or manipulate materials in new and different ways" (Smith, 1981).

This statement seems to be a clue to new and different uses for nuclear tracks, suggested by their ability to influence global properties through structural changes on a local (often still microscopic) scale. The fining of magneto-optic iron garnets is an example, in which latent tracks as well as etched tracks can be applied for the purpose of changing magnetic properties.

Epitaxially grown single-crystal ferrimagnetic garnet films were originally conceived of for use in bubble memories, which vitally depend on a high magnetic domain-wall mobility. For this purpose, garnet films were developed for low intrinsic coercivity and, in order to achieve this, low dislocation density. Thus their magnetic properties are highly susceptible to nuclear track damage.

More recently, the application of this well-studied class of materials in stable, fast switchable displays and printers has become attractive (Hill and Schmidt, 1978). The main advantage of these elements is that they combine memory and display functions in one and the same piece of hardware. They are based on locally fixed magnetic domains in a thin ferrimagnetic garnet film of composition $(Gd,Bi)_3(Fe,Al,Ga)_5O_{12}$, supported by a magnetically inactive garnet substrate. The thin film possesses a uniaxial magnetic anisotropy whose easy axis is perpendicular to the film. This magnetically bistable system is capable of storing binary information. The stored pattern can be displayed directly using the Faraday rotation of polarized light, transmitted through the garnet film. The switching of domains of given magnetization requires the application of an external magnetic field, whose action is localized by heating the desired region of the film far enough above the "compensation point" at which the film is insensitive to external magnetic fields. Discrete bits in the memory can be addressed at random by an array of leads connected to resistive heaters on top of each cell.

The conventional technique for magnetic isolation of neighboring storage sites is based on lithography. It resolves the epitaxial film into a regular array of discrete islands, corresponding to elementary information cells, separated by grooves etched down to the substrate. In this way, the cross-talk between neighboring domains of different magnetic orientation is eliminated.

Because of the restricted aspect ratio (depth to width) of the etched grooves, this lithographic approach limits the storage density. Moreover, the steep slopes of the grooves hamper the deposition of auxiliary layers on top of the island array (e.g., the conductor network), that eventually may prevent coherent deposits. These disadvantages can be circumvented by the use of nuclear tracks (Heitmann *et al.*, 1978). The inherently high susceptibility of the material to crystal dislocations makes it possible for nuclear tracks to increase the coercivity of the garnet by several orders of magnitude. This approach leaves a continuous planar surface that is much better suited for depositing auxiliary layers than a grooved surface. Also, the Faraday contrast can be enhanced by increasing the film thickness without the necessity of simultaneously increasing the depth of the grooves. Either etched or latent nuclear tracks can be used to stabilize the inscribed domain pattern, giving one-to-one correspondence between the magnetic domains and the recorded data, and a safe storage under normal environmental conditions. Latent track fining requires higher doses than etched track fining. Track fining offers simultaneously the possibility of influencing the magnetic anisotropy. This feature can be utilized as an additional parameter to tailor the storage properties according to specific requirements.

Figure 22 shows the effect of domain-wall pinning by etched nuclear tracks, observed by optical microscopy. The magnetic domains are observed between crossed polarizers, using the effect of Faraday rotation. It is evident that the domain walls cross preferentially through the etched tracks in which domain walls cannot exist. This "strategic" behavior decreases their average free energy. At the same time, any domain-wall movement requires the input of external energy to regenerate a corresponding piece of the wall. Therefore the domain walls are immobilized. The resulting frictional force corresponds to an increased coercivity.

For etched tracks in epitaxial films with compressive or tensile misfit strain, the pinning effect can be drastically enhanced by magnetostriction (Krumme *et al.*, 1977). Thereby strain relaxation in the vicinity of the etched track results in a steep gradient of the magnetic domain-wall energy around the track. The strain halos extend beyond the etched channels and thus increase the effective cross section for interaction with the domain walls.

By latent nuclear tracks, a compressive strain field is induced, analogous to that in crystal dislocations. Even at relatively small heavy-ion track densities on the order of 10^8 ions per cm^2, overlap between neighboring strain fields occurs. This results in a lateral compression of the irradiated volume and in an observable global lattice expansion normal to the crystal surface (Strocka *et al.*, 1980). At high ion doses around 10^{12} ions per cm^2, depending on ion and energy, the stored energy can lead to a spontaneous destructive disruption of the crystal during or after the irradiation.

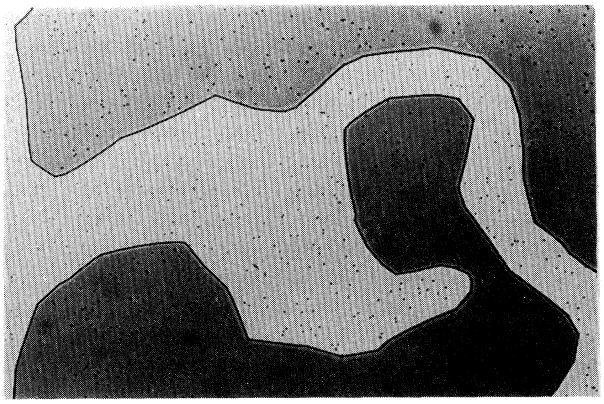

FIG. 22. Pinning of magnetic domain walls by etched nuclear tracks (Hansen *et al.*, 1983). Optical micrograph of magnetic iron garnet film, observed under nearly crossed polarizing conditions. Antiparallel magnetic domains appear as gray and white zones. The domains are separated by domain walls, observed here as black zigzagging lines. Nuclear tracks (black dots) decrease the magnetic domain-wall energy locally and thus result in a short-range pinning force. The global effect of many such local pinning centers is to increase the domain wall coercivity. Thus the inscribed domain pattern is "frozen" and the corresponding information stabilized.

In addition to their practical relevance, track studies in ferrimagnetic iron garnets can shed new light on the structure of latent tracks in crystals via their interaction with magnetic and magneto-optic properties (Heitmann and Hansen, 1982). Nuclear track radii can be determined from the dose dependence of the saturation magnetization and the Faraday rotation (Hansen *et al.*, 1982). Both effects decrease exponentially with the heavy-ion dose. Also, saturation magnetization and Faraday rotation show quite different annealing behaviors corresponding to their preferential dependence on defects of different size and stability.

4. Prospects of surface texture

Not only the chemical composition, but also the texture of a surface has an important influence on most of its other properties (Auciello, 1981), such as surface wetability, adhesion, friction, and electrical surface resistance. Textured surfaces can be used for enhanced absorption of radiant energy; in the realm of biomedical materials, they may help to solve the problem of prosthesis rejection; finally, they are of interest as highly efficient vehicles for heat transfer (Robinson and Rossnagel, 1982).

In graphoepitaxy, a surface texture induces a controlled orientation of a deposited film (Smith, 1981). The characteristic dimension of such a texture must be small compared to the grain or domain size of the film. In this

way, nucleation, coalescence, and recrystallization can be controlled at an early stage of film growth. For example, liquid-crystal technology depends on the texture of the electrode surfaces.

Surface texturing, therefore, finds an increasing range of possible applications in modern materials science. A promising aspect of the nuclear track technique in this field is its ability to produce etch pits of well-defined orientation and size and thereby to increase the effective surface area much more than other techniques.

a. Increasing adhesion

Innovation in materials technology is often based on improved mechanical contact between adjacent materials. This holds true for phenomena of the macroworld as well as of the microworld. In aeronautics and space technology, many high-strength connections nowadays use glue, where formerly rivets had been applied. Polymer adhesion on interfaces has become a field of intense study (Souheng, 1982). In microelectronics, system reliability depends essentially on thin-film adhesion on solids. In addition to glue and cleanliness, a necessary condition for a successful adhesive joint between two solid bodies is their surface roughness, which increases the available contact area and improves the mutual interlock between the neighboring solids. Ultimately, extreme degrees of interlock can be obtained by increasing the roughness on a microscopic scale.

Latent nuclear tracks have been successfully used to improve the adhesion of thin films to substrates at areal doses above the discrete track realm (10^{13}–10^{15} ions per cm^2) (Griffith *et al.*, 1982). In the future, etched heavy-ion nuclear tracks may be used to impart a well-defined microscopic roughness to adhesive joints. The technique generates a texture with precisely known orientation, peak-to-valley amplitude, and surface enhancement factor. The texture is determined by the angle of incidence, the areal dose, and the etching properties of the material used.

b. Improving insulator surfaces

High-voltage breakdown along surfaces is a common problem in high-voltage technology. The deposition of metal vapors on insulators is a nuisance in high-vacuum technology. The conventional way to cope with this problem is to undulate the insulator surface, thereby decreasing the field strength and causing shading in the deposition of metal vapors. The enlargement of the insulator surface made possible by conventional means, however, is moderate, and the protection against metal-vapor deposition not very effective.

Nuclear tracks can increase the area as well as the shadow-casting features of a surface dramatically. In this way, the electrical resistance of surfaces exposed to metal vapor can be improved by 10 orders of magnitude (Fischer *et al.*, 1982). This is probably the greatest global property change achieved in nuclear track technology up to now. The effect depends on the "nominal porosity" of the sample, which is equivalent to the porosity of a regular track array (see Sec. II.C.5). The resistance shows a sharp increase around 70% nominal porosity, when multiple-hole rings occur (Riedel and Spohr, 1979). The rings divide the continuous upper surface of the track recorder into discrete islands. A maze texture results which very effectively prevents electron conduction along the still existing conductive paths (Fig. 23). With increasing nominal porosity, the effect increases until finally the bottom of the track structure develops sufficiently large coherent patches to become conductive. This transition back to conduction is observed above a nominal porosity of about 200%.

5. Optical properties

Nuclear track technology opens up new possibilities in the field of light scattering, optical reflection, resonance, and absorption (McNulty *et al.*, 1982). Etched tracks may provide a severe test for models of elastic scattering of light by particles of arbitrary size, shape, orientation, and refractive index.

a. Surface-enhanced Raman scattering

In the future, etched tracks may be used for studies of fluorescence and Raman scattering by molecules embedded in or adsorbed onto track microcavities. Such investigations are suggested by recent observations of surface-enhanced Raman scattering by molecules adsorbed on highly conductive antennalike microstructues (McNulty *et al.*, 1982; Rowe *et al.*, 1980).

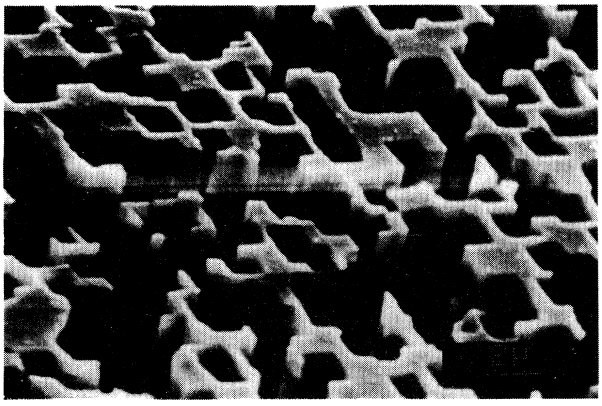

FIG. 23. Superinsulating maze texture generated in thick mica sample (Fischer *et al.*, 1982). Beyond a certain porosity, the surface of a thick track recorder, which is not traversed by the impinging ions, divides into discrete islands separated by deep canyons due to multiple-hole rings (Riedel and Spohr, 1979). A maze structure results, retaining its high electrical surface resistance even if a highly conductive metal film is evaporated on top of it. The metal-coated maze structure has an electrical resistance about 10 orders of magnitude higher than that of an identically treated flat surface.

b. Graded refractive-index matching

Another application of nuclear track technology may be graded refractive-index matching (Craighead *et al.*, 1982). Optical reflectance can be drastically reduced by hairy surface projections with cross sections smaller than the wavelength of visible light. The textured surface can be considered as a thin film with a refractive index smoothly varying in depth, as long as the wavelength is long compared to the characteristic distance between neighboring projections. For shorter wavelengths, the reflectivity approaches that of a rough interface.

c. High-pass filters

Multilayers of aluminized foils are very efficient heat shields under vacuum conditions. They are known as "superinsulators" in low-temperature physics. Unfortunately, such heat shields have large outgassing surfaces, detrimental to high-vacuum applications. Track perforation can alleviate this outgassing problem (Flerov *et al.*, 1982). In this process, the track-recording polymer foil is first irradiated, then etched to the desired hole diameter, and finally given a one-sided thin aluminum coating by vapor deposition. The remaining gas between the aluminized foil layers of the "superinsulator" can be pumped out quite efficiently through the track holes. At the same time, the high thermal reflectivity for long-wavelength radiation is maintained. The long-wavelength cutoff of such a perforated metal film is similar to that of long conductive channels (Keilmann, 1981). The thermal radiation spectrum below 300 K has a wavelength maximum above 5 μm. Therefore it suffices to use track holes with diameters smaller than 2.5 μm.

6. Replica techniques

At first sight, the nuclear track etching technique seems to be limited to dielectric materials and concave (hollow) structures. Moreover, the shape of the etched track seems, inherently, to be strictly dependent upon the specific chemical properties of the recording material. Replica techniques can circumvent these limitations, and fill etched track holes with almost any material, even metals. The track-recording matrix can be selectively removed afterwards to reveal the replica. In this way, convex (protruding) structures with the same shape as the original etched tracks can be created. Furthermore, double-replication techniques can be used to transform an etched track structure from a track recorder of suitable shape into an identical structure of a different material. Today, a wide variety of replication processes are available for this purpose, including techniques such as resin moulding, metal evaporation, electrochemical deposition, chemical vapor deposition, sputtering, and reactive ion etching and deposition.

a. Field emission of electrons

A field emitter is a metallic needle-electrode held at a high negative voltage with respect to a flat counter electrode. Under good vacuum conditions, the needle cusp emits a strongly bundled electron beam of high intensity. The brightness of field emitters [current/(cm^2 sr)] can be several orders of magnitude higher than that of thermal cathodes. Therefore field emitters are beginning to replace directly heated tungsten filaments in many applications, for example, in scanning electron microscopy.

The most important parameter of a field-emitter pin is its smallest radius of curvature at the outermost tip: the maximum field strength is inversely proportional to the tip radius. Tip radii below 100 nm are obtained for individual tungsten wires by using conventional techniques.

Large-area field-emitter arrays are promising devices for many applications ranging from high-quantum-yield photocathodes to energy-saving radar tubes. Their working depends critically on keeping tip radii as closely as possible within the given specifications.

In principle, the following techniques are available for manufacturing large planar field-emitter arrays:

Bunching of fine wires.

Etching of undirectionally solidified eutectic alloys, yielding quasiregular arrays.

Preferential sputtering of oriented single crystals, yielding quasiregular arrays (Auciello, 1981).

Chemical vapor deposition of metals on flat surfaces (such surfaces could even be porous to transmit gases for creating field-ion sources).

A microlithographic shaping technique for generating regular arrays, incorporating a perforated gate electrode (Brodie and Spindt, 1979). Tip radii as small as 30 nm have been achieved. Arrays of 1 mm^2 area can be routinely produced with an areal density of the order of $\geq 10^5$ cones per cm^2. A current density of ≥ 10 A/cm^2 can be drawn from this array.

Microlithographic production of large semiconductor field-emission photocathodes, consisting of regular arrays of fine silicon points (Schroder *et al.*, 1974) and tip radii of the order of 10 nm have been obtained. This type of photocathode is unique in that it produces observable photoemission without requiring cesium as a low-work-function material. In addition, the silicon field-emitter array does not have a long-wavelength threshold like those of conventional photocathodes. Quantum yields as high as 25% have been measured at 0.86-μm wavelength. Uniform emission over several cm^2 has been obtained with a resolution of 10^4 pixels per cm^2.

An interesting alternative method for fabricating such large-area field-emitter arrays is the nuclear track technique: in this case, the field-emitter pins are statistically distributed. Much higher areal densities (above 10^8 pins per cm^2) can be easily achieved. Because the formation of conical shapes is already inherent in track etching, nuclear tracks should make much better starter structures than microlithographic techniques. The main advantage of track etching over conventional techniques is that several tedious processing steps, which have to be interrupted at just the right time, can be avoided. Since etched tracks are hollow structures, however, a replica technique has to be employed that fills the holes with a suitable ma-

terial. The shape, length, and direction of the needles can be adapted to given specifications over a broad range. The total area of such a field-emission device could be made much larger than 10^2 cm^2. However, up until now, field emission has not been observed experimentally for track-generated pin arrays. But large-area metallic pin arrays can be easily obtained by a metal deposition into etched tracks (Fig. 24).

b. Field emission of ions

Recently metallic-alloy-wetted field emitters have yielded very bright beams of singly-charged positive ions (Clampitt, 1981). In this case, the pins are at positive voltage with respect to the flat counterelectrode. Field-ion sources provide the missing link in generating high-intensity ion beams for scanning ion microscopes.

Such ion-optical systems depend vitally on the availability of high-emission ion sources. An interesting alternative to electron-impact ion sources is the "volcano" field-ion source (Aberth and Spindt, 1977). In this model, gas molecules are transmitted through the throat of the "volcano" from the back side of the field-ion source. They are drawn to its rim by dipole forces generated by its strong field gradient, and finally ionized in the close vicinity of the rim. At present, only single "volcano" field emitters can be manufactured, with a diameter of about 10 μm.

The nuclear track technique provides an interesting alternative method for generating such volcanos, using replica techniques. Hollow metallic microtubes can be obtained by metal deposition into etched tracks, followed by the selective removal of the matrix material (Fig. 25). Even large field-ion-emitter arrays could be produced in this way.

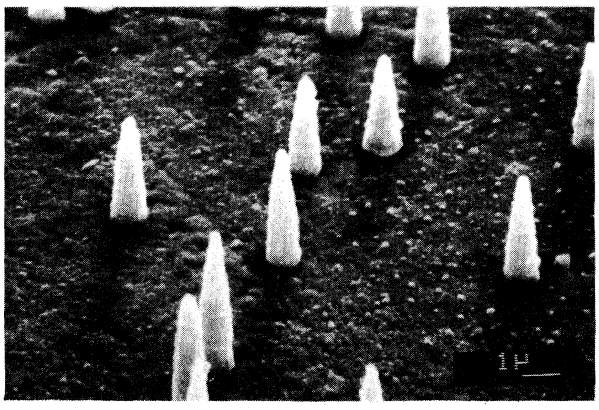

FIG. 24. Random field-emitter array, produced by a replica technique. The microscopic metal pins were obtained by a catalyst-activated copper deposition into etched nuclear track cones, followed by selective removal of the track-recorder material. Such field-emitter arrays could be used in the future as energy-saving cold cathodes in vacuum electronics devices.

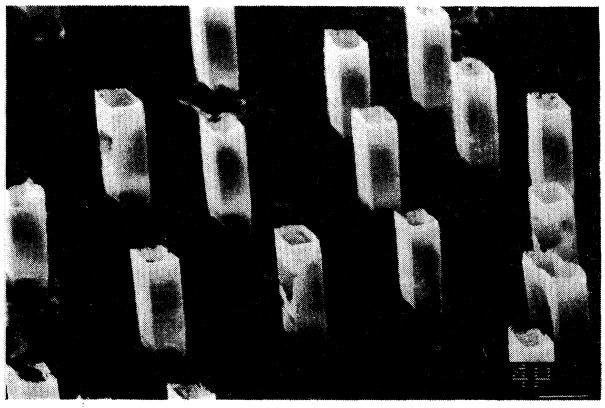

FIG. 25. Random array of hollow metallic microtubes of rhombic shape. The microtubes are obtained by metal deposition into etched nuclear tracks in mica, followed by selective removal of the matrix. Such microtube arrays could be used in the future as field-ion emitters, whereby a suitable gas would be admitted from the back of the structure, would penetrate through the microtubes, and would finally be ionized in the high electrostatic field at the rim of the microtubes.

c. Microcomposite materials

An essential feature of the weathering of fiber-reinforced polymer resins is the gradual destruction of the adhesion between fiber and resin matrix by diffused water. Polyester molding compounds, using thermosetting resins and reinforcing glass fibers, are important in the production of components for the aerospace and automotive industries, as well as for appliances, business machinery, and electrical equipment (Burns, 1982). Nuclear tracks provide a new approach to this adhesion problem, at least on the microscale, by forming "fused" fiber strands. Crisscrossing nuclear track arrays have a predictable intersection probability, which is governed by the mutual angle between the two track arrays and by the nominal porosity. The resulting pore structures can be filled by almost any arbitrary material. The track intersections lead to microcomposites with "fused" strands. Such microcomposites can be compared to three-dimensional polymerized resins in which strand breaking is a necessary condition for mechanical disruption. Figure 26 shows the "fused" fibers of such a track microscomposite generated for demonstration purpose. First, the crisscrossing track-etched holes in mica have been filled by polystyrene. Then the mica matrix has been removed by selective etching in order to be able to observe the fibers.

d. New electron devices

Nuclear tracks could be used for generating metal/oxide/metal point-contact diodes. This could be achieved, for example, by metal-replicating a conical nuclear track hole and overlaying a thin foil on top of the resulting metal pin. Point-contact diodes are used as

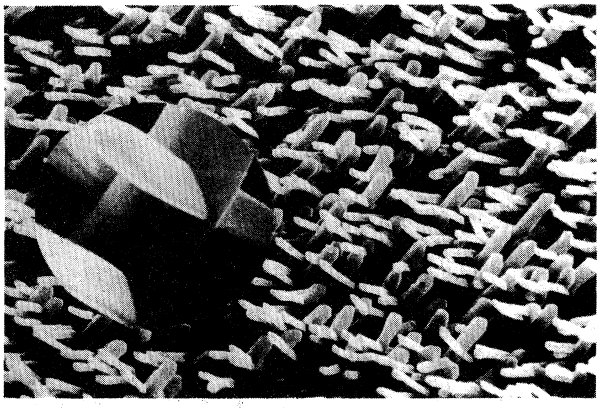

FIG. 26. Fused-fiber architecture of a nuclear track microcomposite. The mutually intersecting "fused" fibers form one coherent network, comparable to a three-dimensionally cross-linked polymer. For the purpose of observation, the matrix of the composite has been removed by selective etching. Nuclear track composites may eliminate the problem of slippage between fiber and matrix, common to conventional composite materials. In track-produced microcomposites the strands of different directions intersect each other, forming homogeneous "fused" joints (enlarged inset).

detectors, harmonic generators, and mixers in the ultrahigh-frequency range up to optical wavelengths. Their useful properties arise from their nonlinear current-voltage characteristics, based on their geometric asymmetry. This asymmetry leads to a potential barrier which is different for forward and backward bias. They can function as receiving antennas, converting laser radiation to an optical-frequency voltage across the diode.

Metal-filled tracks can be used for investigating the phenomenon of superconductivity in a one-dimensionally confined conductor (Possin, 1970).

B. Influencing local properties

1. Single-pore membranes

Single-pore membranes are the earliest example of a local structural change brought about by only one particle. They have several interesting applications.

a. Size and deformability of biological cells

The counting, sizing, and separation of individual living cells is rapidly becoming important in medical diagnostics. Conventional flow cytometry uses capillaries with inner diameters between 10 and 100 μm. One of the most ingenious and economical uses of etched tracks employs one single etched track to count, size, and measure the electrokinetic mobility of submicron-size particles (DeBlois *et al.*, 1977). It thus extends the scope of flow cytometry into the submicroscopic range.

The technique has been applied, more recently, to measure even an internal particle parameter, i.e., the deformability of individual red blood cells, which can be determined by the use of a measuring pore slightly smaller in diameter than the red blood cell itself (Roggenkamp *et al.*, 1981).

Red blood cells are doughnut shaped. They have a diameter of about 7.5 μm and a thickness between 1 and 2 μm. Under normal circumstances, the extremely flexible cells have no problem at all "squeezing" through the considerably finer capillaries of the human body, whose minimum diameters are between 3 and 5 μm. However, disturbances in the plasticity of red blood cells can have far-reaching consequences. Many diseases of the heart and circulatory system have been traced, in recent years, to an insufficient deformability of the red blood cells; consequently, extensive research on the flow behavior of blood in the capillary network has been and is currently being carried out. Blood rheology has been considerably advanced by new methods for observing the flow of blood in the microcirculatory system and influencing this flow by drugs. One of these methods is the measurement of the passage times of red blood cells through a single-pore membrane (Fig. 27). The passage times are directly related to the rigidity of the red blood cells: The stiffer a cell is, the longer it takes to pass through the pore.

To produce a single-pore membrane, one shoots a very fine ion beam of very low intensity through a plastic foil. A particle which has passed through the foil is registered by an electronic particle counter, and the ion beam is switched off to avoid double irradiation.

The single-pore membrane becomes the central unit of a measuring cell, dividing the cell into upper and lower compartments (Roggenkamp *et al.*, 1982). The measuring pore has a precisely known diameter of 5 μm, and its length corresponds to the thickness of the membrane. Only one human red blood cell at a time, can "squeeze"

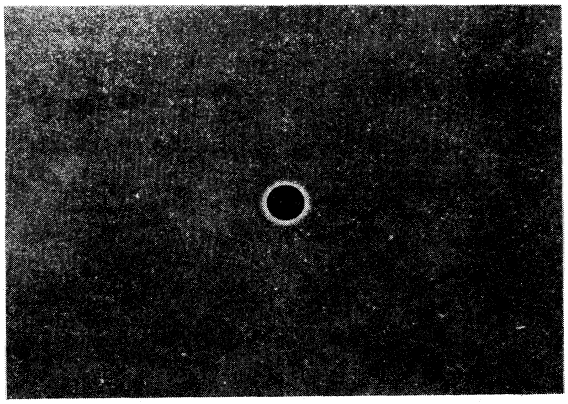

FIG. 27. Single-pore membrane generated in a thin polycarbonate foil. Single pores are used in biology and medicine, for example, as counting apertures for measuring the number, size, mobility, and deformability of particles suspended in solution. The etched track hole shown in this micrograph is produced by the passage of exactly one ion through a foil of 30 μm thickness and 30 mm diameter. The central hole has a diameter of 5 μm (0.005 mm).

itself through this artificial capillary. The pressure difference between the upper and lower compartments of the measuring cell is kept constant and corresponds to the conditions in the human body.

The red blood cell activates an optical or electrical switch as it enters and exits from the capillary. The time difference is registered in a microprocessor system. Many red blood cells are measured in succession to obtain the passage time spectrum, representing the different degrees of deformability. Immediate conclusions on the health of the blood can be drawn from this curve. The effects of a drug, as studied in pharmacology, can be assessed on the level of the individual cells before starting any experiments with patients.

b. Pinhole apertures

Laser technology requires high-precision apertures for defining point sources. Apertures have the additional function of suppressing fringe beams in electron and ion optical systems for obtaining a defined beam profile without a halo of scattered particles. At present, the smallest commercially available pinholes are about 1 μm in diameter. Nuclear track technology provides an economic alternative for even much smaller holes. Figure 28 shows a cross section through an asymmetric aperture generated in a thin cover glass used in optical microscopy. Due to the very high homogeneity of the glass, a very smooth circular aperture is obtained.

c. Gas-inlet leaks

Single-pore membranes can be used, in vacuum technology, as calibration leaks with a leak ratio defined by the pore size. On the other hand, single-pore membranes can be used, in mass spectrometry, as gas-inlet leaks withstanding pressure differences of several atmospheres. The gas enters directly from the high-pressure side of the pore into the vacuum, thereby eliminating the problem of diffusion-induced separation of molecules of different weight, a phenomenon that is encountered in differentially pumped systems.

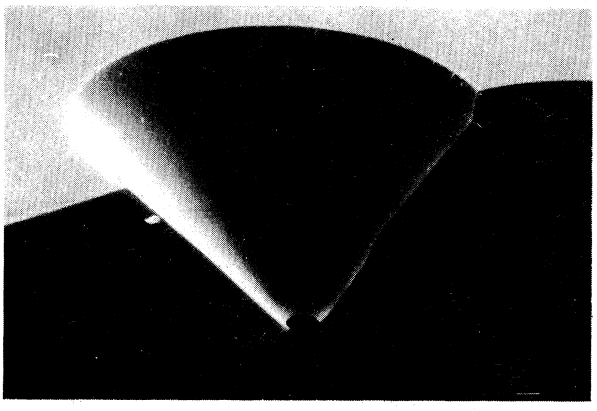

FIG. 28. Cross section through an asymmetrically etched track cone in a thin cover glass used in optical microscopy, obtained by breaking. Due to the very high homogeneity of glass, very smooth circular apertures can be obtained. The perforation was performed in a conductivity cell, exclusively attacking from the top surface, and was interrupted as soon as a preset electrical conductivity through the etched holes had been reached.

d. Superfluidity

Present-day cryogenics requires an understanding of the behavior of small leaks at liquid-helium temperatures. Tapered holes of 0.1 μm minimum diamater can be generated using conventional techniques (Sinharoy and Lange, 1982). The procedure involves laser drilling, followed by galvanotechnic copper deposition. The nuclear track technique provides a simpler way to obtain even smaller holes. Commercial nuclear track membranes have already been used to investigate the superfluid flow in liquid helium (Gamota, 1973).

2. Heavy-ion lithography

Photolithography, one of the important technological developments of applied science, evolved into its present-day scientific status from a rather obscure art initiated around the middle of the 19th century. During the last decades, this technique has been dramatically refined, by the use of uv light, x rays, and electron-beam exposure, making possible submicrometer structures of about 0.1 μm width, with a maximum aspect ratio (depth to width) of ten to one. Within the above context, nuclear track technology seems to be the next natural step toward finer and deeper structures.

Lithographic techniques (Broers, 1979), which conventionally involve irradiation with visible and uv light, x rays, or electron beams, have played a major role in the progress of semiconductor technology. They are one of the main tools used to create fine structures on solid surfaces. Over the last few decades, almost every year the packing density of integrated circuits has doubled, and the price per active element has decreased continuously. For some years, microprocessors have been performing tasks of ever increasing complexity. More recently, highly focused ion beams have been used to obtain very fine patterns for microelectronics applications (Seliger *et al.*, 1979; Stengl *et al.*, 1979).

However the capabilities of conventional techniques using visible light, uv, x rays, or electron beams are almost realized by now, at least in the research laboratory. Simultaneously with electron beam scribing and x-ray lithography (Spiller and Feder, 1977), at present, the applicability of heavy-ion beams in microstructure technology is being explored (Hall *et al.*, 1980). In contrast to conventional techniques, heavy-ion lithography offers a way to generate very fine and, at the same time, very deep structures (Yang *et al.*, 1978; Seliger *et al.*, 1979; Fischer *et al.*, 1980). Heavy-ion lithography involves the use of a mask, which is projected onto a track-sensitive substrate by using a heavy-ion beam (Fig. 29). The high beam col-

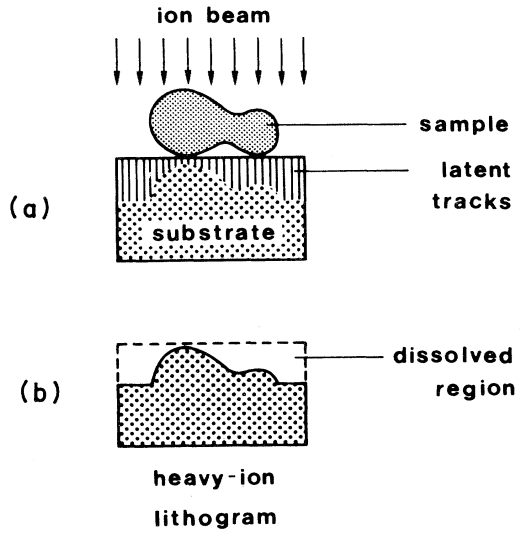

FIG. 29. Principle of heavy-ion lithography: recording and revealing. (a) *Recording* the areal density distribution of the sample in a track-recording substrate in the form of latent tracks of different lengths. The use of a highly parallel ion beam allows the maintenance of a considerable distance between the object and the track-recording substrate. (b) *Revealing* the resulting range envelope by track etching in the form of a relief, achieved as soon as a sufficient overlap occurs between neighboring tracks. The relief elevation corresponds directly to the areal density of the sample, projected along the axis of the ion beam.

limation attainable with this technique is an essential condition for such a projection scheme, and allows one, at the same time, to locate the object and track-recording material at a relatively large distance from each other. The resulting relief elevation is directly related to the projected areal density of the mask. This feature adds a third dimension to conventional planar lithography, in which relief elevation depends very sensitively on the time of development and is therefore, in most cases, defined directly by the thickness of the deposited layer. Up until now, depth could not be defined directly by the depth dependence of the irradiation itself. Rather it was defined by the depth of the sensitive layer on top of the substrate. The well-defined depth observed in ion lithography, however, is inherent in the well-defined ion range. Exponentially decaying radiation damage, occurring for photons and electrons, is not suited for this purpose. Another important advantage of ion lithography over x-ray lithography is the ease with which ion beams can be created, accelerated, and deflected. Heavy-ion lithography may ultimately be used to create structures close to the natural limits of digital electronics (Keyes, 1975; Wallmark, 1975), as given by local fluctuations due to the finite size of the atoms.

Owing to the very high damage density of heavy ions, the technique is not restricted to photosensitive materials. Almost any insulating material is sensitive to heavy ions. This enables one to use silicon dioxide layers, for example, already existing on commerically available silicon wafers, as a new type of "photoresist." The silicon dioxide film serves as a passivation layer of very uniform thickness on top of the silicon. Its thickness can be adjusted by heat treatment in an oxidizing atmosphere. Compared to organic polymers, silicon dioxide is a very homogeneous material down to the atomic scale. Therefore this inorganic "resist" has a very high resolution.

Figure 30 shows the heavy-ion lithogram of a very fine metal grid which has been used as a shadow-casting mask. The mask has been projected onto a silicon dioxide layer of about 0.2 μm thickness on top of a silicon wafer. The distance of projection (about 1 mm) was more than ten thousand times larger than the observed resolution (about 0.1 μm). The use of this large projection distance is possible due to the high collimation of the ion beam.

Nuclear stopping yields the strongest contribution to range and angular straggling, and is a limiting factor for the lateral and depth resolution that can ultimately be achieved in heavy-ion lithography. It is responsible for most of the permanent radiation damage observed in metals. Nuclear stopping close to the stopping point ($\lesssim 1$ μm) provides sufficient damage density in single-crystal semiconductors to make them susceptible to a preferential etching process. Very likely this holds also for metals. The amorphizing action of heavy ions (Gibbons, 1972) gives rise to drastic changes in the bulk etch rate of the material. For example, silicon single crystals can be selectively etched just at the onset of amorphization using dislocation-sensitive etchants. In this way, grating patterns with submicron periods can be engraved on Si sub-

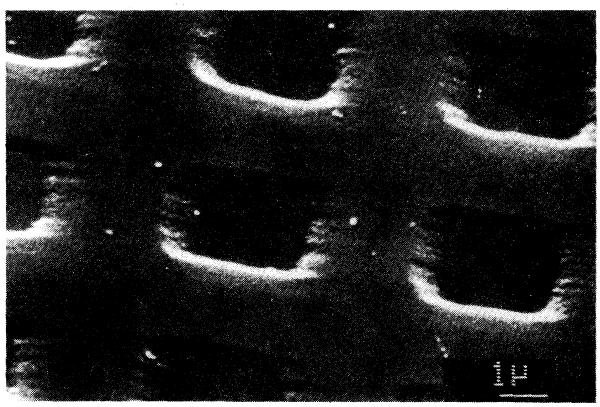

FIG. 30. Silicon dioxide, applied as a high-resolution "resist." SiO_2 exists as a passivating layer of very uniform thickness and homogeneity on commercially available silicon wafers. Subjected to heavy ions, it can be thought of as an "inherent" resist of very uniform thickness. Its high spatial resolution is due to the high homogeneity of the glassy material. In this scanning electron micrograph, $\lesssim 0.1$ μm can be discerned in the toothed fine structure, replicating the irregularities of the projected metallic micromesh. The mesh was kept at a projection distance of 1000 μm, which is very large compared to the finest resolved structure (the observed lateral smearing is due to slipping between mask and resist during the exposure). The metallic micromesh was provided through courtesy of P. Tischer, Siemens AG, Munich, FRG.

strates with an accuracy of 0.01 μm (Moriwaki *et al.*, 1979).

In addition to its use as a microlithographic structuring tool, heavy-ion lithography has a considerable potential as a tool for observing the inner details of microscopic objects. This is possible without dissecting the object (Fig. 31). Already a single ion is capable of measuring density variations of the order of a few percent, making possible observation with very little associated radiation damage per picture element.

Heavy-ion radiography (Benton *et al.*, 1973), which involves relativistic energies, is an extension of heavy-ion lithography. For specific ion energies of the order of a hundred MeV per nucleon, where ion ranges are of the order of 10 cm, medical diagnostics and cancer treatment become possible. Heavy-ion radiography uses a thick stack of plastic sheets for recording the projected areal density of a macroscopic object. The different plastic sheets are etched separately after the irradiation. Only the track "endpoints" are revealed by etching due to the low energy loss of relativistic ions. Computer tomograms with high-density contrast can be obtained, by using multiple irradiations under different angles.

3. Prospects of scanning ion microbeams

The nuclear track technique has been almost exclusively employed, until now, for generating many statistically independent tracks. Because of the broad-beam radiation used, the tracks are distributed homogeneously but randomly over the sample area. Nevertheless, an astonishingly wide range of effects can be observed. Etched nuclear tracks depend mainly on the material, the irradiation, and the etching conditions. Accordingly, global property modifications are achieved by the "concerted" action of many randomly distributed tracks of defined size, range, and orientation.

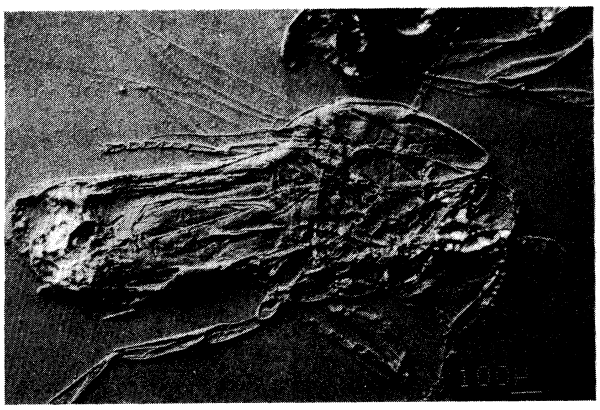

FIG. 31. Density mapping of a small insect by heavy-ion lithography. Because of their well-defined range, heavy ions are very sensitive probes for sampling the density of inhomogeneous objects. Like diagnostic x rays in medicine, they make the inner details of an object accessible from outside, without dissecting the object. The relief elevation corresponds directly to the projected areal density distribution of the object. Density differences of a few percent can easily be discerned.

There exist already two exceptions in the above described examples pointing to the controllability of two further beam properties:

Local confinement of the ion beam. A single-pore membrane is generated by exactly one, locally confined heavy ion, for example.

Modulation of ion range. In this case, heavy-ion lithography uses a broad beam that is laterally modulated in its ion range.

A qualitatively new aspect of nuclear track technology is the generation of tracks at predetermined sites on a solid surface. Regular track arrays can be generated in this way, as well as arbitrary track patterns. Thus the full spectrum of possibilities of a "micromilling machine" can be achieved, in constrast to conventional lithographic techniques, which are confined to relatively shallow structures close to the surface. Nuclear track technology, "drills" submicron-size holes of many microns length and arbitrary direction. It may even be possible, in the future, to modulate the penetration range of the scanning ion beam. Therefore, the scanning ion microprobe has a good chance of becoming the "ultimate" tool in a future microstructure technology. At present, several scanning ion microprobes are being constructed worldwide, which could be used for producing nuclear tracks in a precisely controlled manner.

IV. CONCLUSION

During the past decade, when the nuclear track technique has been used mainly as a "detector" of heavy ions in nature, the scientific community has gradually become aware of the applicability of the technique as a structuring tool. This technique surpasses all previously available "drilling" tools with respect to the smallest attainable hole size, rate of production, and hole length-to-diamater ratio. It can be applied to a wide variety of homogeneous dielectric materials. Replica techniques can be used to transfer the generated structures to virtually any arbitrary material, for example, metals. Developing techniques other than track etching, such as track grafting and other decoration techniques, while still in their infancy, multiply the shaping potential of the technique tremendously.

At present, mainly statistical distributions of tracks are used, to change the global (bulk) properties of solids. With such distributions, an arbitrary axis of anisotropy, given by the track direction, can be simultaneously introduced into an originally isotropic solid. These global applications cover a wide range of surface and volume properties. Easily accessible radiation sources, such as fission-fragment sources, nuclear reactors, and small heavy-ion accelerators (for example, ion implanters used in microcircuit technology) can provide a valuable testing ground for commercial applications that eventually will require larger heavy-ion accelerators. In the future, scanning ion machines will also be able to confine the scribing ion beams locally, thus creating a very powerful microtool

in which individual particles can be used to generate three-dimensional submicroscopic patterns.

ACKNOWLEDGMENTS

Substantial contributions to this review were provided through critical comments and suggestions from the following persons: O. Auciello, R. Brandt, R. L. Fleischer, K. O. Groeneveld, G. Haase, P. Hansen, H. Heitmann, R. W. Keyes, H. Kiesewetter, G. zu Putlitz, H. G. Roggenkamp, E. Schopper, K. Thiel, L. Tommasino, F. Zoergiebel.

REFERENCES

Aberth, W., and C. A. Spindt, 1977, "Characteristics of a Volcano Field Ion Quadrupole Mass Spectrometer," Int. J. Mass Spectrom. Ion Phys. **25**, 183.

Ahlen, S. P., P. B. Price, and G. Tarle, 1981, "Track-Recording Solids," Phys. Today **34**, No. 9, 32.

Ahlen, S. P., and G. Tarle, 1983, "Observation of Large Deviations from the Bethe-Bloch Formula for Relativistic Uranium Ions," Phys. Rev. Lett. **50**, 1110.

Ahlen, S. P., G. Tarle, and P. B. Price, 1982, "Studies of Relativistic Uranium Nuclei with Dielectric Track Detectors," Science **217**, 1139.

Albrecht, D., P. Armbruster, B. E. Fischer, C. Riedel, and R. Spohr, 1981, "Small Angle Neutron Scattering from Oriented Latent Nuclear Tracks," Gesellschaft für Schwerionenforschung, Nachrichten 12-81, p.3.

Albrecht, D., P. Armbruster, M. Roth, and R. Spohr, 1982, "Small Angle Neutron Scattering Observations from Oriented Latent Nuclear Tracks," in *Proceedings of the 11th International Conference on Solid State Nuclear Track Detectors, Bristol, 7–12 September, 1981,* edited by P. H. Fowler and V. M. Clapham (Pergamon, Oxford), available as Nucl. Tracks Suppl. 3, p. 55.

Ali, A., and S. A. Durrani, 1977, "Etched-Track Kinetics in Isotropic Detectors," Nucl. Track Detection **1**, 107.

Amin, S. A., and D. L. Henshaw, 1981, "Effect of Various Etching Solutions on the Response of CR-39 Plastic Track Detector," Nucl. Instrum. Methods **190**, 415.

Anderson, J. L., and J. A. Quinn, 1974, "Restricted Transport in Small Pores. A Model for Steric Exclusion and Hindered Particle Motion," Biophys. J. **14**, 130.

Aschenbach, J., G. Fiedler, H. Schreck-Köllner, and G. Siegert, 1974, "Special Glasses as Energy Detectors for Fission Fragments," Nucl. Instrum. Methods **116**, 389.

Auciello, O., 1981, "Ion Interaction with Solids: Surface Texturing, Some Bulk Effects, and their Possible Applications," J. Vac. Sci. Technol. **19**, 841.

Bangert, U., K. Thiel, and W. Herr, 1979, "Untersuchung schwerionen-induzierter Thermolumineszenz," Gesellschaft für Schwerionenforschung, Darmstadt, FRG, Report 79-11, p. 142.

Barraud, A., 1980, "Interface and Monomolecular Film Solid State Reactions. Application to Microlithography," in *Proceedings of the Symposium on Electron and Ion Beam Science and Technology, 9th International Conference,* edited by R. Bakish (Electrochemical Society, Pennington, New Jersey), p. 365.

Beck, R. E., and J. S. Schultz, 1972, "Hindrance of Solute Diffusion within Membranes as Measured with Microporous Membranes of Known Pore Geometry," Biochim. Biophys. Acta **255**, 273.

Belyaev, A. D., I. I. Bahromi, N. V. Beresina, Z. S. Bikbova, A. A. Gorevoi, V. I. Kogan, A. I. Muminov, V. P. Pikul, and A. M. Usmandiarov, 1979, "Relation of Fission-Fragment Ranges to Mica Crystal Orientation," Nucl. Tracks **4**, 53.

Benton, E. V., 1970, "On Latent Track Formation in Organic Nuclear Charged Particle Detectors," Radiat. Eff. **2**, 273.

Benton, E. V., and R. P. Henke, 1969, "Heavy Particle Range-Energy Relations for Dielectric Nuclear Track Detectors," Nucl. Instrum. Methods **67**, 87.

Benton, E. V., R. P. Henke, and C. A. Tobias, 1973, "Heavy Particle Radiography," Science **182**, 474.

Blok, H., F. Hanappe, F. M. Kiely, B. D. Pate, and J. Peter, 1974, "Further Measurements of the Track Lengths of Heavy Ions in Mica," Nucl. Instrum. Methods **119**, 307.

Bogenschütz, A. F., 1967, *Aetzpraxis für Halbleiter* (Carl Hanser, München).

Brault, R. G., and L. J. Miller, 1980, "A Method for Rapidly Screening Polymers as Electron-Beam Resists," in *Proceedings of the Symposium on Electron and Ion Beam Science and Technology, 9th International Conference,* edited by R. Bakish (Electrochemical Society, Pennington, New Jersey), p. 341.

Brodie, I., and C. A. Spindt, 1979, "The Application of Thin-Film Field-Emission Cathodes to Electronic Tubes," Appl. Surf. Sci. **2**, 149.

Broers, A. N., 1979, "High-Resolution Systems for Microfabrication," Phys. Today **32**, No. 11, 38.

Burns, R., 1982, *Polyester Molding Compounds* (Dekker, New York).

Cannel, D. S., and F. Rondelez, 1980, "Diffusion of Polystyrenes through Microporous Membranes," Macromolecules **13**, 1599.

Cartwright, B. G., E. K. Shirk, and P. B. Price, 1978, "A Nuclear-Track-Recording Polymer of Unique Sensitivity and Resolution," Nucl. Instrum. Methods **153**, 457.

Chatterjee, A., and J. L. Magee, 1980, "Energy Transfer from Heavy Particles," Lawrence Berkeley Laboratory Report LBL-112 20/UC-48, p. 53.

Clampitt, R., 1981, "Advances in Molten Metal Field Ion Sources," Nucl. Instrum. Methods **189**, 111.

Craighead, H. G., R. E. Howard, J. E. Sweeney, and D. M. Tennant, 1982, "Textured Surfaces: Optical Storage and Other Applications," J. Vac. Sci. Technol. **20**, 316.

Dartyge, E., J. P. Duraud, Y. Langevin, and M. Maurette, 1981, "New Model of Nuclear Particle Tracks in Dielectric Minerals," Phys. Rev. B **23**, 5213.

Datz, S., and C. D. Moak, 1982, "Heavy Ion Channeling," Oak Ridge National Laboratory, Physics Division preprint.

Dearnaley, G., 1975, "Ion Implantation," Nature **256**, 701.

DeBlois, R. W., C. P. Bean, and R. K. A. Wesley, 1977, "Electrokinetic Measurements with Submicron Particles and Pores by the Resistive Pulse Technique," Colloid Interface Sci. **61**, 323.

DeForest, W. S., 1975, *Photoresist Materials and Processes* (McGraw-Hill, New York).

DeSorbo, W., 1979, "Ultraviolet Effects and Aging Effects on Etching Characteristics of Fission Tracks in Polycarbonate Film," Nucl. Tracks **3**, 13.

DeSorbo, W., and H. E. Cline, 1970, "Metal Membranes with Uniform Submicron-Size Pores," J. Appl. Phys. **41**, 2099.

Dienes, G. J., and G. H. Vineyard, 1957, *Radiation Effects in*

Solids, Vol. 2 of Interscience Monographs in Physics and Astronomy, edited by R. E. Marshak (Interscience, New York).

Dole, M., 1973, Ed., *The Radiation Chemistry of Macromolecules* (Academic, New York), Vols. 1 and 2.

Dran, J. C., M. Maurette, and J. C. Petit, 1980, "Radioactive-Waste Storage Materials: Their Alpha-Recoil Aging," Science **209**, 1518.

Dürolf, H., B. Genswürger, and R. Spohr, 1978, "Eignungsuntersuchung von photoaetzbarem Glas als Kernspurmaterial," Gesellschaft für Schwerionenforschung Jahresbericht 1977, GSI-J-1-78, p. 131.

Edmonds, E. A., and S. A. Durrani, 1979, "Relationships between Thermoluminescence, Radiation-Induced Electron Spin Resonance and Track Etchability of Lexan Polycarbonate," Nucl. Tracks **3**, 3.

Enge, W., 1980, "Introduction to Plastic Nuclear Track Detectors," Nucl. Tracks **4**, 283.

Fain, J., M. Monnin, and M. Montret, 1974, "Energy Density Deposited by a Heavy Ion around Its Path," in *Proceedings of the 4th Symposium on Microdosimetry, Verbania, Italy, 1973* (Commission of the European Communities, Luxembourg), NSA **30**, No. 14379, 169.

Fischer, B. E., D. Albrecht, and R. Spohr, 1982, "Preparation of Superinsulating Surfaces by the Nuclear Track Technique," Radiat. Eff. **65**, 143.

Fischer, B. E., B. Genswürger, and R. Spohr, 1980, "Heavy Ion Lithography: A Tool for the Investigation and Replication of Microscopic Objects," Int. J. Appl. Radiat. Isot. **31**, 297.

Fleischer, R. L., 1980, "Isotopic Disequilibrium of Uranium: Alpha-Recoil Damage and Preferential Solution Effects," Science **207**, 979.

Fleischer, R. L., 1981, "Nuclear Track Production in Solids," Prog. Mater. Sci. ***X***, 97.

Fleischer, R. L., P. B. Price, and R. M. Walker, 1975, *Nuclear Tracks in Solids: Principles and Applications* (University of California, Berkeley).

Fleischer, R. L., P. B. Price, and R. T. Woods, 1969, "Nuclear Particle Track Identification in Inorganic Solids," Phys. Rev. **188**, 563.

Flerov, G. N., Joint Institute for Nuclear Reactions, Dubna, USSR, private communication.

Flerov, G. N., V. I. Kuznetsov, B. I. Verkin, R. S. Mikhal'chenko, and N. P. Pershin, 1982, "Waermephysikalische und gasdynamische Eigenschaften von Waermeabschirmisolation im Vakuum auf der Basis von polymeren Kernspurfiltern," in *Bericht der 4. Konferenz über die Anwendung neuer kernphysikalischer Methoden zur Loesung von wissenschaftlich-technischen und volkswirtschaftlichen Aufgaben,* Gesellschaft für Schwerionenforschung Translation 82-16. Original in Russian: Joint Institute for Nuclear Reactions P 18-82-117, Dubna.

Fowler, P. H., and V. M. Clapham, 1982, Eds., *Proceedings of the 11th International Conference on Solid State Nuclear Track Detectors, Bristol, 7—12 September, 1981* (Pergamon, Oxford), available as Nucl. Tracks Suppl. 3.

François, H., N. Kurtz, J. P. Massue, M. Monnin, R. Schmitt, and S. A. Durrani, 1980, Eds., *Proceedings of the 10th International Conference on Solid State Nuclear Track Detectors, Lyon, 2—6 July, 1979* (Pergamon, Oxford), available as Nucl. Tracks Suppl. 2.

Frischkorn, H. J., K. O. Groeneveld, P. Koschar, R. Latz, and J. Schader, 1982, "Observation of Heavy Ion Induced Wake Potential Interference Effects," Phys. Rev. Lett. **49**, 1671.

Gamota, G., 1973, "Creation of Quantized Vortex Rings in Superfluid Helium," Phys. Rev. Lett. **31**, 517.

Geissel, H., 1982, "Untersuchungen zur Abbremsung von Schwerionen in Materie im Energiebereich von (0.5—10) MeV/*u*," Gesellschaft für Schwerionenforschung Report 82-12.

Geissel, H., P. Armbruster, T. Kitahara, G. Kraft, H. Spieler, and K. Guettner, 1980, "Energy Loss of Heavy Particles in Solid Materials," Nucl. Instrum. Methods **170**, 217.

Geissel, H., Y. Laichter, W. F. W. Schneider, and P. Armbruster, 1981, "Energy Loss and Energy Loss Straggling of Fast Heavy Ions in Matter," Gesellschaft für Schwerionenforschung, Darmstadt, FRG, preprint GSI-81-33.

Geissel, H., Y. Laichter, W. F. W. Schneider, and P. Armbruster, 1982a, "Stopping Powers and Ranges of (0.1—2.4) GeV Uranium Ions in Solids," in *Proceedings of the Symposium on Accelerator Aspects of Heavy Ion Fusion, Darmstadt, FRG, May 29—April 2, 1982,* (Gesellschaft für Schwerionenforschung, Darmstadt), GSI Report 82-8, p. 578.

Geissel, H., Y. Laichter, W. F. W. Schneider, and P. Armbruster, 1982b, "Stopping Powers and Ranges of (0.1—2.4) GeV Uranium Ions in Solids," in Ph.D. Thesis (Justus Liebig-Universitaet, Fachbereich 13, Giessen D26, FRG).

Gemmel, D. S., 1974, "Channeling and Related Effects in the Motion of Charged Particles through Crystals," Rev. Mod. Phys. **46**, 129.

Gibbons, J. F., 1972, "Ion Implantation in Semiconductors. Part II: Damage Production and Annealing," Proc. IEEE **62**, 1062.

Glaser, D. A., 1954, Nuovo Cimento **2**, Suppl. No. 2, 361.

Glaser, D. A., 1958, "The Bubble Chamber," in *Encyclopedia of Physics. Vol. XLV. Nuclear Instrumentation II,* edited by S. Flügge and E. Creutz (Springer, Berlin), p. 314.

Gold, R., J. H. Roberts, and F. H. Ruddy, 1981, "Annealing Phenomena in Solid State Track Detectors," Nucl. Tracks **5**, 253.

Granzer, F., and E. Moisar, 1981, "Der Photographische Elementarprozess in Silberhalogeniden. Teil II," Phys. in unserer Zeit. **12.2**, 36.

Granzer, F., H. Paretzke, and E. Schopper, 1978, Eds., *Proceedings of the 9th International Conference on Solid State Nuclear Track Detectors, Munich, 30 Sept.—6 Oct., 1976* (Pergamon, Oxford), available as Nucl. Tracks Suppl. 1.

Griffith, J. E., Y. Qiu, and T. A. Tombrello, 1982, "Ion-Beam-Enhanced Adhesion in the Electronic Stopping Region," Nucl. Instrum. Methods **198**, 607.

Groeneveld, K. O., E. Schopper, and S. Schumann, 1980, "Atomic Displacement Effects from Heavy Ion Induced Coulomb Explosions," in *Proceedings of the 9th International Conference on Solids State Nuclear Track Detectors, Munich, 30 Sept.—6 Oct., 1976,* edited by F. Granzer, H. Paretzke, and E. Schopper (Pergamon, Oxford), available as Nucl. Tracks Suppl. 1, p. 81.

Gruhn, T. A., and E. V. Benton, 1982, "The Chemical Basis of the Photo-Oxidative Enhancement of Track Etching in the Polycarbonate of Bisphenol-A," Nucl. Tracks Suppl. **3**, 69.

Guillot, G., and F. Rondelez, 1981, "Characteristics of Submicron Pores Obtained by Chemical Etching of Nuclear Tracks in Polycarbonate Film," J. Appl. Phys. **52**, 7155.

Güttner, K., S. Hofmann, D. Marx, G. Münzenberg, and F. Nickel, 1977, "Range and Range Straggling of Heavy Ions in Solids," Nucl. Instrum. Methods **146**, 413.

Haase, G., E. Schopper, and F. Granzer, 1977, "Solid State Nuclear Track Detectors: Track Forming, Stabilizing and Development Processes," Radiat. Eff. **34**, 25.

Haase, G., E. Schopper, and F. Granzer, 1978, "Solid State Nuclear Track Detectors: Track Forming, Stabilizing and Development Processes," in *Proceedings of the 9th International Conference on Solid State Nuclear Track Detectors, Munich, 30 Sept.—6 Oct., 1976,* edited by F. Granzer, H. Paretzke, and E. Schopper (Pergamon, Oxford), available as Nucl. Tracks Suppl. 1, p. 199.

Haase, G., F. Zörgiebel, E. Schopper, F. Granzer, G. Henig, J. U. Schott, and F. Wendnagel, 1973, "Silver Halide Crystals as Particle Track Detectors," Photog. Sci. Eng. **17**, 409.

Hall, T. M., A. Wagner, and L. F. Thompson, 1980, "Ion Beam Exposure Characteristics of Resists," J. Vac. Sci. Technol. **16**, 1889.

Hansen, P., and H. Heitmann, 1979, "Influence of Nuclear Tracks on the Magnetic Properties of a $(Gd,Bi)_3(Fe,Ga)_5O_{12}$ Garnet Film," Phys. Rev. Lett. **43**, 1444.

Hansen, P., H. Heitmann, and P. H. Smit, 1982, "Nuclear Tracks in Iron Garnet Films," Phys. Rev. B **26**, 3539.

Hansen, P., H. Heitmann, B. Strocka, and R. Spohr, 1983, "Der Einfluss von Ionenstrahlen auf die magnetischen Eigenschaften von ferrimagnetischen Schichten," BMFT Report FB T83-048, Fachinformationszentrum Karlsruhe, D-7514 Eggenstein-Leopoldshafen 2, FRG.

Heitmann, H., C. Fritzsche, P. Hansen, J. P. Krumme, R. Spohr, and K. Witter, 1978, "Influence of Irradiation with High Energetic Ions on Storage Properties of Magneto-Optic $(Gd,Bi)_3(Fe,Ga)_5O_{12}$ Epitaxial Films," J. Magn. Magn. Mater. **7**, 40.

Heitmann, H., and P. Hansen, 1982, "The Healing Behavior of Nuclear Tracks in Yttrium Iron Garnet Films," J. Appl. Phys. **53**, 7321.

Henke, R. P., and E. V. Benton, 1971, "On Geometry of Tracks in Dielectric Nuclear Track Detectors," Nucl. Instrum. Methods **97**, 483.

Henschel, H., A. Kohnle, H. Hipp, and G. Goennenwein, 1981, "Absolute Measurement of Velocities, Masses and Energies of Fission Fragments from Californium-252 (SF)," Nucl. Instrum. Methods **190**, 125.

Hepburn, C., and A. H. Windle, 1980, "Solid State Nuclear Track Detectors," J. Mater. Sci. **15**, 279.

Hilderbrand, D., and E. V. Benton, 1980, "The Chemical Etching Behavior of Cellulose Nitrate," Nucl. Tracks **4**, 77.

Hill, B., and K. P. Schmidt, 1978, "Fast Switchable Magneto-Optic Memory Display Components," Philips Res. Rep. 33, 211.

Huang, W. H., and R. M. Walker, 1967, "Fossil α-Particle Recoil Tracks: A New Method of Age Determination," Science **155**, 1103.

Hubert, F., A. Fleury, R. Bimbot, and D. Gardes, 1980, "Range and Stopping-Power Tables for 2.5—100 MeV/Nucleon Heavy Ions in Solids," Ann. Phys. (Paris) **5**, 1.

Hyde, E. K., 1964, *The Nuclear Properties of the Heavy Elements. Volume III. Fission Phenomena* (Prentice-Hall, Englewood Cliffs, New Jersey).

Jones, F., and J. Paraszszak, 1981, "RD3D (Computer Simulation of Resist Development in Three Dimensions)," IEEE Trans. Electron Devices **ED-28**, 1544.

Katz, R., 1978, "Track Structure Theory in Radiobiology and in Radiation Detection," Nucl. Track Detection **2**, 1.

Katz, R., and E. J. Kobetich, 1968, "Formation of Etchable Tracks in Dielectrics," Phys. Rev. **170**, 401.

Keilmann, F., 1981, "Infrared High-Pass Filter with High Contrast," Int. J. Infrared Millimeter Waves **2**, 259.

Kendall, D. L., 1979, "Vertical Etching of Silicon at Very High Aspect Ratios," Annu. Rev. Mater. Sci. **9**, 373.

Keyes, R. W., 1975, "Physical Limits of Digital Electronics," Proc. IEEE **63**, 740.

Khan, H. A., N. A. Khan, and R. Spohr, 1981, "Scanning Electron Microscope Analysis of Etch Pits Obtained in a Muscovite Mica Track Detector by Etching in Hydro-Fluoric Acid and Aqueous Solutions of NaOH and KOH," Nucl. Instrum. Methods **189**, 577.

Khan, H. A., and K. Kristiansson, 1980, Eds., "Solid State Nuclear Track Detectors," *International Spring School on the Development and Application of Solid State Nuclear Track Detectors, Rawalpindi, March 5—14, 1979,* Nucl. Instrum. Methods **173**.

Klein, N., 1969, "Electrical Breakdown in Solids," Adv. Electron. Electron Phys. **26**, 309.

Klump, B., and D. Woermann, 1977, "Study of Mica Membranes with Known Pore Geometry. Measurements of Electrical Conductivity," Ber. Bunsenges. Phys. Chem. **81**, 92.

Knippelberg, W., O. Becker, and K. Wien, 1982, "A Comparison of Fission Fragment Induced Ion Emission from Metallic and Dielectric Films," Nucl. Instrum. Methods **198**, 59.

Koh, W. H., and J. L. Anderson, 1975, "Electroosmosis and Electrolyte Conductance in Charged Microcapillaries," AIChE J. **21**, 1176.

Komaki, Y., 1979, "Growth of Fine Holes by the Chemical Etching of Fission Tracks in Polyvinylidene Fluoride," Nucl. Tracks **3**, 33.

Krumme, J. P., I. Bartels, B. Strocka, K. Witter, Ch. Schmelzer, and R. Spohr, 1977, "Pinning of 180° Bloch Walls at Etched Nuclear Tracks in LPE-Grown Iron Garnet Films" J. Appl. Phys. **48**, 5191.

Kuznetsov, V. I., P. Yu. Apel, and L. I. Samojlova, 1982, "Nukleare Mikrofilter," in *Bericht der 4. Konferenz über die Anwendung neuer kernphysikalischer Methoden zur Loesung von wissenschaftlich-technischen und volkswirtschaftlichen Aufgaben,* Gesellschaft für Schwerionenforschung Translation 82-16. Original in Russian: Joint Institute for Nuclear Reactions P 18-82-117, Dubna.

Lin, B. J., 1978, "A Double-Exposure Technique to Macroscopically Control Submicrometer Linewidths in Positive Resist Images," IEEE Trans. Electron Devices **ED-25**, 419.

Lindhard, J., M. Scharff, and H. E. Schiott, 1963, "Range Concepts and Heavy Ion Ranges," K. Dan. Vidensk. Selsk. Mat. Fys. Medd. **33**, No. 14, 1.

Lück, H. B., 1982, "Mechanism of Particle Track Etching in Polymeric Nuclear Track Detectors," Nucl. Instrum. Methods **202**, 497.

Malone, D. M., and J. L. Anderson, 1978, "Hindred Diffusion of Particles through Small Pores," Chem. Eng. Sci. **33**, 1429.

Märk, E., and T. D. Märk, 1982, "Fission Track Temperature Age Theory," in *Proceedings of the 11 International Conference on Solid State Nuclear Track Detectors, Bristol, 7—12 Sept., 1981,* edited by P. H. Fowler and V. M. Clapham (Pergamon, Oxford), available as Nucl. Tracks Suppl. 3, p. 389.

Marshall, S., 1982, Ed., *1982 Solid State Processing and Production Buyers Guide and Directory* (Technical Publishing, Port Washington, New York).

Martin, B., and H. Stelzer, 1978, "Detectors for Heavy Ions," in *Experimental Methods in Heavy Ion Physics,* edited by K. Bethge (Springer, Berlin), p. 150.

McNulty, P. J., S. R. Palmer, and D. D. Cooke, 1982, "Optical Properties of Particle Tracks in SSNTD Detectors," in *Proceedings of the 11th International Conference on Solid State Nuclear Track Detectors, Bristol, 7—12 Sept. 1981,* edited by P.

H. Fowler and V. M. Clapham (Pergamon, Oxford), available as Nucl. Tracks Suppl. 3, p. 807.
Messing, R. A., 1974, "Controlled-Pore Ceramics," Res./Dev. 25, 32.
Moriwaki, K., H. Aritome, and S. Namba, 1979, "Submicron Pattern Fabrication by Ion-Beam Lithography," in *Proceedings of the Conference on Microcircuit Engineering: Microstructure Fabrication, Sept. 25—27, 1979, Aachen,* edited by H. Beneking (Institute of Semiconductor Electronics), p. 153.
Naeser, C. W., and H. Faul, 1969, "Fission Track Annealing in Apatite and Sphene," J. Geophys. Res. **74**, 705.
Nakada, Y., and M. A. Giles, 1971, "X-Ray and Scanning Electron Microscope Studies of Laser-Drilled Holes in Al_2O_3 Substrates," J. Am. Ceram. Soc. **54**, 354.
Northcliffe, L. C., and R. F. Schilling, 1970, "Range and Stopping-Power Tables for Heavy Ions," Nucl. Data Tables **A7**, 233.
Ollerhead, R. W., J. Bøttiger, J. A. Davies, J. L'Ecuyer, and H. K. Haugen, 1980, "Evidence for a Thermal Spike Mechanism in the Erosion of Frozen Xenon," Radiat. Eff. **49**, 203.
O'Sullivan, D., P. B. Price, K. Kinoshita, and C. G. Willson, 1982, "Predicting Radiation Sensitivity of Polymers," J. Electrochem. Soc. **129**, 811.
Paretzke, H. G., 1982, "Can Dosimetric Quantities Describe Charged Particle Tracks in Matter?" in *Proceedings of the 11th International Conference on Solid State Nuclear Track Detectors, Bristol, 7—12 Sept. 1981,* edited by P. H. Fowler and V. M. Clapham (Pergamon, Oxford), available as Nucl. Tracks Suppl. 3. p. 3.
Paretzke, H. G., E. V. Benton, and R. P. Henke, 1973, "On Particle Track Evolution in Dielectric Track Detectors and Charge Identification through Track Radius Measurement," Nucl. Instrum. Methods **108**, 63.
Perez, A., J. Davenas, and C. H. S. Dupuy, 1976, "Ionization Induced Defects in Alkali Halide Single Crystals," Nucl. Instrum. Methods **132**, 219.
Possin, G. E., 1970, "A Method for Forming Very Small Diameter Wires," Rev. Sci. Instrum. **41**, 772.
Price, P. B., D. O'Sullivan, and S. P. Ahlen, 1982, "Thin-Film Dosimetry for Neutrons and Alpha Particles," in *Proceedings of the 11th International Conference on Solid State Nuclear Track Detectors, Bristol, 7—12 Sept. 1981,* edited by P. H. Fowler and V. M. Clapham (Pergamon, Oxford), available as Nucl. Tracks Suppl. 3, p. 925.
Price, P. B., and R. M. Walker, 1962, "Observation of Charged-Particle Tracks in Solids," J. Appl. Phys. **33**, 3400.
Price, P. B., and R. M. Walker, 1967, "Molecular Sieves and Methods for Producing Same," United States Patent Office, No. 3,303,085, Feb. 7, 1967.
Pusch, W., and A. Walch, 1982, "Synthetic Membranes—Preparation, Structure, and Application," Angew. Chem. Int. Ed. Engl. **21**, 660.
Quinn, J. A., J. L. Anderson, W. S. Ho, and W. J. Petzny, 1972, "Model Pores of Molecular Dimension. The Preparation and Characterization of Track-Etched Membranes," Biophys. J. **12**, 990.
Remillieux, J., J. C. Poizat, and M. J. Gaillard, 1982, Eds., *Proceedings of the 9th International Conference on Atomic Collisions in Solids, Lyon, July 6—10, 1981,* Nucl. Instrum. Methods **194**, 1.
Riedel, C., and R. Spohr, 1979, "Statistical Properties of Etched Nuclear Tracks. I. Analytical Theory and Computer Simulation," Radiat. Eff. **42**, 69.
Riedel, C., and R. Spohr, 1980a, "Statistical Properties of Etched Nuclear Tracks. II. Experiment and Filter Design," Radiat. Eff. **46**, 23.
Riedel, C., and R. Spohr, 1980b, "Transmission Properties of Nuclear Track Filters," J. Membr. Sci. **7**, 225.
Robinson, R. S., and S. M. Rossnagel, 1982, "Ion-Beam-Induced Topography and Surface Diffusion," J. Vac. Sci. Technol. **21**, (3), 790.
Roff, W. J., J. R. Scott, and J. Pacitti, 1971, *Fibres, Films, Plastics and Rubbers: A Handbook of Common Polymers* (Butterworths, London).
Roggenkamp, H. G., H. Kiesewatter, T. Schmeink, and H. G. Hollweg, 1982, "Ein neues Verfahren zur Quantifizierung der Verformbarkeit von Erythrocyten," Biomedizinische Technik **27**, 162.
Roggenkamp, H. G., H. Kiesewetter, R. Spohr, U. Dauer, and L. C. Busch, 1981, "Production of Single-Pore Membranes for the Measurement of Red Blood Cell Deformability," Biomedizinische Technik **26**, 167.
Rowe, J. E., C. V. Shank, D. A. Zwemer, and C. A. Murray, 1980, "Ultrahigh-Vacuum Studies of Enhanced Raman Scattering from Pyridine on Ag Surfaces," Phys. Rev. Lett. **44**, 1770.
Ruault, M. O., J. Chaumont, and H. Bernas, 1982, "Transmission Electron Microscopy Study of Ion Implantation Induced Si Amorphization," in *Proceedings of the Third International Conference on Ion Beam Modification of Materials, Grenoble, 6—10 Sept., 1982,* Nucl. Instrum. Methods **209/210**, Pt. I, p. 351.
Salamon, M. H., S. P. Ahlen, G. Tarle, and K. C. Crebbin, 1981, "Measurement of Higher-Order Corrections to Stopping Power for Relativistic Ne, Ar, and Fe Beams," Phys. Rev. A **23**, 73.
Schmidt, H., G. Haase, and F. Zörgiebel, 1977, "Investigations on the Photographic Elementary Process in AgCl Single Crystal Foils," Radiat. Eff. **34**, 43.
Schmidt-Boecking, H., 1978, "Penetration of Heavy Ions in Matter," in *Experimental Methods in Heavy Ion Physics,* edited by K. Bethge (Springer, Berlin), p. 81.
Schmitt, H. W., and F. Pleasonton, 1966, "Evaluation of a Semiconductor Detector for Fission Fragment Energy Measurements," Nucl. Instrum. Methods **40**, 204.
Schnoor, G., H. Schütt, R. Beaujean, and W. Enge, 1982, "Electrolytical Studies of Submicroscopic Nuclear Tracks in Plastic Detectors," in *Proceedings of the 11th International Conference on Solid State Nuclear Track Detectors, Bristol, 7—12 Sept. 1981,* edited by P. H. Fowler and V. M. Clapham (Pergamon, Oxford), available as Nucl. Tracks Suppl. 3, p. 51.
Schopper, E., Institute for Nuclear Physics, Frankfurt, FRG, private communication.
Schroder, D. K., R. N. Thomas, J. Vine, and H. C. Nathanson, 1974, "The Semiconductor Field-Emission Photocathode," IEEE Trans. Electron Devices **ED-21**, 785.
Seiberling, L. E., J. E. Griffith, and T. A. Tombrello, 1980, "A Thermalized Ion Explosion Model for High Energy Sputtering and Track Registration," Radiat. Eff. **52**, 201.
Seliger, R. L., R. L. Kubena, R. D. Olney, J. W. Ward, and V. Wang, 1979, "High-Resolution, Ion-Beam Processes for Microstructure Fabrication," J. Vac. Sci. Technol. **16**, 1610.
Shapiro, M. M., 1958, "Nuclear Emulsions," in *Encyclopedia of Physics. Vol. XLV. Nuclear Instrumentation II,* edited by S. Flügge and E. Creutz (Springer, Berlin), p. 342.
Siegmund, P., 1981, "Sputtering by Ion Bombardment: Theoretical Concepts," Topics Appl. Phys. **47**, 9.
Siegrist, A., and R. Balzer, 1977, "Investigations on the Forma-

tion of Tracks in Crystals," Radiat. Eff. **34**, 75.
Sinharoy, S., and W. J. Lange, 1982, "Behavior of Small Leaks in the Presence of Liquid or Gaseous Helium at 4.2 K," J. Vac. Sci. Technol. **20**, 978.
Smith, H. T., 1981, "The Impact of Submicrometer Structures in Research and Applications," in *Proceedings of the International Conference on Microlithography,* Amsterdam, 30 Sept.—2 Oct., 1980, edited by R. P. Kramer (Delft University, Delft).
Somogyi, G., 1980, "Development of Etched Nuclear Tracks," Nucl. Instrum. Methods **173**, 21.
Somogyi, G., K. Grabisch, R. Scherzer, and W. Enge, 1976, "Revision of the Concept of Registration Threshold in Plastic Track Detectors," Nucl. Instrum. Methods **134**, 129.
Somogyi, G., and S. A. Szalay, 1973, "Track-Diameter Kinetics in Dielectric Track Detectors," Nucl. Instrum. Methods **109**, 211.
Somogyi, G., M. Toth-Szilayi, M. Monnin, and J. Gourcy, 1979, "Non-Etching Nuclear Track Visualization in Polymers: Fluorescent and Dyed Tracks," Nucl. Tracks **3**, 151.
Souheng, W., 1982, *Polymer Interface and Adhesion* (Dekker, Basel).
Spiller, E., and R. Feder, 1977, "X-Ray Lithography," Topics Appl. Phys. **22**, 35.
Spohr, R., 1980, "Nuclear Track Irradiations at GSI," Nucl. Tracks **4**, 101.
Spurny, K. R., J. P. Lodge, E. R. Frank, and D. C. Sheesley, 1969, "Aerosol Filtration by Means of Nuclepore Filters. Structural and Filtration Properties," Environ. Sci. Technol. 3, 453.
Stengl, G., R. Kaitna, H. Löschner, P. Wolf, and R. Sacher, 1979, "Ion Projection System for IC Production," J. Vac. Sci. Technol. **16**, 1883.
Strocka, B., G. Bartels, and R. Spohr, 1980, "Lattice Strain in Garnet Single Crystal Caused by High-Energy Heavy Ion Irradiation," Appl. Phys. **21**, 141.
Tarle, G., S. P. Ahlen, and P. B. Price, 1981, "Energy Straggling Eliminated as a Limitation to Charge Resolution of Transmission Detectors," Nature **293**, 556.
Tarle, G., and M. Solarz, 1978, "Evidence of Higher-Order Contributions to the Stopping Power of Relativistic Iron Nuclei," Phys. Rev. Lett. **41**, 483.
Teicher, M., and R. Beserman, 1982, "Heavy Ion Implantation in Diamond," J. Appl. Phys. **53**, 1467.
Thiel, K., and H. Külzer, 1978, "Anisotropy of Track Registration in Natural Feldspar Crystals," Radiat. Eff. **35**, 87.
Thiel, K., H. Külzer, and W. Herr, 1978, "Some Track Registration Properties of Artificial Gd-Ga Garnets," Nucl. Track Detection **2**, 127.
Tommasino, L., 1980, "Solid Dielectric Detectors with Breakdown Phenomena and Their Applications in Radiation Protection," Nucl. Instrum. Methods **173**, 73.
Tress, G., M. Ellinger, E. U. Khan, H. A. Khan, P. Vater, P. Brandt, and M. Kadner, 1982, "Mica Track Microfilters Applied in a Cascade Particle Fractionator at an Industrial Plant," Nucl. Tracks **6**, 87.
Turi, E. A., 1981, Ed., *Thermal Analysis in Polymer Characterization* (Heyden and Son, New York).
Vater, P., G. Tress, R. Brandt, B. Genswürger, and R. Spohr, 1980, "Nuclear Track Microfilters Made of Mica," Nucl. Instrum. Methods **173**, 205.
von Dobeneck, D., 1975, "Materialbearbeitung mit Elektronenstrahlen," TZ Prakt. Metallbearbeitung **69**, 1.
Wallmark, J. T., 1975, "Fundamental Physical Limitations in Integrated Electronic Circuits," Inst. Phys. Conf. Ser. **25**, 133.
Washington, D., V. Duchenois, R. Polaert, and R. M. Beasley, 1971, "Technology of Channel Plate Manufacture," Acta Electron. **14**, 201.
Wendnagel, T., E. Schopper, and F. Granzer, 1980, "Properties and Technology of AgCl Detectors. II. Experiments and Technological Performance," in *Proceedings of the 10th International Conference on Solid State Nuclear Track Detectors, Lyon, 2—6 July, 1979,* edited by H. François, N. Kurtz, J. P. Massue, M. Monnin, R. Schmitt, and S. A. Durrani (Pergamon, Oxford), available as Nucl. Tracks Suppl. 2, p. 147.
Willson, C. G., H. Ito, J. M. J. Frechet, and F. Houlihan, 1982, "Chemical Amplification in the Design of Polymers for Resist Applications," in *28th Macromolecular Symposium of the International Union of Pure and Applied Chemistry, Amherst, MA, July 1982* (University of Massachusetts, Amherst).
Wilson, C. T. R., 1897, Proc. R. Soc. London, Ser. A **189**, 265.
Wittels, N. D., 1980, "Fundamentals of Electron and X-Ray Lithography," in *Fine Line Lithography,* edited by R. Newman (North-Holland, Amsterdam), p. 1.
Yang, T. C., G. Welch, C. A. Tobias, H. Maccabee, T. Hayes, L. Craise, E. V. Benton, and F. Abrams, 1978, "The Feasibility of Heavy Charged-Particle Microscopy," Ann. N.Y. Acad. Sci. **306**, 322.
York, C. M., 1958, "Cloud Chambers," in *Encyclopedia of Physics. Vol. XLV. Nuclear Instrumentation II,* edited by S. Flügge and E. Creutz (Springer, Berlin), p. 260.
Young, D. A., 1958, "Etching of Radiation Damage in Lithium Fluoride," Nature **182**, 375.
Zettlemoyer, A. C., 1969, Ed., *Nucleation* (Dekker, New York).
Ziegler, J. F., 1977, *The Stopping and Ranges of Ions in Matter,* Vols. 1—5 (Pergamon, London).

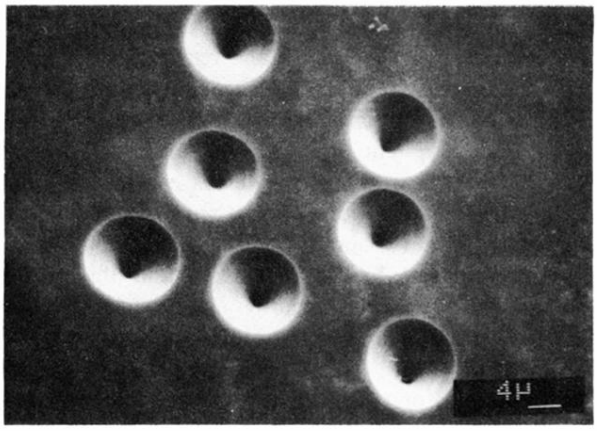

FIG. 16. Etch cones obtained in regular glass after a short etching.

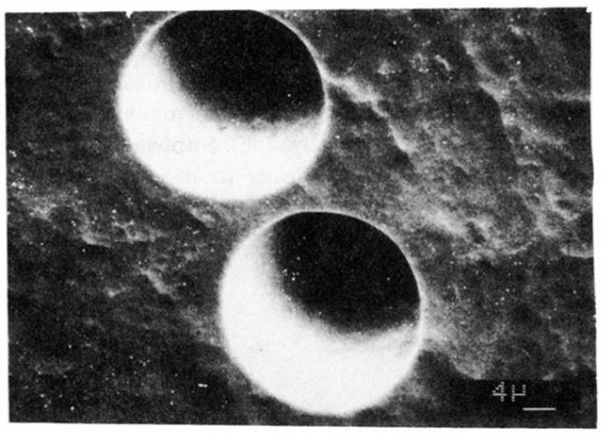

FIG. 17. Spherical etch pits in regular glass after prolonged etching.

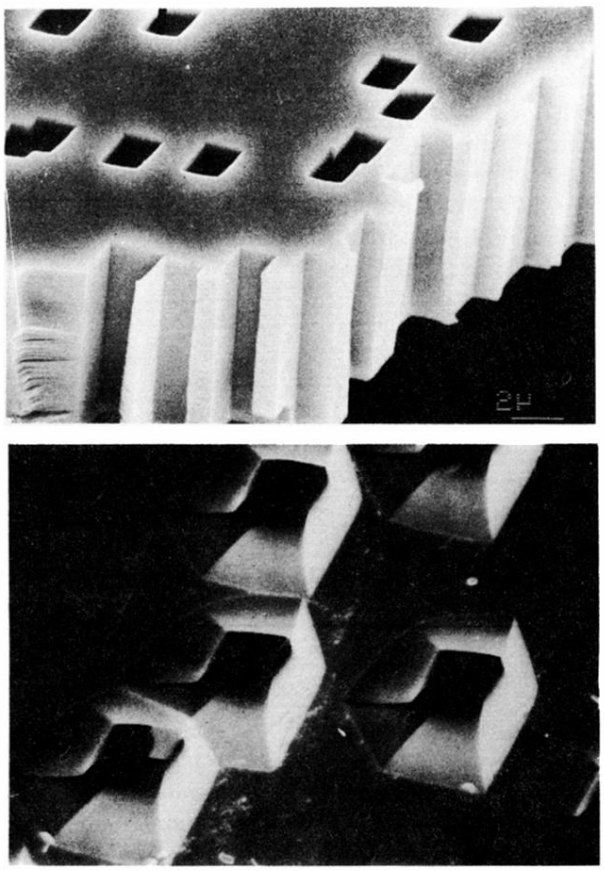

FIG. 18. Influence of the etchant on the track morphology in mica (Khan *et al.*, 1981). In addition to the composition of the recording material and the irradiating ion and energy, track morphology depends on the chemical nature, reactivity, viscosity, and temperature of the etchant. *Top*: Etching of the latent tracks by hydrofluoric acid leads to rhombic holes with sharp edges. *Bottom*: Etching in boiling sodium hydroxide solution leads to smooth hexagonal funnels.

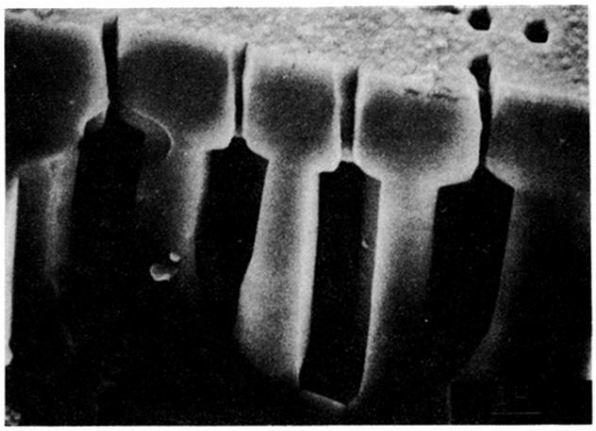

FIG. 19. Microcavities generated in a double-layer track recorder (Hansen *et al.*, 1983). Epitaxially grown iron garnet film on top of a single-crystal garnet substrate with etched nuclear tracks. The different lateral etch rates in the top film and in the substrate lead to hexagonal microcavities, connected to the outside world only by fine bottlenecks.

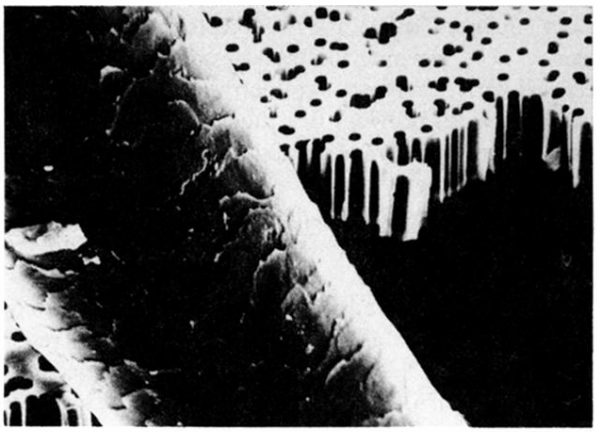

FIG. 21. Nuclear track filter dimensions, compared to a human hair. The etched track holes (background right) are about ten times smaller in diameter than a human hair (foreground left; diameter about 100 μm). The track-etch technique enables one to make holes with a minimum diameter of about 0.01 μm (10 nm), that is, about a thousand times smaller than the etched track holes shown here.

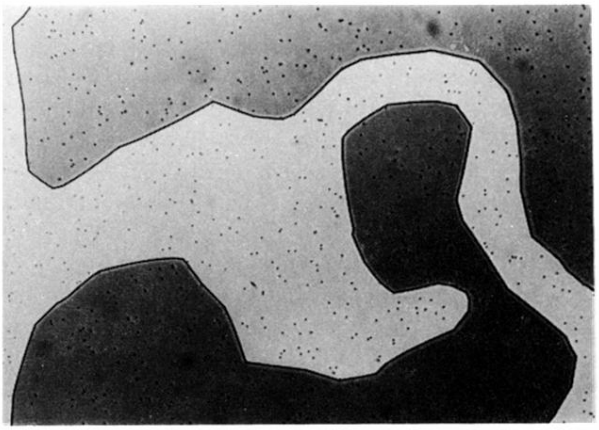

FIG. 22. Pinning of magnetic domain walls by etched nuclear tracks (Hansen *et al.*, 1983). Optical micrograph of magnetic iron garnet film, observed under nearly crossed polarizing conditions. Antiparallel magnetic domains appear as gray and white zones. The domains are separated by domain walls, observed here as black zigzagging lines. Nuclear tracks (black dots) decrease the magnetic domain-wall energy locally and thus result in a short-range pinning force. The global effect of many such local pinning centers is to increase the domain wall coercivity. Thus the inscribed domain pattern is "frozen" and the corresponding information stabilized.

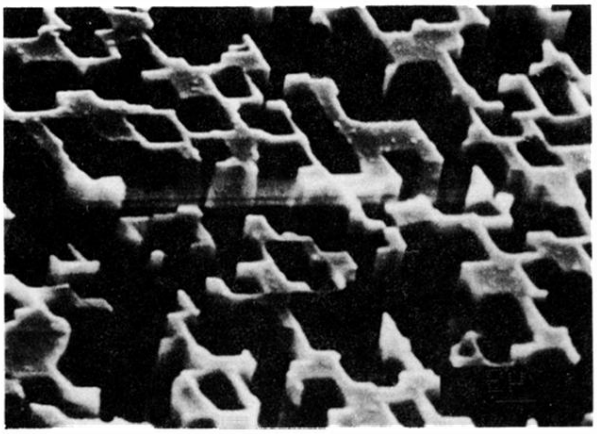

FIG. 23. Superinsulating maze texture generated in thick mica sample (Fischer *et al.*, 1982). Beyond a certain porosity, the surface of a thick track recorder, which is not traversed by the impinging ions, divides into discrete islands separated by deep canyons due to multiple-hole rings (Riedel and Spohr, 1979). A maze structure results, retaining its high electrical surface resistance even if a highly conductive metal film is evaporated on top of it. The metal-coated maze structure has an electrical resistance about 10 orders of magnitude higher than that of an identically treated flat surface.

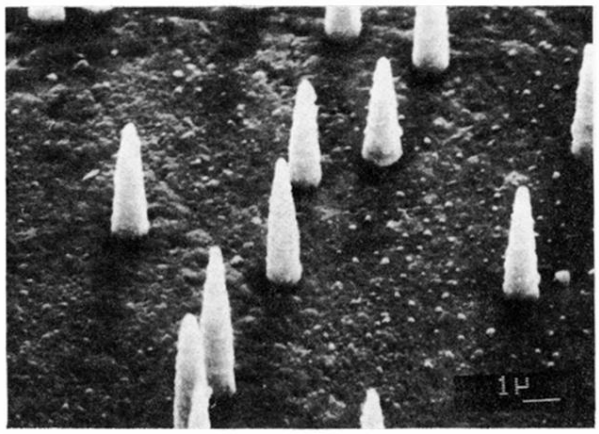

FIG. 24. Random field-emitter array, produced by a replica technique. The microscopic metal pins were obtained by a catalyst-activated copper deposition into etched nuclear track cones, followed by selective removal of the track-recorder material. Such field-emitter arrays could be used in the future as energy-saving cold cathodes in vacuum electronics devices.

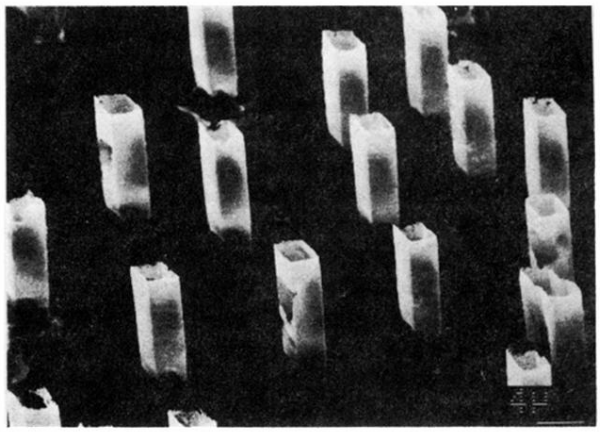

FIG. 25. Random array of hollow metallic microtubes of rhombic shape. The microtubes are obtained by metal deposition into etched nuclear tracks in mica, followed by selective removal of the matrix. Such microtube arrays could be used in the future as field-ion emitters, whereby a suitable gas would be admitted from the back of the structure, would penetrate through the microtubes, and would finally be ionized in the high electrostatic field at the rim of the microtubes.

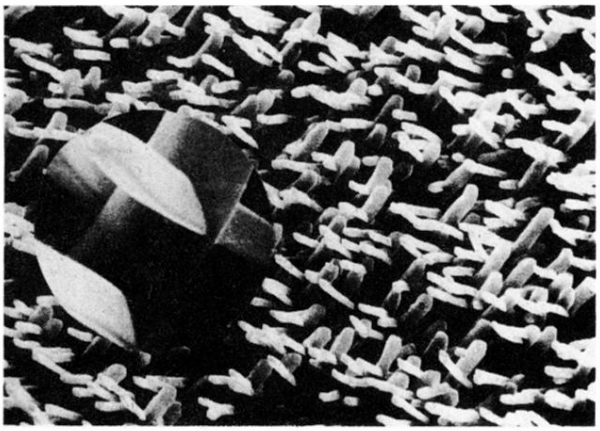

FIG. 26. Fused-fiber architecture of a nuclear track microcomposite. The mutually intersecting "fused" fibers form one coherent network, comparable to a three-dimensionally cross-linked polymer. For the purpose of observation, the matrix of the composite has been removed by selective etching. Nuclear track composites may eliminate the problem of slippage between fiber and matrix, common to conventional composite materials. In track-produced microcomposites the strands of different directions intersect each other, forming homogeneous "fused" joints (enlarged inset).

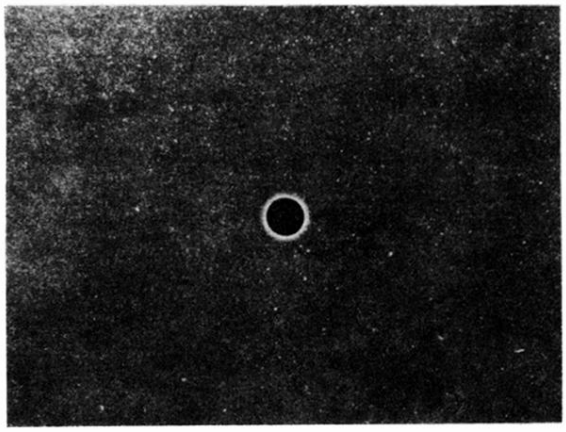

FIG. 27. Single-pore membrane generated in a thin polycarbonate foil. Single pores are used in biology and medicine, for example, as counting apertures for measuring the number, size, mobility, and deformability of particles suspended in solution. The etched track hole shown in this micrograph is produced by the passage of exactly one ion through a foil of 30 μm thickness and 30 mm diameter. The central hole has a diameter of 5 μm (0.005 mm).

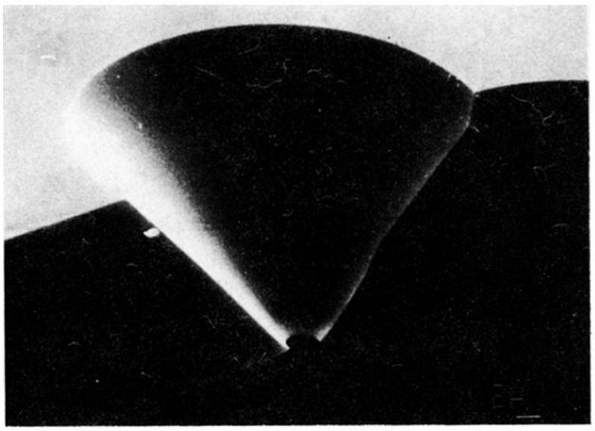

FIG. 28. Cross section through an asymmetrically etched track cone in a thin cover glass used in optical microscopy, obtained by breaking. Due to the very high homogeneity of glass, very smooth circular apertures can be obtained. The perforation was performed in a conductivity cell, exclusively attacking from the top surface, and was interrupted as soon as a preset electrical conductivity through the etched holes had been reached.

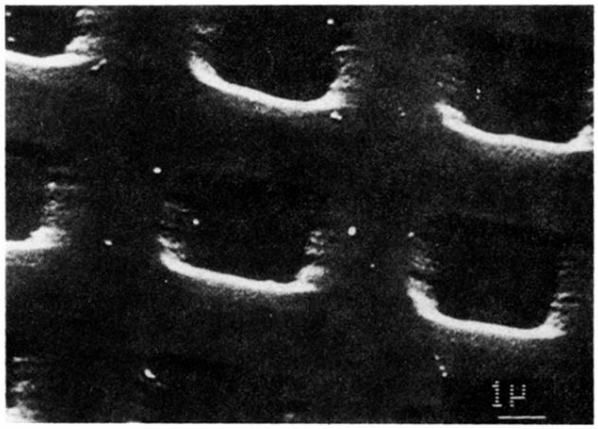

FIG. 30. Silicon dioxide, applied as a high-resolution "resist." SiO_2 exists as a passivating layer of very uniform thickness and homogeneity on commercially available silicon wafers. Subjected to heavy ions, it can be thought of as an "inherent" resist of very uniform thickness. Its high spatial resolution is due to the high homogeneity of the glassy material. In this scanning electron micrograph, ≤ 0.1 μm can be discerned in the toothed fine structure, replicating the irregularities of the projected metallic micromesh. The mesh was kept at a projection distance of 1000 μm, which is very large compared to the finest resolved structure (the observed lateral smearing is due to slipping between mask and resist during the exposure). The metallic micromesh was provided through courtesy of P. Tischer, Siemens AG, Munich, FRG.

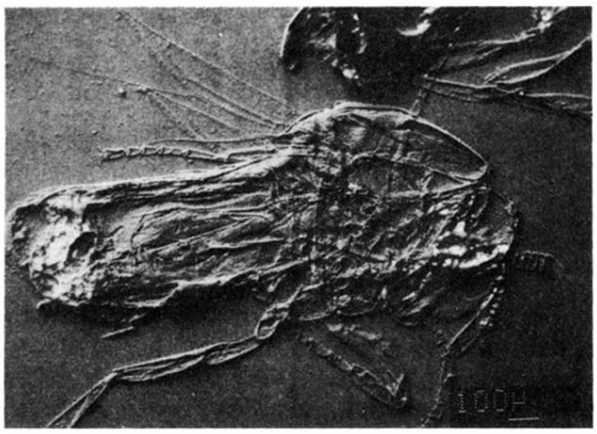

FIG. 31. Density mapping of a small insect by heavy-ion lithography. Because of their well-defined range, heavy ions are very sensitive probes for sampling the density of inhomogeneous objects. Like diagnostic x rays in medicine, they make the inner details of an object accessible from outside, without dissecting the object. The relief elevation corresponds directly to the projected areal density distribution of the object. Density differences of a few percent can easily be discerned.